Indian hedgehog function in skin development and tumour formation

Inaugural-Dissertation

zur

Erlangung des Doktorgrades

der Mathematisch-Naturwissenschaftlichen Fakultät

der Universität zu Köln

vorgelegt von

Parisa Kakanj

aus Teheran

Köln 2011

Berichterstatter/in:	Prof. Dr. med. Jens C. Brüning
	Prof. Dr. rer. nat. Carien M. Niessen
Vorsitzender:	Pof. Dr. rer. nat. Martin Hülskamp
Schriftführerin:	Dr. rer. nat. Catherin Niemann

Tag der mündlichen Prüfung: 28.06.2011

To my beloved parents

تقدیم به مادر و پدر عزیزم

با عشق و احترام قلبی

“The pipette is my clarinet.”

Max Delbrück (1970)

Table of contents

Figure index

Table index

1 Abbreviations

A	adenine
Ab	antibody
B	bulge
BCA	bicinchonic acid
BCC	basal cell carcinoma
BL	basal layer
BM	basement membrane
BMP	Bone Morphogenetic Protein
BP	base pairs
BrdU	Bromodeoxyuridine (5-bromo-2'-deoxyuridine)
BSA	bovine serum albumin
°C	degree Celsius
cDNA	complementary DNA
CL	cornified layer
c-Myc	cellular myelo cytomatosis oncogene
CO_2	carbon dioxide
Cre	site specific recombinase from phage P1 (causes recombination)
CS	Cockayne syndromeb
DAPI	4`6-Diamidino-2-phenylindol
DE	dermis
Dhh	Desert hedgehog
DMBA	7,12-dimethylbenz-[*a*]-anthracene
DMEM	Dulbecco`s modified Eagle's Medium
DMSO	dimethylsulfoxide
DNA	deoxyribonucleic acid
DP	dermal papilla
DSB	double stand breaks
E	embryonic day
ECL	enhanced chemiluminescence
ECM	extracellular matrix

EDTA	ethylene diamine tetra acetic acid
EGF	epidermal growth factor
EtOH	ethanol
FACS	fluorescence activated cell sorting
FCS	fetal calf serum
Ihh	Indian hedgehog
Ihh EKO	epidermal specific *Ihh* knockout
g	gram
GFP	green fluorescent protein
GL	Granular layer
Gli	glioma-associated oncogene homolog
GSK3	Glycogen synthase kinase 3
GTP	Guanosintriphosphat
H	hours
HCL	hydrochloric acid
H&E	hematoxylin-eosin
HF	hair follicle
HG	hair germ
Hh	Hedgehog
HR	homologous recombination
HRP	horse radish peroxidase
Hz	hertz
IF	immunofluorescent
IFE	interfollicular epidermis
IRS	inner root sheath
IU	international unit
IZ	isthmus zone
JZ	junctional zone
K	keratin
K6a	keratin 6a
K10	keratin 10
K14	keratin 14

kDa	kilo Dalton
Ki67	Kiel 67 (university of Kiel)
KO	knockout
Lef1	Lymphoid enhancer-binding factor 1
LRC	label retaining cells
M	Mol
mAB	monoclonal antibody
Mdm2	Murine double minute 2
µg	micro geram
mg	milligram
min	minute
µl	micro liter
ml	milliliter
µm	micro molar
mM	millimolar
mRNA	messenger RNA
MZ	mature sebocytes
n	nano
NER	nucleotide excision repair
Ng	nanogram
NGS	normal goat serum
nm	nanometer
NP-40	nonidet P-40
ORS	outer root sheat
P	postnatal day
PAGE	polyacrylamide gel electrophoresis
PAP	papilloma
PBS	phosphate buffered saline
PCR	polymerase chain reaction
PDK1	phosphoinositide-dependent protein kinase 1
PFA	paraformaldehyde
PI	propidium iodide

PI3K	phosphatidylinositol 3 kinase
PKA	protein kinase A
Ptch	patched
RNA	ribonucleic acid
RNAi	RNA interference
Rpm	rounds per minute
SC	stem cell
SDS	sodium dodecyl sulphate
Sec	seconds
Ser	Serine
SG	sebaceous gland
Shh	Sonic hedgehog
SL	Spinous layer
s-Me	s-mercaptoethanol
Smo	smoothened
Sufu	Suppressor of Fused
TAE	Tris-acetic acid-EDTA-buffer
TBS	tris buffered saline
TE	Tris-EDTA buffered
TF	Transcription factor
Tg	Transgenic
TPA	12-*O*-Tetradecanoylphorbol-13-acetat
U	unit
UV	ultraviolet
V	volt
vs.	versus
v/v	volume/volume
WB	western blot
WM	whole mounts
Wt	wild-type
w/v	weight per volume
XP	Xeroderma pigmentos

2 Abstract

The Hedgehog (Hh) signalling pathway plays an essential role during mammalian skin development and epidermal regeneration. Out of the three mammalian Hh homologs, Sonic hedgehog (Shh) is the best characterised Hh ligand in the skin. Shh is expressed during hair morphogenesis and is required for hair follicle formation and cyclic hair regeneration. Mutations in *Shh* and other components of the Hh pathway result in skin abnormalities and tumour formation, e.g. Basal Cell Carcinoma (BCC), the most common cancer in humans. Indian hedgehog (Ihh) is expressed in the sebaceous gland (SG), a hair follicle associated epidermal appendage, which secretes sebum to lubricate and protect the skin. However, an *in vivo* function for Ihh has not been identified in the skin. *In vitro* studies indicated that components of the Hh pathway are up-regulated and activity of the pathway is increased upon differentiation of human sebocytes. Furthermore, it was shown that activation of Hh signalling in basal keratinocytes promotes ectopic SG and sebaceous duct formation. Analysis of sebaceous tumours in mouse models and in humans demonstrated expression of Ihh in mature tumour cells. These observations led to the hypothesis that Ihh could be an important factor regulating differentiation and tumour formation in the skin. To address these issues, an epidermis-specific *Ihh* knockout (*Ihh* EKO) was generated. The absence of epidermal Ihh significantly inhibits proliferation in early skin development however; morphogenesis of SGs, hair follicles and the interfollicular epidermis was not altered. Importantly, a function of Ihh for tumourigenesis was identified. In particular, Ihh increases the size of tumours and induces SG and sebaceous duct fate differentiation and this was accompanied by a reduced number of follicular progenitors. In addition, Ihh signalling promoted proliferation and regulated p53 in squamous epidermal tumours. The results indicate that regulation of p53 constitutes a general function of Ihh in keratinocytes and that Ihh plays an important role in patho-physiological conditions of the skin.

2.1 Zusammenfassung

Der Hedgehog (Hh) Signalweg spielt für die Entwicklung und Regeneration der Haut der Säugetiere eine wichtige Rolle. Unter den drei Hh Liganden, Sonic Hedgehog (Shh), Indian Hedgehog (Ihh) und Dessert Hedgehog (Dhh), ist die Rolle von Shh am besten untersucht. Shh wird im wachsenden Haarfollikel exprimiert, wo es während der Haarfollikelbildung und der zyklischen Regeneration des Haares inbesondere die Proliferation der Keratinozyten kontrolliert. Die Aktivierung des Signalweges, z.B. durch Mutationen in dem Rezeptor Patched, führt zu Störungen der Hautentwicklung und zu Tumoren, unter denen das Basalzellkarzinom (BCC) die am häufigsten auftretende menschliche Krebserkrankung darstellt. Der Ligand Ihh wird in der Talgdrüse exprimiert, die häufig mit dem Haarfollikel assoziiert vorliegt. Bisher ist über die Funktion von Ihh in der Haut wenig bekannt. In vitro Studien zeigten, dass während der Differenzierung humaner Sebozyten die Expression von Komponten und die Aktivität des Hh Signalwegs erhöht sind. Eine Aktivierung des Hh Signalwegs in der Basalschicht der Epidermis führt zur Bildung ektopischer Talgdrüsen und Talgdrüsengänge. Die Analyse von Talgdrüsentumoren beim Menschen und der Maus zeigt, dass Ptch1 und Gli1 erhöht exprimiert sind, was darauf hinweist, dass der Hh Siganlweg in diesen Tumoren aktiviert ist. Ihh wird in Talgdrüsentumoren ebenfalls stark expimiert, wohingegen Shh und Dhh nicht detektierbar sind. Diese Beobachtungen führten zur Hypothese, dass Ihh für die Proliferation, Differenzierung und Tumorbildung in der Haut von großer Bedeutung ist. Um die Funktion von Ihh in der Haut zu untersuchen, wurden Mäuse generiert, in denen Ihh spezifisch im Epithel der Haut ausgeschaltet wurde (*Ihh* EKO). Der Verlust von Ihh in der Haut führt zwar zu einer verringerten Proliferation in der Epidermis von jungen Tieren, jedoch wurden keine offensichtlichen morphologischen Defekte beobachtet. Im Gegensatz dazu führt der Verlust von Ihh zu reduzierter Proliferation und zu veränderter Differenzierung in Talgdrüsentumoren. In Plattenephitelkarzinomen waren in *Ihh* EKO Mäusen ebenfalls die Proliferation und Differenzierung der Kerationzyten deutlich verändert. Des Weiteren führt der Verlust von Ihh in der normalen Haut als auch in Tumoren zu einer nuklearen Akkumulation von p53. Die Daten zeigen deutlich, daß Ihh neben der Regulation der Differenzierung von Sebozyten eine wichtige Funktion in der Kontrolle von Proliferation und p53 Aktivität der Haut hat.

3 Introduction

Genetic studies have revealed that a small number of evolutionarily conserved pathways are used repeatedly in different contexts to control many cell fate decisions in all animals during their development. These include: the Bone morphogenetic protein (Bmp), Wnt, receptor tyrosine kinase, Notch and Hedgehog (Hh) pathways (Huangfu and Anderson, 2006). However, gene duplications and the increase of organism complexity during evolution led to increased numbers of pathway components and their divergent functions.

3.1 Hedgehog (Hh) signalling

The Hh signalling cascade is one of the key pathways for mammalian development. The *Hh* gene was first identified in a *Drosophila* genetic screening by Christiane Nüsslein-Volhard and Eric Wieschaus in 1980 and was observed to be important for embryonic segmentation and imaginal discs specifications in *Drosophila* (Nüsslein-Volhard and Erik Wieschaus, 1980; Basler and Struhl, 1994; Mohler, 1988; Tabata et al., 1992). Hh is conserved from insects to mammals and has been studied in greatest depth in *Drosophila*, in which forward genetic screens allowed identification of various components of the Hh signalling pathway (Hooper and Scott, 2005; Huangfu and Anderson, 2006). However, recent genetic studies have defined a surprisingly large number of proteins required for Hh signalling in vertebrates and mammals that have no apparent role in *Drosophila* Hh signalling.

3.1.1 Mechanisms of Hh signal transduction in mammalian tissues

Vertebrate Hh genes were first reported in 1993 across different species (fish, chick and mouse) by several groups (Echelard et al., 1993; Krauss et al., 1993; Riddle et al., 1993; Chang et al., 1994; Roelink etal., 1994). The obvious difference between invertebrates and vertebrates is that the genes encoding the specific Hh pathway components have been duplicated during vertebrate evolution (Kumar et al., 1994, Meyer and Schartl, 1999; Mazet

and Shimeld, 2002). Three Hh homologs, *Sonic hedgehog* (*Shh*), *Indian hedgehog* (*Ihh*) and *Desert hedgehog* (*Dhh*) have been identified in mammals. Dhh is most closely related to the *Drosophila* Hh protein and regulates spermatogenesis whereas Shh and Ihh are more closely related to each other (90% amino acid identity) than to Dhh (80% amino acid identity). Shh and Ihh also play essential roles during embryonic development (Echelard et al., 1993). All three Hh proteins are synthesized as a precursor of ~45-kDa which undergoes auto-processing to generate a ~19-kDa amino-terminal fragment (Hh-N). The Hh-N fragment is activated after two post-translational modifications: covalent attachment of a cholesterol moiety to the carboxy-terminus and palmitoylation at the amino-terminus (Lee et al., 1994; Porter et al., 1995; Porter et al., 1996; Li et al., 2006; Li et al., 2011). These lipid modifications are crucial and contribute to the mobility and full signalling capacity of Hh proteins (Lewis et al., 2001; Chen et al., 2004).

Secretion of Hh ligands induces various effects dependent on the cellular context. Hh can act as an on-off switch that regulates the fate of immediately adjacent cells. Alternatively, Hh can act as short-range morphogen over a distance of around 10-15 cell diameters or as long-range morphogen spanning over more than 100 cell diameters (Ingham and Hidalgo, 1993, Stone et al., 1996; Strigini and Cohen, 1997; Huangfu and Anderson, 2006). The Hh signalling cascade is initiated upon binding of a Hh ligand to its receptor Patched (Ptch), a protein with 12-transmembrane spanning domains (Fig. 1). There are two *Ptch* homologs in mice, *Ptch1* and *Ptch2*. Ptch1 and Ptch2 are differentially expressed during development suggesting specific roles for each protein. Ptch1 is more widely expressed during embryonic development and in mouse and human it is known as a tumour suppressor. The function of Ptch2 however has not been fully clarified inspite of loss-of-function studies. A recent study suggests that Ptch2 may also act as a Hh receptor and modulates signalling in various cellular environments (Smyth et al., 1999; Rahnama et al., 2004, Lee et al., 2006; Eriken Nieunenhuis???).

Smoothened (Smo) a 7-transmembrane spanning protein is repressed by Ptch1 in the absence of the Hh-ligand. In the presence of high levels of Hh ligand, Ptch1 inhibition is released and Smo transduces the signal to the downstream Glioma-associated family of zinc finger transcription factors Gli1, Gli2 and Gli3. The precise mechanism by which Smo activates this cascade remains unclear. It is known that a conformational change of Smo protein and its translocation to the primary cilium are the two critical events for activation of the Hh pathway

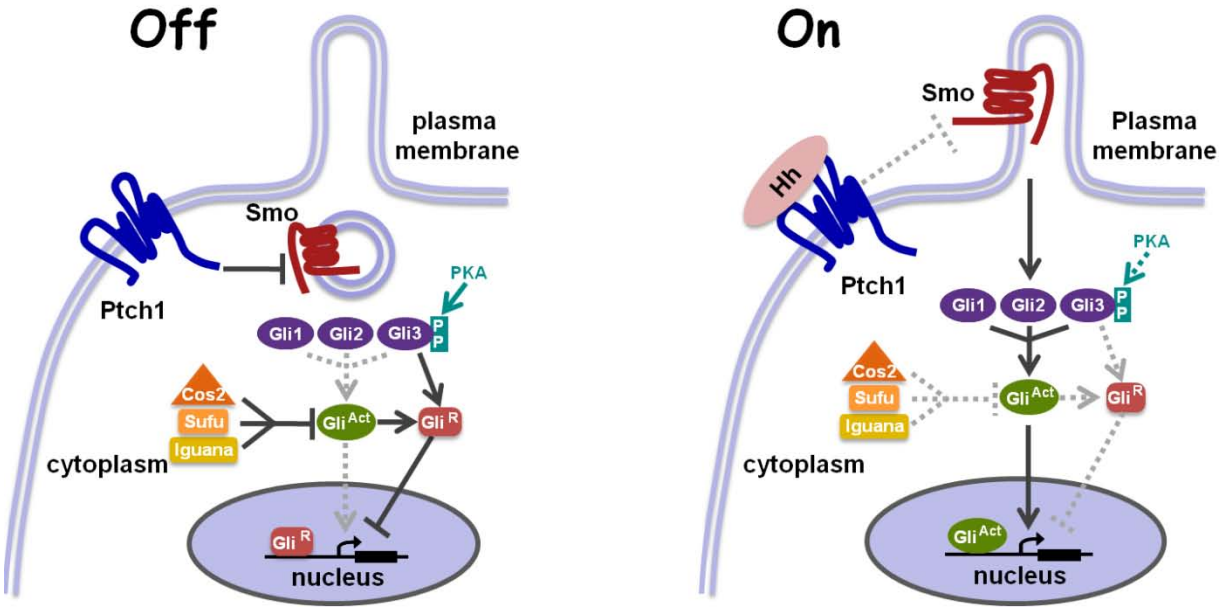

Figure 1: Scheme of the Hh pathway in vertebrates and mammals.
In the absence of Hh ligand **(left)** Ptch1 represses the transmembrane protein Smo; preventing the accumulation of Smo in cilia and turning off downstream signalling. Activation of Gli transcription factors is inhibited by a group of proteins: Sufu, Iguana (for zebrafish) and Cos2. Gli2 and Gli3 are processed (phosphorylated and cleaved) into a repressor form (Gli^R) in a cilia-dependent manner. The short form of Gli (Gli^R) accumulates in the nucleus and represses the transcription of target genes. In the presence of high levels of Hh ligand **(right)**, Ptch1 inhibition is released; Smo is recruited to cilia and activates Gli proteins. The Gli proteins are no longer cleaved and full length Glis activate the transcription of Hh-target genes. Ptch1 (Patched1), Smo (Smoothened), Gli (Glioma-associated family of transcription factors), Sufu (Suppressor of Fused), p (phosphorylation), PKA (protein kinase A). (Modified after Huangfu and Anderson, 2006)

in vertebrates (Zhao et al., 2007; Taipale et al., 2002). Smo controls both the activation of Gli transcription factors and the proteolytic processing event that generates a repressor form of Gli. However, this does not occur for all Gli proteins (Huangfu and Anderson, 2006). Gli3 and Gli2 are bifunctional and can be processed into a repressor or a transcriptional activator (Wang et al., 2000; Aza-Blanc et al., 2000). Gli1 cannot be proteolytically processed and is solely a transcriptional activator (Dai et al., 1999; Lee et al., 1997; Ruiz i Altaba, 1998). The three Gli proteins are characterised by a homologous zinc finger domain and have limited homology outside this region (Matise and Joyner 1999). Upon activation of the Hh pathway, the active form of the Glis (Gli^{Act}) induces the expression of target genes including Ptch1 and Gli1, which provide a negative (Ptch1) and a positive (Gli1) feedback for Hh signalling (Ruiz i Altaba et al., 2007; Wang et al., 2000; Pan et al., 2006; Litingtung et al., 2002; Bai et al., 2004).

3.1.2 Expression and function of Hh ligands during mammalian development

Hh ligands act as morphogens and regulate multiple developmental processes (Fig. 2). All mammalian Hh ligands have similar signalling capacities but exert different roles during development due to their diverse expression patterns (Ingham and McMahon, 2001; McMahon et al., 2003; Sagai et al., 2005; Varjosalo and Taipale, 2008).

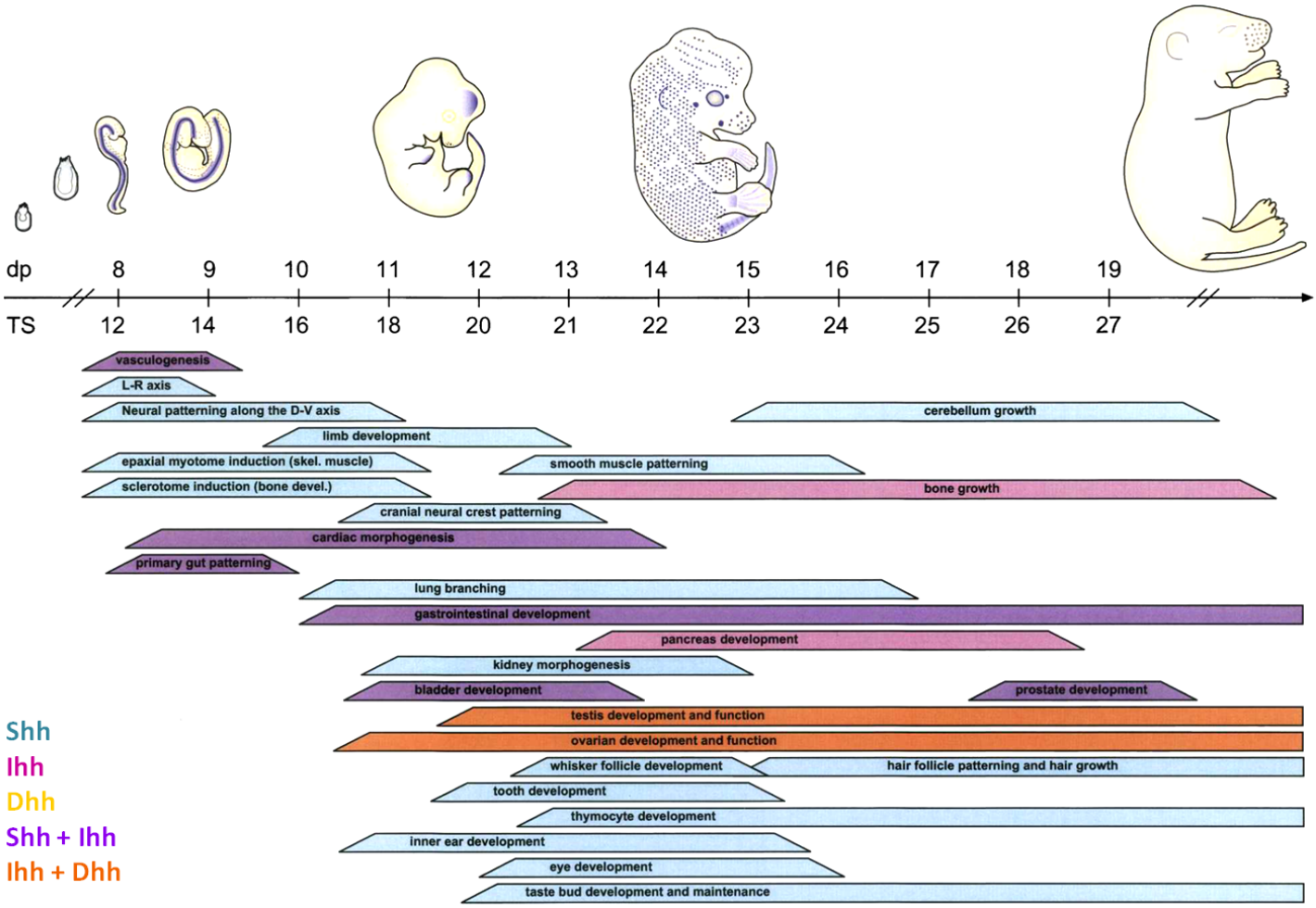

Figure 2: Temporal control of Hh expression and function during mammalian development.
(Top) Embryo cartoons show regions of the Hh target gene expression depicted by the embryos. *Ptch1* (blue) during mouse embryonic development. **(Bottom)** Bars show approximate embryonic stages when Shh, Ihh, and/or Dhh (color code in bottom left) control developmental processes in the indicated tissues or cell types. The embryonic stage is indicated by postcoital (dpc) (Varjosalo and Taipale, 2008; Ingham and McMahon, 2001).

Shh, the best characterised Hh ligand, is the most broadly expressed during mammalian development. Shh expression has been detected in the notochord, floor plate, limbs and many other developing organs (Huangfu and Anderson, 2006). Shh is an essential factor for patterning of the dorso-ventral axes as well as for the morphogenesis of different organs (Ingham and McMahon, 2001, McMahon et al., 2003; Varjosalo and Taipale, 2008). In contrast, Dhh expression and function is restricted to the regulation of spermatogenesis and development of the perineural sheath (Bitgood et al. 1996; Parmantier et al., 1996; Yao et al. 2002; Wijgerde et al. 2005). Ihh expression is limited to a few tissues during development, including primitive endoderm (Dyer et al. 2001), gut (Ramalho-Santos et al., 2000; van den Brink 2007) and growth plates of the bones (Vortkamp et al., 1996; St-Jacques et al. 1999, Karp et al., 2000). Importantly, more than one ligand is often expressed in the same tissue and therefore, can act redundantly.

Hh signalling also plays important roles beyond development and controls tissue maintenance and differentiation in adult organs (Varjosalo and Taipale, 2008), for instance in the gastrointestinal tract, pancreas, uterus, mammary gland and skin (St-Jacques et al., 1998; Oro at al. 2002; Ingham and McMahon, 2001; Varjosalo and Taipale, 2008).

3.2 Structure and function of mammalian skin

The skin is the only organ in mammals which is in direct contact with the surrounding milieu and forms an effective barrier between the organism and the environment. Its' functions are to protect the body against pathogens, UV radiation, chemical and mechanical stress as well as the regulation of temperature, water and electrolyte balance (Wokalek, 1992, Chuong et al., 2002; Blanpain and Fuchs, 2006; Segre 2006). In addition, animals can perceive their environment through the tactile sense of the skin. In mammals, the skin is the largest organ and consists of the epidermis, dermis and subcutaneous tissue, the hypodermis (Fig. 3). The subcutis is the fat tissue below the dermis composed of adipocytes (Alberts, 2008; Montagna and Parakkal, 1974). The dermis is a mesenchymal connective tissue, which underlies the epidermis. It is composed of fibroblasts and extracellular matrix (ECM) components (e.g. collagen and elastic fibers) and provides stability and nutrients for the epidermis. The cross talk between dermis and epidermis is important for proliferation and morphogenesis of the

epidermal compartment. The epidermis, the outer most layer of the skin, is separated by a basement membrane from the dermis and is composed of two major compartments, the interfollicular epidermis (IFE) and the pilosebaceous unit (Fig. 3, 4). The epidermis is a stratified squamous epithelium, composed of several layers. The basal layer of IFE consists of the proliferating and transit amplifying cells giving rise to suprabasal differentiated cells of the spinous, granular, and cornified layer (Fig.3). The pilosebaceous unit is made of hair follicles (HFs) and sebaceous glands (SGs).

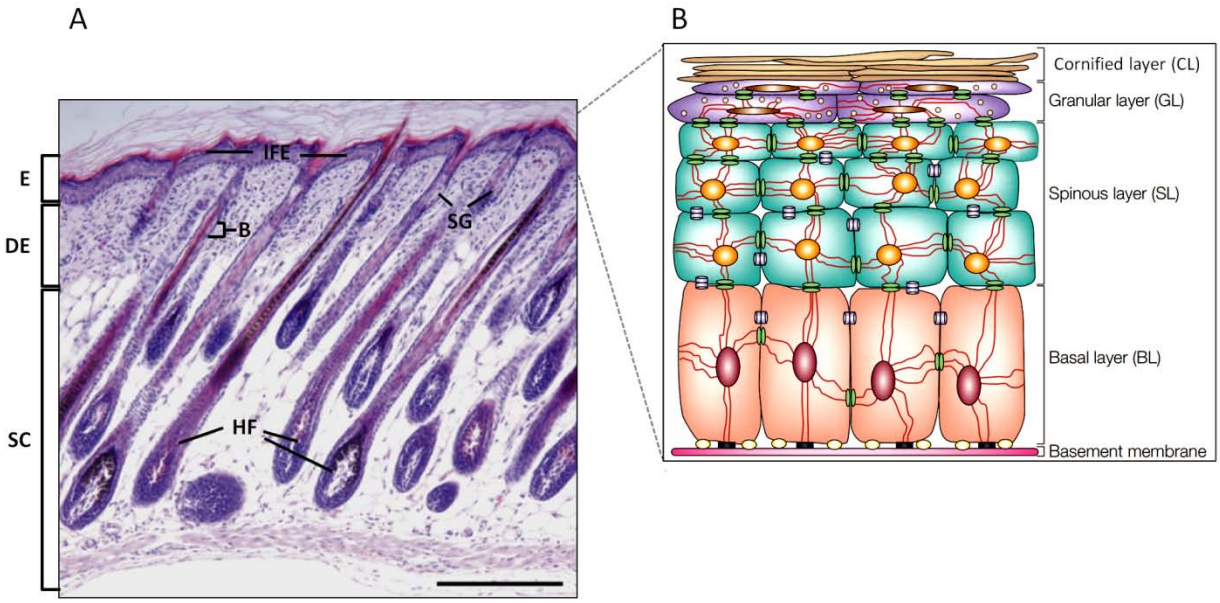

Figure 3: Skin morphology and structure of the interfollicular epidermis (IFE).
(A) Haematoxylin- and eosin-stained section of the dorsal skin of an adult mouse demonstrating epidermis (E), dermis (DE), and subcutis (SC). The epidermis consists of different compartments such as the interfollicular epidermis (IFE), Hair follicles (HF), bulge (B) and sebaceous glands (SG) **(B)** The IFE is composed of different layers: basal layer (BL), spinous layer (SL), granular layer (GL) and cornified layer (CL) (Niemann and Watt, 2002; modified after Fuchs and Raghavan, 2002).

The HF is composed of the outer root sheath (ORS), companion layer, inner root sheath (IRS), hair shaft and the rapidly proliferating matrix cells in the hair bulb, which give rise to the different hair lineages (Fig. 4) (Niemann and Watt, 2002; Blanpain and Fuchs, 2006; Shimomura and Christiano, 2010). Continuous renewal of the HF throughout life requires multipotential SC. The best characterised Hair follicle stem cell (HFSC) compartment is the bulge region which is established within the permanent part of the HF (Nowak et al., 2008). The SG is an epidermal appendage associated with HFs. The SG consists of an undifferentiated

layer of keratinocytes at the periphery of the gland and differentiated sebocytes in the center. (Fig. 4) (Niemann, 2009; Schneider and Paus, 2009). One important feature of the mature sebocytes is the accumulation of lipid droplets. Once mature sebocytes burst, the lipid containing sebum is delivered via the sebaceous duct to the hair channel and surface of the skin. The secreted sebum lubricates the hair channel and the surface of the skin. It also protects the skin against pathogens and environmental stress factors (Thody and Shuster, 1989; Schneider and Paus, 2009). Therefore, the proper function of SGs is crucial for maintenance of the skin barrier. Furthermore, malfunctions of the SGs are associated with diseases including Acne vulgaris and cancers (Zouboulis, 2004).

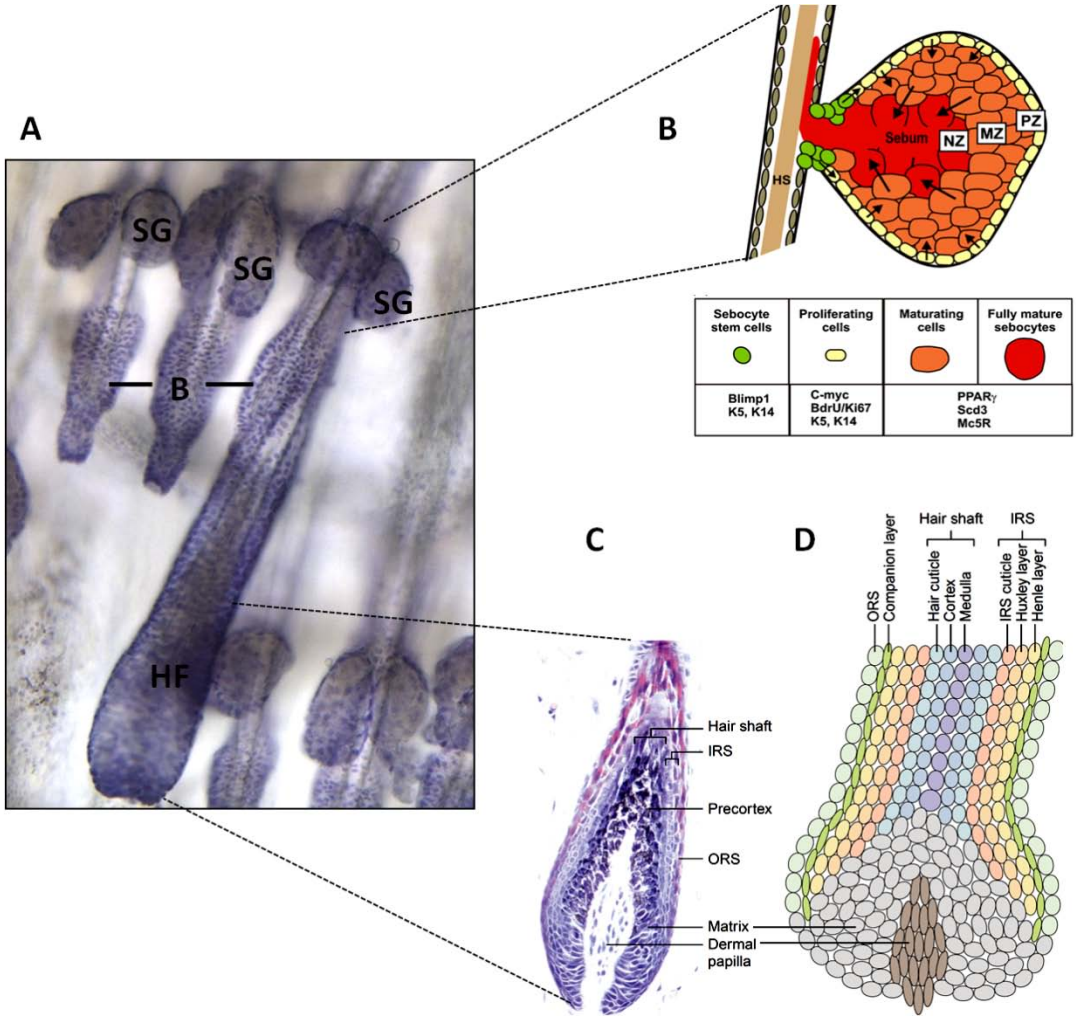

Figure 4: Structure of the pilosebaceous unit.
(A) Haematoxylin- and eosin-stained whole mount of mouse tail skin demonstrating HFs, SGs and the bulge region (B) of the HF. **(B)** Schematic drawing of the SG illustrating three regions: basal cell layer (PZ), partially mature sebocytes (MZ) and fully mature sebocytes (NZ). **(C)** Haematoxylin- and eosin-stained section through the base of a growing follicle. **(D)** Schematic drawing of the HF consisting of different cell layers: outer root sheath (ORS), companion layer, inner root sheath (IRS), hair shaft, matrix containing HF progenitor cells and the dermal papilla (DP), a specialized mesenchymal component embedded in the hair bulb which induces HF proliferation. (Niemann and Watt, 2002; Schneider and Paus, 2009).

3.3 Hedgehog signalling during skin development and regeneration

During skin development, a complex signalling network controls the morphogenesis and regeneration of each epidermal compartment. Hh signalling is one of the essential pathways during skin development and homeostasis (St-Jacques et al., 1998; Oro and Higgins, 2003). In mammalian skin, *Shh* is expressed in the matrix of the hair bulb and promotes cell proliferation and cyclic hair regeneration (Fig. 5A, G, H, I) (Oro at al., 2001; St-Jacques et al., 1998; Chiang et al., 1999; Sato et al., 1999; Wang et al., 2000; Oro and Higgins, 2003). During early skin development, expression of *Shh* in placodes of the HF and expression *of Ptch1, Smo, Gli1* and *Gli2* in both the epithelial and dermal compartment suggests Shh signalling activity in cell types derived from both compartments (Fig. 5A-F). (Oro et al., 1997; St-Jacques et al., 1998, Oro and Higgins, 2003). Lower levels of *Ptch1*, *Smo*, *Gli1* and *Gli2* expression were also detected in keratinocytes and in the dermis of the interfollicular region (Fig. 5A-F) (Oro et al., 1997; St-Jacques et al., 1998). However, the function of the Hh pathway in the IFE has not been elucidated yet.

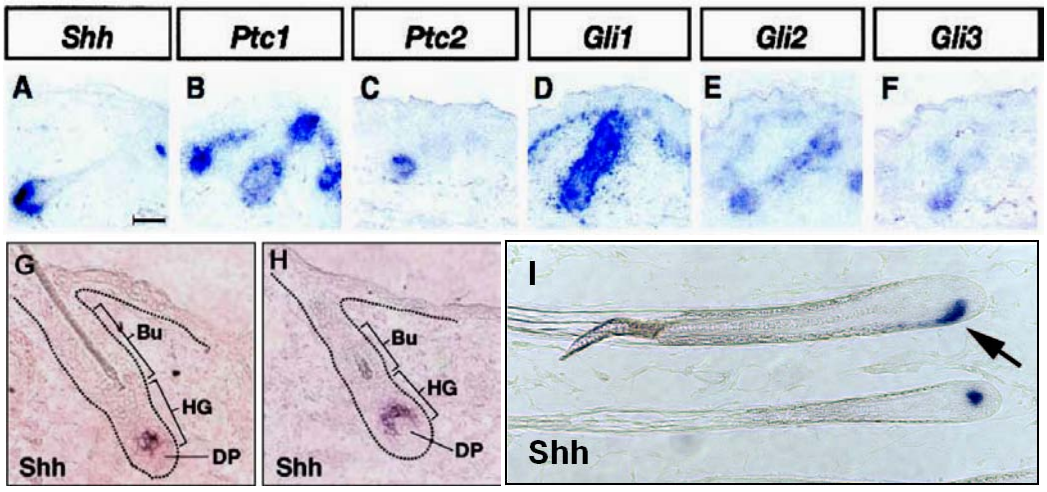

Figure 5: Expression pattern of Shh and Hh pathway components during HF morphogenesis and hair regeneration.
(A-F) Expression of Shh **(A)**, Ptch1 **(B)**, Ptch2 **(C)**, Gli1 **(D)**, Gli2 **(E)**, and Gli3 **(F)** at E18.5 in wild-type skin.
(G-H) Shh expression in the cyclic, adult HF during hair development**. (I)** Shh expression in late anagen HFs. Bulge (BU), hair germ (HG), dermal papilla (DP), (Mill et al., 2003; Blanpain and Fuchs, 2006 review; Levy et al., 2007).

3.4 Ihh signalling during epidermal development

Previous studies indicate that *Ihh* is expressed in differentiated sebocytes in murine and human skin (Niemann et al. 2003; Takeda et al., 2006; Lo Celso et al., 2008; Bonfanti et al., 2010). In addition, a nuclear accumulation of Gli1 was observed in undifferentiated sebocytes at the periphery of the SG (Fig. 6) (Niemann et al. 2003). *In vitro* studies also indicate increased amounts of Ihh protein in differentiated human sebocytes (SZ95 cell line) and a nuclear accumulation of Gli1 and Gli2 in undifferentiated sebocytes. This increase in Gli expression correlates with proliferation of undifferentiated cells (Niemann et al., 2003; Takeda et al., 2006; Lo Celso et al., 2008). The data suggest a paracrine mechanism of Ihh signalling in modulating proliferation of sebocyte progenitors *in vitro* (Niemann et al. 2003). More detailed analyses indicated that components of the Hh pathway including Ihh, Ptch1, Smo, Gli2 and Gli3 are up-regulated upon differentiation in human sebocytes (Sequaris et al., unpublished data). The up-regulation of a Gli reporter construct upon sebocytes differentiation shows that not only components of the Hh pathway but also Hh signalling activity increases during sebocyte differentiation (Sequaris et al., unpublished data).

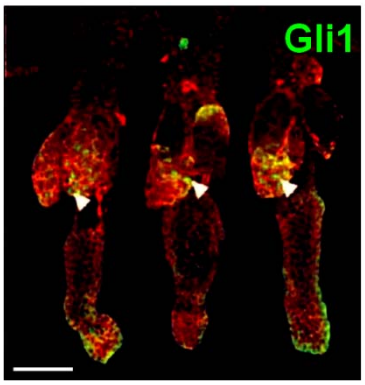

Figure 6: Expression of Gli1 in the SG of mouse skin.
Immunostaining for Gli1 protein (green) in whole mounts of wild type tail epidermis. Scale bars 50µl. (Niemann et al., 2003)

Gain and loss of function studies of components of the Hh pathway support the concept that Hh signalling plays an important role for SG differentiation (Table 1) (Niemann, 2009). For instance, ectopic activation of Hh signalling by overexpression of a gain-of-function mutant of the Smo receptor, *K5-SMOM2*, increases size and number of sebaceous glands (Fig. 7B) (Allen et al. 2003). In addition, constitutive *Gli2* expression in the basal layer of all epidermal compartments (*K5-Gli2*) induces formation of ectopic sebaceous ducts and highly branched SGs not only in association with HFs but also with the IFE (Fig. 7D) (Gu and Coulombe 2008). In contrast, inhibition of Hh signalling in the skin by a dominant-negative form of Gli2 (K5-Gli2ΔC4) leads to suppression of sebocyte development (Fig. 7C) (Allen et al. 2003). Taken together, these data led to the hypothesis that Ihh signalling could be an important mediator of sebocyte differentiation and SG formation in mammals.

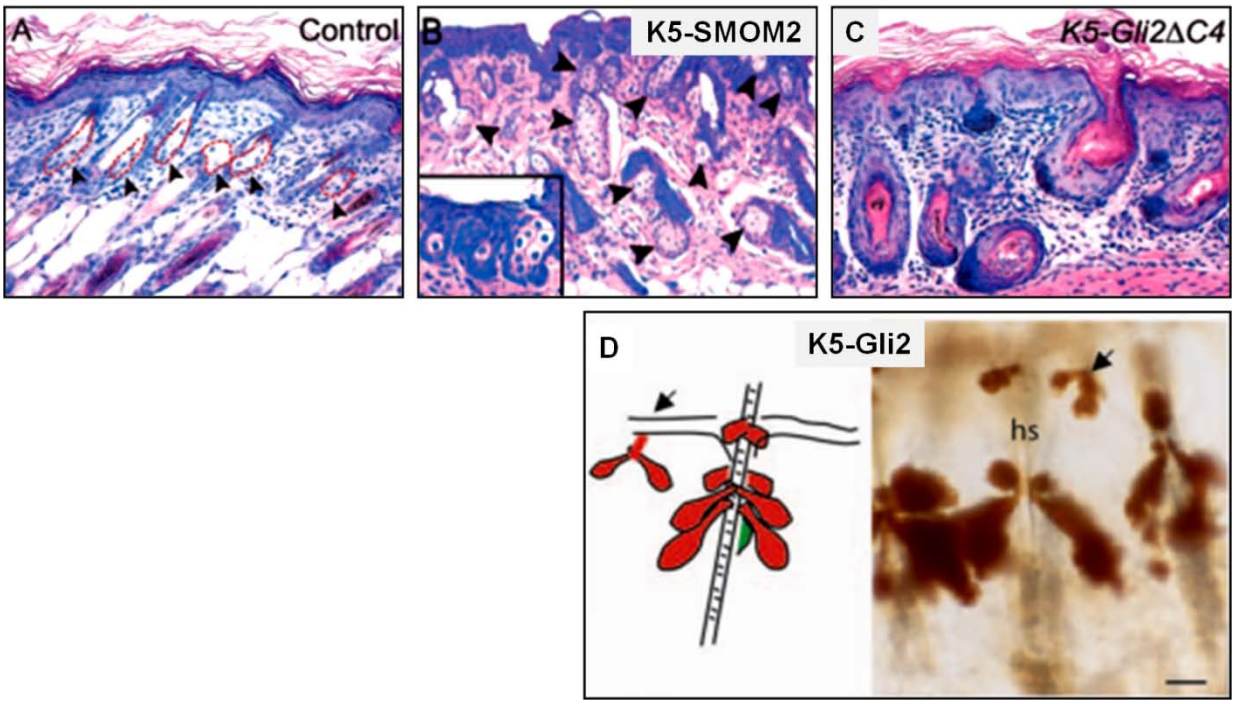

Figure 7: Modification of SG formation in transgenic mouse models.
(A) Wild type skin. The black arrows indicate HF associated SGs. **(B**) K5-SMOM2 transgenic (tg) mice expressing a constitutive active SMO mutant in keratinocytes, indicates increased number of SGs. **(C)** K5-Gli2ΔC4 tg mice with a constitutively expressed dominant-negative Gli2 allele in keratinocytes do not develop SG. **(D)** K5-Gli2 tg mice with constitutive expression of Gli2 develop prominent sebaceous ducts and additionally highly branched SGs (Allen et al. 2003; Gu and Coulombe 2008).

Table 1: Mouse models with Hh-dependent SG malformation

Mouse model	Tumour type	References
epidermal overexpression of *SMOM2* (*K5-SMOM2*)	increasing size and number of SG	Xie et al., 1998 Allen et al., 2003 Grachtchouk et al., 2003
epidermal overexpression of *Gli2* (*K5-Gli2*)	formation of ectopic of sebaceous duct and highly branched SG	Grachtchouk et al., 2000
epidermal expression of dominant-negative form of Gli2 (*K5-Gli2⊿C4*)	suppression of sebocyte development	Allen et al., 2003

3.5 Hh signalling in skin cancer

Aberrant regulation of the Hh pathway is implicated in several human developmental abnormalities and diseases including cancer. The first link between the Hh pathway and cancer was discovered in humans in 1992 (Gailani et al., 1992). Inherited loss of function mutations in the human *PTCH1* gene were identified as the underlying cause of the Nevoid Basal Cell Carcinoma Syndrome (NBCCS), also called Gorlin syndrome (Hahn et al., 1996; Johnson et al., 1996). The NBCCS causes developmental defects within different organs such as the nervous system, eyes, bones, endocrine system and skin. Also sporadic Basal Cell Carcinoma (BCC) are frequently caused by inactivating mutations in *PTCH1* or to a lesser extent, by activating mutations in *SMO*, both causing a constitutive activation of the Hh pathway (Hahn et al. 1996; Johnson et al. 1996; Gailani et al. 1996; Xie et al., 1998; Pasca di Magliano and Hebrok, 2003). BCC is the most common human cancer among Caucasians (Epstein, 2008 review). The main trigger of BCC is exposure of the skin to ultraviolet (UV) light. People with fair skin are especially at risk.

Many transgenic mouse models exist for BCC or BCC-like lesions. These include mice with reduced levels of Ptch1 (*Ptch*$^{+/-}$, Ptch fl/fl:K14, Ptch fl/fl:K6), an activated form of human *SMO* (K5-SMOM), epidermal overexpression of mouse *Shh* (K14-Shh), *Gli2* (*K5-Shh*) and mouse and human *Gli1* (*K5-Gli1; K14-GLI1*) mimic BCC or BCC like lesions (Table 2) (Goodrich et al., 1997, Hahn et al., 1998; Xie et al., 1998; Grachtchouk et al., 2003; Oro et al. 1997, Grachtchouk et al., 2000, Dahmane et al., 1997; Nilsson et al., 2000; Oro and Higgins, 2003).

In addition to BCC Hh pathway activity is also involved in the pathogenesis of other skin cancers including Squamous Cell Carcinoma (SCC) (Asplund et al., 2005; Snijders et al., 2005; Wakabayashi et al., 2007), Merkel cell carcinoma (Brunner et al., 2010), Basal Follicular Hamartoma (BFH) (Svärd et al., 2006), tumour of the follicular infundibulum (TFI) (Grachtchouk et al., 2011) and Sebaceous adenoma (Niemann et al., 2003).

Table 2: Mouse models with Hh-depending skin tumours

Mouse model	Tumour type	References
epidermal overexpression of *Shh* (*K14-Shh*)	BCC	Oro et al. 1997
Ptch inactivation (*Ptch* $^{+/-}$)	Basal follicular hamartoma, Medulloblastoma and other tumours	Goodrich et al., 1997 Hahn et al., 1998
Ptch conditional loss-of-function (*K14Cre ; Ptch*$^{fl/fl}$)	BCC	Siggins et al., 2009 Villani et al., 2010
epidermal overexpression of *SMOM2* (*K5-SMOM2*)	Basal follicular hamartoma	Xie et al., 1998 Grachtchouk et al., 2003
epidermal overexpression of *GLI1* (*K5-Gli1, K14-GLI1*)	BCC, trichoepithelioma	Dahmane et al., 1997 Nilsson et al., 2000 Oro & Higgins, 2003
epidermal overexpression of *Gli2* (*K5-Gli2*)	BCC	Grachtchouk et al., 2000
Sufu inactivation (*Sufu*$^{+/-}$)	Basal follicular hamartoma	Svärd et al., 2006

3.5.1 Hh signalling activity in sebaceous tumours

Mice expressing N-terminally truncated Lef1 (ΔNLef1), which blocks β-catenin signalling, in the basal layer of the epidermis (K14ΔNLef1 transgenics) develop spontaneous sebaceous tumours including sebaceous adenoma and sebeceoma (Niemann et al. 2002). In humans sebaceous tumours are relatively rare benign age-related tumours. Lesions are usually located on sun-damaged skin of the head and neck area (LeBoit, 2006). One third of human sebaceous tumours are associated with mutations in Lef1 which impair Lef1 binding to β-catenin (Takeda et al., 2006).

A previous study showed that treatment of K14ΔNLef1 transgenic mice with the carcinogen DMBA induced high frequencies of sebaceous tumours in those mice (Niemann et al., 2007). The ΔNLef1 mutant appears to act as tumour promoter by preventing accumulation of the tumour suppressor p53. Analysis of sebaceous tumours of K14ΔNLef1 transgenic mice revealed high expression of Ptch1 and Gli1. The increased Ptch1 RNA and protein levels and the nuclear localisation of Gli1 indicate that Hh signalling is activated in sebaceous tumours (Niemann et al., 2002, Niemann et al., 2003). Ihh is the prominent Hh ligand expressed in mature sebocytes of sebaceous tumours whereas no Shh and Dhh was detected. In human sebaceous adenoma high levels of IHH, PTCH1, GLI1 and GLI2 expression were also observed whereas SHH and DHH were not significantly expressed (Niemann et al., 2003). In contrast, Ihh protein was not detectable in Pliomatricomas which are benign skin tumours derived from the HF, indicating a specific function of Ihh during sebaceous tumour formation. Together these data suggest an involvement of Ihh signalling during epidermal lineage selection in normal skin and sebaceous tumours.

3.5.2 Hh signalling and p53

p53 is one of the most well known tumour suppressor genes in mammals. It is mutated in majority of human cancers (Vogelstein et al., 2000). Its importance can be explained by the fact that it acts as a transcriptional regulator in a number of processes, which protect the organism against cell damage and uncontrolled proliferation. Thus, it is involved in cell-cycle control, apoptosis and maintenance of genetic stability (Vogelstein et al., 2000; Vousden and Lane, 2007). Undamaged cells are characterised by low levels of p53 protein where it is efficiently ubiquitinilated and targeted for degradation by the proteasome. However upon hypoxia, radiation-induced DNA damage (UV, X-ray) and induction of proliferation, p53 protein degradation is blocked resulting in a fast accumulation of the protein. p53 acts mainly as a transcription factor controlling a large number of genes, including the cell cycle inhibitor *p21*, several DNA repair genes (*p53R2, XpC, XpG*,) and many regulators of apoptosis (*BAX, Bcl-2, Puma*) (Polager and Ginsberg, 2009; Weinberg, 2007).

Mutational analyses of p53 indicate that p53 is not a typical tumour suppressor gene. Surprisingly, p53 inactivation does not lead to lethality while the inactivation of most tumour suppressor genes has profound developmental defects and results in lethality. Mice lacking p53 (p53-/-) show largely normal development but have a shorter life span and develop cancer (lymphoma and sarcoma) before reaching 10 months of age (Jacks et al., 1994). A closer examination *Trp53* knockout mice (*p53*-/-) has however revealed that p53 negatively regulates proliferation and self-renewal of neural stem cells (Meletis et al, 2006). Recent studies on the production of induced pluripotent stem cells derived from somatic cells uncovered an even more general function of p53 in preventing cellular reprogramming and de-differentiation (Zhao and Xu, 2010, Puzio-Kuter and Levine, 2009). On the basis of these findings p53 has been suggested to contribute to the balance between tumour suppression and long-term cell proliferative potential, which is essential for the longevity of organisms with renewable tissues such as mammals (Vousden and Lane, 2007).

Recent studies indicate that, in particular for stem cell biology, Hh signalling is involved in regulating p53. In humans and mice the level of Gli1 is critical in maintaining neural stem cell number (Stecca and Ruiz i Altaba, 2009). In addition, downregulation of Gli1 activity limits brain tumour formation by reducing the number of cancer stem cells (Clement et al., 2007;

Stecca and Ruiz i Altaba, 2009). This regulation depends on the interaction between the p53 and Gli1. Mechanistically p53 blocks nuclear localisation, expression levels, and consequently the activity of Gli1. Conversely, Gli1 represses p53 thereby establishing a sensitive balance between p53 and Gli1. Furthermore it was shown that stimulation of cerebellar granular neural precursor cells (GNP) with Shh promotes the accumulation and activity of the p53 inhibitor Mdm2 (Malek et al., 2011). Studies in zebrafish also indicate that Shh signalling controls p53 activity, which is required for cell cycle exit of retinal cells and differentiation of photoreceptors (Prykhozhij, 2010).

Previous studies have shown that p53 nuclear accumulation is increased in papilloma and SCC of wild-type mice, when induced by oncogenic Ras (Vousden et al. 2002). Interestingly, in sebaceous tumours induced in K14ΔNLef1 transgenic mice the opposite trend was observed, nuclear p53 being significantly reduced (Niemann et al., 2007). Since in these tumours Ihh is up-regulated the question arises whether the unusual behaviour of p53 in sebaceous tumours is due to negative regulation by Hh signalling (Fig. 8).

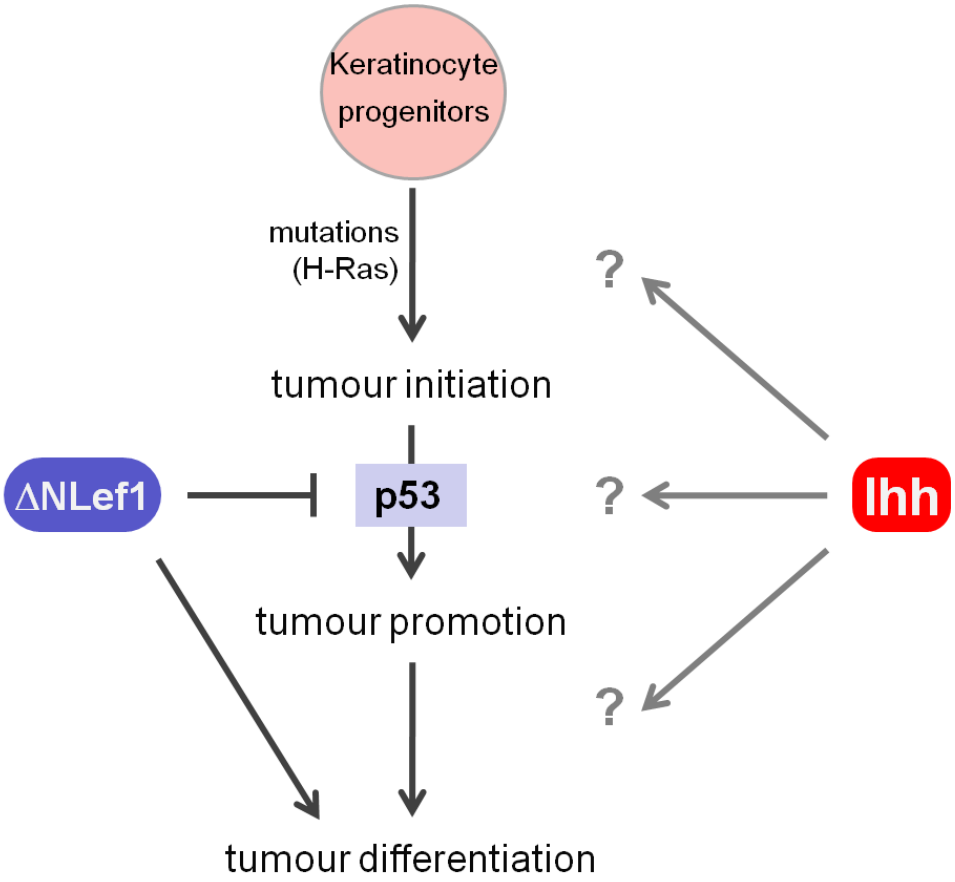

Figure 8: Schematic view of sebaceous tumour development.
The molecular mechanism which causes initiation of spontaneous sebaceous tumour in not clear yet, however chemical induction of H-Ras mutation is sufficient to induce sebaceous tumours in K14ΔNLef1 transgenic mice. The ΔNLef1 specifies tumor type and prevents accumulation of p53 by acting as a tumour promoter. The Ihh signal is proposed to be produced by differentiated sebocytes in the sebaceous tumours and is suggested to be involved in the differentiation process in sebaceous tumour.

3.6 Aims of this study

Many essential components of the Hh pathway, including the ligand Ihh, are expressed in mature sebocytes of SGs and sebaceous tumours in humans and mice. *In vitro* studies demonstrate that Ihh is involved in controlling differentiation and proliferation of sebocytes. However an *in vivo* function of Ihh for morphogenesis and homeostasis of the skin has not been identified yet. Therefore, the aims of this project are:

- Generation and analysis of an epidermis-specific KO mouse model for *Ihh*.

- Investigation of a potential function of Ihh signalling during skin development and epidermal homeostasis, focusing on sebocyte differentiation and SG formation

- Determining the consequences of loss of epidermal Ihh for sebaceous tumour formation, as well as for development and progression of squamous skin tumours.

- Unravelling the molecular mechanism of Ihh signalling in skin and skin tumours including an analysis of the relationship between Hh signalling and p53.

4 Materials and Methods

4.1 Materials

4.1.1 Chemicals, solvents, media and additives

Table 3: Chemicals and Reagents

Chemical	Supplier
Agarose (Star pure9	Starlab, Ahrensburg
Ampicillin	Fluka, Buchs, CH, Germany
Automation Buffer (10x)	GenTex Inc., Germany
Bovine Serum Albumin (BSA)	Sigma-Aldrich, Steinheim
BrdU (5-bromo-2'-deoxyuridine)	Sigma-Aldrich, Germany
Cholera toxin	Sigma-Aldrich, Germany
Collagen G	Biochrom AG
Complete Mini protease inhibitor	Roche, Mannheim
Deoxycholic Acid (DCA)	Fluka, Buchs, CH
Diamidino-2-phenylindol (DAPI)	Sigma-Aldrich, Steinheim
Diazabicycloloctan (DABCO)	Sigma-Aldrich, Steinheim
7,12-dimethylbenz-[*a*]-anthracene (DMBA)	Sigma-Aldrich, Steinheim
Dimethyl Sulfoxide (DMSO)	Sigma-Aldrich, Steinheim
Dithiothreitol (DTT)	Biochemika, Duesseldorf
D-MEM/Ham`s F12	Biochrome, Berlin, Germany
EDTA pH 8.0 (0.5M)	Gibco, Germany
Epidermal Growth Factor (EGF)	Biochrom, Berlin
Ethanol	Roth, Karlsruhe
Ethidium bromide	Amersham Biosciences, Uppsala, S
Ethylenediaminetetraacetic Acid (EDTA)	Roth, Karlsruhe
Fetal Calf Serum (FCS)	Biochrom, Berlin
Glycerol	Roth, Karlsruhe
Glycine	Roth, Karlsruhe

HEPES	Merck, Darmstadt
Hydrochloric acid (HCl)	Fluka, Buchs, CH
Isopropanol	Roth, Karlsruhe
Keratinocyte Growth Factor (KGF)	Biochrom, Berlin
Kanamycin	Fluka, Buchs, CH
MassRuler DNA Ladder, high range	Fermentas; Germany
MassRuler DNA Ladder, low range	Fermentas, Germany
Magnesium Chloride (MgCl2)	Sigma-Aldrich, Steinheim
Methanol	Roth, Karlsruhe
Milk powder	Heirler, Radolfzell
MOPS (10x)	Invitrogen, Karsruhe
Mowiol	Calbiochem, Darmstadt
Mitomycin C	Sigma, Aldrich Steinheim
Mowiol	Calbiochem
NaCl	Roth, Karlsruhe
Normal goat serum (NGS)	Sigma-Aldrich Steinheim
NuPAGE Antioxidant	Invitrogen, Karsruhe
NuPAGE LDS Sample Buffer	Invitrogen, Karsruhe
NuPAGE MOPS SDS Running Buffer	Invitrogen, Karsruhe
Optimem I	Invitrogen, Karlsruhe
Paraformaldehyde (PFA)	Merck, Darmstadt
Protease inhibitor cocktail tablets	Roche, Mannheim
PBS	Biochrom, Germany
PCR-Mastermix “Ready to load”	Bio-Budget, Germany
Penicillin/Streptomycin	Biochrom, Germany
Pertex	Leica, Germany
PFA	Merck, Darmstadt
Sebomed basal culture medium	Biochrom, Berlin
Sodium Dodecyl Sulfate (SDS)	Roth, Karlsruhe
Sodium chloride (NaCl)	Roth, Karlsruhe
Sodium hydroxide (5M NaOH)	Roth, Karlsruhe
SOC-Medium	Invitrogen, Karlsruhe
12-*O*-Tetradecanoylphorbol-13-acetat (TPA)	LC laboratories, USA

Transfer buffer	Invitrogen, Karlsruhe
Tris	Roth, Karlsruhe
TritonX-100	Merck, Darmstadt
Trypsin/EDTA	Biochrom, Berlin
Tween-20	Roth, Karlsruhe
Xylol	Roth, Karlsruhe

4.1.2 Kits, devices and accessories

Table 4: Kits	**Supplier**
Pierce BCA Protein Assay Kit	Pierce Biotechnology, USA
QIAGEN Plasmid Purification Mini Kit	Qiagen, Hilden
ECL Plus Western blotting detection reagent	GE Healthcare, Germany
DeadEnd™ Fluorometric TUNEL System	Promega, Germany

Table 5: Devices and accessories	**Supplier**
Cameras:	
Nikon eclips-E800	Nikon Instech Co, Japan
Nikon DMZ1200 camera	Nikon Instech Co, Japan
Olympus U-TB190, 8M14203	Olympus GmbH, Japan
Leica DM 4000B	Leica Microsystems, Germany
Leica JVC 3-Chip-Kamera KY-F75U	Leica Microsystems, Germany
Centrifuges	
Refrigerated Microcentrifuge, 5415 R	Eppendorf AG, Hamburg
Microcentrifuge, 5417 C	Eppendorf AG, Hamburg
Films	
Hyperfilm for Western Blots	Amersham, Biosciences, UK

Gel electrophoresis and blotting systems

NuPage Novex high-performance pre-cast gels	Invitrogen, Karlsruhe
XCell II, Blot Module	Invitrogen, Karlsruhe

Heating blocks

Eppendorf Thermomixer compact	Eppendorf AG, Hamburg

Incubators

Hereaus 6000 cell incubator	Kendro Laboratory Products, Germany

Photometer

BioPhotometer plus	Eppendorf AG, Hamburg

Others

BioDoc Analyze	Biometra
Curix 60 developer	AGFA; Belgian
ECL Hyperfilm	Fermentas
Eppendorf Thermomischer kompakt	Eppendorf AG, Hamburg
Loading dye blue 6x	Fermentas, St. Leon-Rot
MagicMark-XP	Invitrogen, Karlsruhe
MasterMix (2,5x) PCR Mix	Eppendorf AG, Hamburg
NuPAGE Novex 4-12% Bis-Tris Mini Gels	Invitrogen, Karlsruhe
PowerPac Universal	Biorad, Germany
PageRuler Plus Prestained	Fermentas, St. Leon-Rot
Pressure cooker (2100-Retriver)	Prestige Medical, France
SERVAGel TG10–Vertical,Tris-Glycine Gel	Serva, Germany
Westram Clear Signal nitrocellulose-Membrane Whatman	Inc, Stanford, USA
Whatman Gel Blot paper	Schleicher & Schuell, Dassel
Xcell II Blot module	Invitrogen, Karlsruhe
Xcell SureLock Mini-Cell	Invitrogen, Karlsruhe

4.1.3 Media, solutions and buffers

Phosphate buffered saline (PBS, Instamed), Biochrom, Berlin

10x TAE:

0.9M Tris Ultra
0.89M Boric acid
20mM EDTA
pH 0.8

1% Ripa buffer (western blot):

150mM NaCl
25mM Tris.HCL pH 7.5
1% sodium deoxycholate
1 % NP-40

➔ add 1 protease inhibitor cocktail tablet to 10ml WCE buffer
➔ after determination of protein concentration 1mM DTT was added

Whole cell extract (WCE) buffer (western blot):

20mM HEPES
0.42M NaCl
0.5% NP-40
0.5% DCA
25% glycerol
0.2mM EDTA
1.5mM MgCl2

➔ add 1 protease inhibitor cocktail tablet to 10ml WCE buffer
➔ after determination of protein concentration 1mM DTT was added

10x TBS (western blot):

0,2M Tris Base
2M NaCl
pH 7.6

1x TBS-T (western blot):

100ml 10x TBS
0.1% Tween
1M Tris-HCl 1M Tris Base
pH 7.5

➔ 1l ddH_2O

Blocking solution (western blot):

1x TBS-T
5% Milchpulver

Glycine strip (western blot):

0,1M Glycine
20% SDS
pH 2.5

1 x Tris glycine running buffer (western blot):

25mM Tris
190mM Glycine
10 % SDS

1 x Tris glycine transfer buffer (western blot):

25mM Tris
190mM Glycine
20 % Methanol

NuPAGE Invitrogen (western blot):

2µl NuPAGE Reducing agent (10x)
5µl NuPAGE LDL Sample Buffer (4x)
13µl Sample

➔ 20µl ddH_2O

5 x Laemmli loading dye (western blot):

60mM Tris.HCL pH 6.8
10% Glycerol
2% SDS
5% s-mercaptoethanol
0.01% bromophenol blue

TNE buffer lysis buffer:

40mM Tris
150mM NaCl
10mM EDTA
pH 7.4

Keratinocytes medium

DMEM/Ham's F12 medium (500ml)

Supplements:

100U/ml penicillin

100µg/ml streptomycin

1.8 x 10^{-4}M (16.6 mg) adenine

2mM L-Glutamine

0.5µg/ml (0.25 mg) hydrocortison

10ng/ml (5 µg) EGF

10^{-5}M cholera enerotoxin

5 µg/ml (2.5 mg) insulin

10 % FCS Gold (chelex-100 resin treated)

➔ FCS was treated with Chelex-100 resin overnight at RT, pH 7.0 and strained through a sterile filter prior to use

J2/3T3 fibroblast medium supplemented with:

DMEM
100U/ml penicillin
100µg/ml streptomycin
10 % FCS

Lysis buffer (isolation of gDNA):

0.2M NaCl
0.1M Tris HCl pH 8,5
5 µM EDTA
0.2% SDS
8.4 ml dH2O

➔ add 5U Proteinase K (20mg/ml) before use

Mowiol/DABKO:

4.8 g Mowiol
12 g Glycerin
12 ml H2O

➔ stirr 3 - 4 h
➔ add 24 ml 0.2 M Tris pH 8
➔ heat to 50 °C and stir overnight
➔ add 1.2 g DABKO (2,5%)

1M Tris-HCl:

1M Tris Base
pH 7.5

Blocking solution for BrdU-IF-staining on cells:

3g BSA
10ml FCS
5g Milk powder
10µl Tween-20

➔ 100ml 1x PBS

4.2 Mice

To generate epidermal specific *Ihh* knockout mice (*Ihh* EKO) (K14Cre+/-//*Ihh* fl/fl) homozygous mice carrying a floxed *Ihh* gene (*Ihh* fl/fl) (Razzaque et al., 2005) were crossed with mice expressing Cre-recombinase under control of the human Keratin 14 promoter (K14Cre+/-) (Hafner, et al. 2004). To generate triple mutant, homozygous *Ihh* EKO mice were crossed with K14ΔNLef1 transgenic mice (Niemann et al., 2002).

The *Ihh* floxed mice have been used in studies of the role of Ihh in other organs (Kobayashi et al., 2005; Lee et al., 2006; Mao et al., 2010; van Dop et al., 2010; Kosinski et al., 2010; Ochiai et al., 2010).

All mouse strains used were backcrossed or maintained on a C57BL/6 background.

In this study K14Cre+/-//*Ihh* fl/fl and *Ihh* fl/fl littermates were analysed for development of postnatal skin and were also used in two-stage carcinogenic tumour experiment.

The K14ΔNLef1 /K14Cre+/-//*Ihh* fl/fl and K14ΔNLef1/*Ihh* fl/fl were used for one-stage carcinogenic tumour experiment. For the number and genotype of animals which were used in this study see table 6, 7 and 8.

4.2.1 Tumour studies in K14ΔNLef1 transgenic mice

To induce sebaceous tumours, skin of 8-9 week old K14ΔNLef1/*Ihh* EKO and K14ΔNLef1 littermates were treated once with a sub-critical threshold dose of 7,12-dimethylbenz-[*a*]-anthracene (100nmol DMBA /200µl acetone) (DMBA, Sigma-Aldrich) or acetone vehicle. 4 weeks after topical DMBA application tumours develop. DMBA induces point mutations at different genes, including codon 61 of the proto-oncogene H-Ras (in K14ΔNLef1/*Ihh* EKO background). With special safety precautions the solution was applied onto the skin of the shaved back of anaesthetized mice. Scoring of tumours was carried out once a week for up to 50 weeks after tumour initiation. For the number and genotype of animals which were used in this study see table 7 and 8

4.2.2 Two-stage skin carcinogenesis experiment

To induce squamous tumours (papilloma and SCC) (Sundberg et al., 1997; Abel et al., 2009), skin of 8-9 week old *Ihh* EKO and *Ihh* fl/fl control littermates were treated once with a sub-critical threshold dose of 7,12-dimethylbenz-[*a*]-anthracene (100nmol DMBA /200µl acetone) (DMBA, Sigma-Aldrich) or acetone vehicle. One week later animals received the tumour promoter TPA (12-*O*-Tetradecanoylphorbol-13-acetat, LC Laboratories) (6nmol/200µl acetone, or acetone vehicle only, three times per week for 25 weeks. Under special safety precaution the solution was applied onto the skin of the shaved back of anaesthetized mice. Scoring of tumours was carried out one a week for up to 50 weeks after tumour initiation. For the number and genotype of animals which were used in this study see table 7 and 8

Table 6: Mice used in this studies

Genotype	number (n)	Treatment	Experiment
Ihh fl/fl	8-15 each stage	___	Studies for postnatal skin development (P0-P10)
K14Cre+/-//Ihh fl/fl	8-15 each stage	___	

Table 7: Mice used in this studies, first set of tumour experiment

Genotype	number (n)	Treatment	Experiment
Ihh fl/fl	19	DMBA/TPA	Two-stage carcinogenic experiment
K14Cre+/-//Ihh fl/fl	20	DMBA/TPA	Two-stage carcinogenic experiment
K14Cre+/-//Ihh fl/fl	5	TPA/Acetone	Two-stage carcinogenic experiment
Ihh fl/fl	4	DMBA/Acetone	Two-stage carcinogenic experiment
K14Cre+/-//Ihh fl/fl	5	DMBA/Acetone	Two-stage carcinogenic experiment
K14ΔNLef1/hh fl/fl	17	DMBA	One-stage carcinogenic experiment
K14ΔNLef1/K14Cre+/-//Ihh fl/fl	19	DMBA	One-stage carcinogenic experiment
K14ΔNLef1/hh fl/fl	4	Acetone	One-stage carcinogenic experiment
K14ΔNLef1/K14Cre+/-//Ihh fl/fl	5	Acetone	One-stage carcinogenic experiment

Table 8: Mice used in this studies, second set of tumour experiment

Genotype	number (n)	Treatment	Experiment
Ihh fl/fl	31	DMBA/TPA	Two-stage carcinogenic experiment
K14Cre+/-//Ihh fl/fl	33	DMBA/TPA	Two-stage carcinogenic experiment
K14ΔNLef1/hh fl/fl	17	DMBA	One-stage carcinogenic experiment
K14ΔNLef1/K14Cre+/-//Ihh fl/fl	17	DMBA	One-stage carcinogenic experiment

4.3 Molecular Biology

Standard methods of molecular biology were performed according to Sambrook and Russell (Sambrook and Russell, 2001; Celis, 2006) unless stated otherwise.

4.3.1 Genotyping and efficiency of deletion

Genotyping was performed by PCR on DNA extracted from tail biopsies using customised primers. PCR analysis on genomic DNA from split epidermis was performed to determine the efficiency of deletion of the floxed region in *Ihh* locus in the presence of keratin 14-driven Cre.

4.3.2 Isolation of genomic DNA (gDNA)

Tail biopsies of 3-week of mice were incubated in lysis buffer containing 0.2M NaCl, 0.1M Tris/HCl, PH8,5; 5µM EDTA; 0,2% SDS and 100µg/ml proteinase K (Sigma [39U/mg]) for 2-3 hours at 55°C. After a centrifugation step, 2 volumes isopropylalcohol were added to the supernatant to precipitate gDNA. 150µl H2O (DNase free) was added to the pellet and subsequently, gDNA was dissolved O/N at RT.

4.3.3 Polymerase Chain Reaction (PCR) for genotyping

PCR (Mullis et al., 1987; Saiki et al., 1988) was used to amplify DNA fragments and genotype mice for the presence of floxed alleles and/or transgenes with customized primers listed in Table 9.

All amplifications were performed in a total reaction volume of 25µl, containing a minimum of 50ng template DNA, 5-25pmol of each primer, 25µM dNTPs Mix, 1U of RedTaq DNA-polymerase and 1xRedTaq Reaction buffer. For genotyping Eppendorf MasterMix and RedTaq ReadyMix PCR kit with MgCl2 (Sigma) was used.

Standard PCR programs started with 5-8min denaturation at 95°C, followed by 30-32 cycles consisting of denaturation at 94°C for 30sec, annealing at oligonucleotide-specific temperatures for 30-60 sec and elongation at 72°C for 30-45 sec and a final elongation step at 72°C for 5-10 min. Based on the number of specific nucleotides in the primer, the following formula was used to estimate the melting temperature of primers: Tm=2(A+T)+4(G+C). All PCR reactions carried out either in T-Gradient Thermocyler or Personal Thermocycler (Biometra). PCR amplification products were analysed by agarose gel electrophoresis. PCR-amplified DNA fragments were applied to 2% (w/v) agarose gels (1x TAE electrophoresis buffer, 0.5mg/ml ethidium bromide) and electrophoresed at 120-200V.

Table9: Oligonucleotides used for genotyping

Mouse strain	Primer	Oligonucleotide (5´➔3´)	T-Annealing [°C]
Ihh floxed	fllhh-for-Lanske	5´-AGC ACC TTT TTT CTC GAC TGC CTG-3´	68
(Razzaque et al., 2005)	fllhh-rev-Lanske	5´-TGT TAG GCC GAG AGG GAT TTC GTG-3´	68
K14Cre	SC1-for	5´-GTC CAA TTT ACT GAC CGT ACA C-3´	59
(Hafner, et al., 2004)	SC3 -rev	5´-CTG TCA CTT GGT CGT GGC AGC-3´	59
K14ΔNLef1	dNLef1-for	5´-TGT CCC TTG TAT CAC CAT GGA CC-3´	49
(Niemann et al., 2002)	dNLef1-for	5´-CCA AAG ATG ACT TGA TGT CGG CT -3´	49

All primer sequences are displayed in 5´➔-3' order. Primer orientation is designated "sense" when coinciding with transcriptional direction. All primers were purchased from MWG, Germany.

4.3.4 PCR anaylsis for efficiency of deletion

PCR analyses were performed to amplify DNA fragment and genotype mice for the deletion of exon1 in floxed alleles to examine the Cre activity and its specific expression in the skin of *Ihh* EKO mice with customised primers listed in Table 10.

All amplifications were performed in a total reaction volume of 25µl, containing a minimum of 50ng template DNA, 5-10pmol of each primer, 25µM dNTPs Mix, 1U of RedTaq DNA-polymerase and 1xRedTaq Reaction buffer. For deletion PCRs, RedTaq ReadyMix PCR kit with MgCl2 (Sigma) was used.

Standard PCR programs started with 4 min denaturation at 95°C, followed by 30 cycles consisting of denaturation at 95°C for 30 sec, annealing at oligonucleotide-specific temperatures (68°C) for 45 sec and elongation at 72°C for 80 sec and a final elongation step at 72°C for 7 min. PCR reactions carried out either in T-Gradient Thermocyler or Personal Thermocycler (Biometra). PCR amplification products were analysed by agarose gel electrophoresis. PCR-amplified DNA fragments were applied to 1% - 3% (w/v) agarose gels (1 x TAE electrophoresis buffer, 0.5mg/ml ethidium bromide) and electrophoresed at 120-200V.

Table10: Oligonucleotides used in PCR analysis for efficiency of deletion

Mouse strain	Primer	Oligonucleotide (5´➔3´)	T-Annealing [°C]
K14Cre/Ihh fl/fl	PK-Ihh-for-1-20	5´-CCG CAG ACG GCA GCA GCT CC-3´	68
	PK-Ihh-For-56-77	5´-TGC TAA CCG CGG GTC CCT TCA G-3´	68
	fllhh-rev-Lanske	5´-TGT TAG GCC GAG AGG GAT TTC GTG-3´	68

All primer sequences are displayed in 5´➔-3' order. Primer orientation is designated "sense" when coinciding with transcriptional direction. All primers were purchased from MWG, Germany.

4.3.5 DNA sequencing

Genomic DNA was sequenced for *Ihh* exon1 deletion using an ABI Big dye terminator sequencing Kit (Applied Biosystems) according to the manufacturer's instructions. The fluorescently labelled DNA was analysed with an ABI Prism3730 DNA analyser (Applied Biosystems).

4.4 Protein biochemical methods

4.4.1 Protein extraction from skin and skin tumours

Skin or tumour tissue were lysed in 1-3ml of 1x Ripa lysis buffer supplemented with Complete Mini protease inhibitor cocktail (Roch) (10ml 1x Ripa buffer 1 tablet of Complete Mini

protease inhibitor). Skin and tumour lysates were generated by homogenising the tissue by a mixer mill (Qiagen) for 3-5 min at 30Hz. Lysates were incubated for 30 min on ice followed by 30 min centrifugation at 13.500rpm, 4°C. The supernatants containing protein were transferred into new eppendorf tubes and after addition of DTT stored at -80°C and -20°C.

4.4.2 Protein quantification by Biuret protein assay

The protein concentration of the lysates was quantified by the bicinchoninic acid (BCA) method using the Pierce BCA Protein Assay Kit (Pierce Biotechnology, Rockford USA) according to the manufacturer's instructions. This method is based on a two step detection system. In alkaline environment proteins form complexes with Cu2+ ions there by reducing them to Cu1+ ions (biuret method). Subsequently the reduced Cu1+ ions form a soluble purple complex with bicinchoninic acid (BCA) that has a maximal absorbance at 562nm. For the quantification of the protein concentration, samples were diluted 1:10. Applying the protocol, 10µl of the diluted sample as well as 10µl of eight BSA samples with known concentrations (0, 25, 125, 250, 500, 750, 1000, 1500 up to 2000µg/ml) for the standard curve were incubated with 200µl supplied BCA-working solution and incubated for 30 min at 37°C in 96 well plates (TPP, Trasadingen, CH). The absorbance of the reaction product was measured by an Immuno Reader NJ-2000 (InterMed Inc., Cambridge USA) at 578nm. Each lysate was quantified as triplicates. The standard curve was made by plotting the absorbance of the BSA standards against their concentration (Fig. 9). The resulting equation of the standard curve was then used to calculate the unknown protein concentrations of the analysed samples.

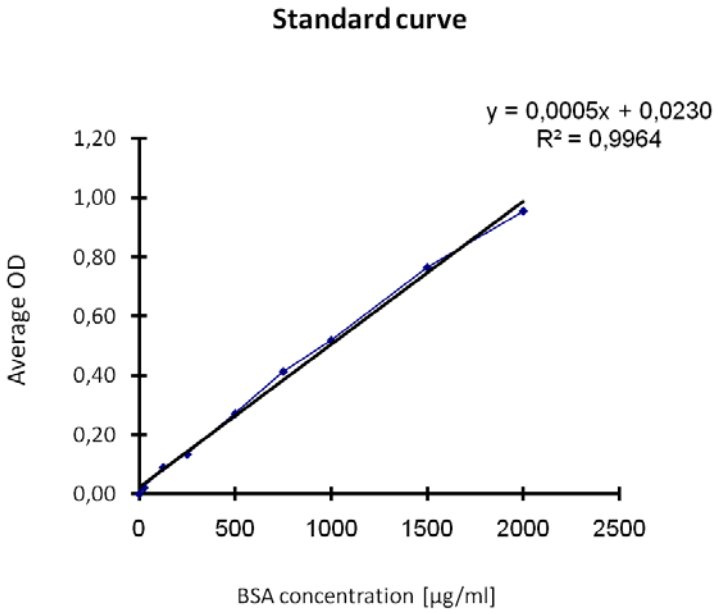

Figure 9: Standard curve for determining unknown protein concentrations.
Absorbance of BSA standards was plotted against their concentration. The corresponding linear equation was used to calculate the protein concentration in the samples.

4.4.3 SDS-polyacrylamide-gel-electrophoresis (SDS-PAGE)

Denaturised proteins were separated according to molecular mass via SDS polyacrylamide-gelelectrophoresis (Laemmli, 1970). Samples were dissolved in 1x SDS-sample buffer (NuPAGE Invitrogen or Laemmli Loading Dye) incubated for 5 min at 92°C. 2-20µg of protein was loaded on the gels, which were separated at 200V per gel for an appropriate time (60-80min) in 1xSDS running buffer (1x MOPS Running Buffer with 500µl NuPAGE Antioxidant). Depending on the molecular mass of the proteins of interest, commercially available gels 4-12% acrylamid and gradient gels (4-12% gradient Bis-Tris Gels, Invitrogen) were used. In addition, 5µl PageRuler Plus Prestained Plus and 2µl and MagicMark XP were applied.
The gel is then used for protein transfer to a nitrocellulose membrane.

4.4.4 Western blot analysis (WB)

Western blot analysis is a method for detection of particular proteins using antibodies that are specific for the target protein. For this purpose, separated proteins were transferred to a methanol-activated nitrocellulose membrane "Westran Clear Signal PVDF membrane", using a wet electorblot apparatus (Xcell Surelock Mini-Cell, Invitrogen, Karlsruhe) and commercially available 1x transfer buffer (Invitrogen). PVDF membrane was equilibrated 5min in methanol and subsequently 5-10 min in transfer buffer. Protein transfer was executed at 30V for 60-80 min. Non-specific binding sites of the membrane were blocked for 1-2 h at RT either with 5% milk powder /1xTBS-T for both p53 and SCD1. In order to detect p53 and SCD1, total protein levels were incubated at O/N at 4°C with primary antibody (Table 11) diluted in 5% milk powder/1xTBS-T. After three 10 min wash steps in 1xTBS-T the membranes were incubated for 1-2h with the appropriate horseradish peroxidase (HRP) conjugated lgG secondary antibody (Table 12), also diluted in 5% milk powder/1xTBS-T. After washing the membrane again three times for 10min in 1x TBS-T immuno-reactive proteins were visualised using ECL Plus Western blotting detection reagent (GE Healthcare) according to the manufacturer's instructions and exposing the blot to ECL Hyperfilm. This detection system is based on the chemoluminescent oxidation of luminal catalysed by the peroxidase reaction in the presence of peroxide. Detection was repeated with different exposure times.

4.4.5 Membrane stripping to detect housekeeping proteins

To control if equal amounts of protein were blotted, detection of an endogenous loading control (here: α tubulin or GAP-DH) was performed. In order to reprobe the membrane it was incubated with glycine-strip for 1h at RT on shaker. Then it was washed two times in TBS-T to detach the previously bound antibodies. Afterwards, the membrane was washed and incubated in 1M Tris HCl for 10min. After three wash steps for 10min in TBS-T the protein detection was performed escribed in (4.3.5).

Quantification of the bands was performed by selecting the area, means gray value and integrated density functions of the ImageJ software (http://rsb.info.nih.gov/nih-image),

on a grayscale picture. To obtain the relative signal intensity for each test sample band, the intensity values were divided to their respective GPA-DH or α-Tubulin band values.

Table 11: Primary antibodies used for WB

Antibody	Host	Dilution	Reference
SCD1 (S-15)	goat	1:400	Santa Cruz
p53	mouse IgG1	1:1000	Cell Signaling
GAP-DH	rabbit	1:3000	Abcam
a-Tubulin	mouse IgG1	1:5000	Merck

Table 12: Secondary antibodies used for WB

Antibody	Dilution	Reference
HRP-conjugated anti-goat IgG	1:2500	GE Healthcare
HRP-conjugated anti-mouse IgG	1:4000	GE Healthcare
HRP-conjugated anti-rabbit IgG	1:3000	GE Healthcare

4.5 Tissue Analysis

Mice were sacrificed and tail and back skin or tumour tissue was dissected as described previously (Paus et al., 1999). 1h before sacrifice, all mice received a single IP injection of 100-150mg/kg BrdU (Owen and Watt, 2001). Skin tumours and dorsal skin sections were harvested. Tissue was either fixed directly in 4% formaldehyde 2h at RT for paraffin embedding or stored at -80°C embedded in tissue Tec OCT (tissue freezing medium, Sakura) to perform cyrosections. Additionally, samples were directly transferred into liquid nitrogen for RNA or protein analysis. For the number and genotype of animals which were used in this study see table 12.

4.5.1 Preparation of whole mount tail skin (WM)

Whole mounts of mouse tail epidermis (WM) were prepared as previously described (Braun et al., 2003; Niemann et al., 2003). Briefly, whole skin was removed from the tail of mice and incubated for 1-4h at 37°C in freshly prepared 5mM EDTA/1xPBS. The epidermis was then separated from the dermis and fixed in 3.4% formaldehyde for 2h at RT. Fixed whole mounts were stored in 1x PBC at 4°C or stained.

4.5.2 Isolation and cultivation of primary keratinocytes

Primary keratinocytes were isolated from the epidermis of wild-type and *Ihh* EKO littermates at postnatal day 1-3 (P1-P3). The skin of these mice was harvested and incubated overnight, floating on dermis side down, in 0.25 % Trypsin/EDTA at 4°C. On the next day the epidermis was separated from dermis using forceps (Rheinwald and Green, 1975; Rheinwald, 1989; Watt, 1994). The epidermis was comminute using scalpels and incubated for 1h at 37°C in DMEM/Ham's F12 in thermocycler. Finally the epidermal cells were seeded onto collagen I coated 6-well plates. In order to provide optimal support for the isolated primary keratinocytes, they were co-cultured with mitomycin c pretreated fibroblasts. J2/3T3 fibroblast was cultured in fibroblast medium (4.1.3) at 37°C and 5% CO_2. Therefore fibroblasts were seeded out onto collagen I coated 6-well plates and treated with mitomycin c for 2-3 h at 37 °C. In order to remove mitomycin c, fibroblasts were washed twice with PBS after incubation. Isolated primary keratinocytes were co-cultured in DMEM/HAM´s F12 keratinocyte medium (4.1.3) at 32°C and 5% CO2.

4.5.3 Passaging of primary keratinocytes

Medium was changed every 2 days. When keratinocytes reached confluency of 80-90% cells were washed with 1x PBS/0.02% EDTA at RT for 5min and incubated with 0.05% (v/w) tyrupsin/0.02% (v/w) EDTA (Gibco/Invitrogen) at 37°C until the cells detached (2-5min).

After centrifugation for 5min at 700rpm, cells were reseeded onto collagen G coated 6 cm dishes, without fibroblasts, to retain only keratinocytes for further cultivation. This collagen G coated culture dishes were prepared before using 40µg/ml collagen G diluted in 1xPBS. Culture dishes were incubated with 4 ml of collagen G/PBS at 4 °C overnight and washed twice with 1x PBS prior use.

4.5.4 Determination of cell number by CASY Counter

Cell numbers were determined by a CASY cell counter. 100µl cell suspension was diluted in 10ml of an electrolyte buffer (CASYton) and aspirated through a precision measuring capillary with a defined size. In the measuring capillary the cells were scanned with a frequency of $1x10^6$ measurements per second. This procedure uses a low voltage field, produced between two platinum electrodes that are traversed by the cells, thus producing electric signals. These signals are analysed by amplitude, pulse, width, course of time and resulting pulse area. Thereby, it is possible to simultaneously separate cell debris, viable cells, dead cells and cell aggregates.

4.6. Histological analysis

4.6.1 Sectioning

Sections of formalin-fixed (4% Formalin, 2h, RT and in 70% ethanol O/N) and paraffin-embedded back skin and tumour tissue (5-10µm) were dehydrated. Subsequently, haematoxylin-eosin (H&E) staining (4.5.3) was performed according to the standard protocols (4.5.2). Skin or tumour section (4-7µm) of OCT-embedded frozen tissue were fixed with 1-4% (w/v) PFA/PBS or acetone, respectively depending on the antibody used in the experiment, and subjected for further immunofluorescent analyses.

4.6.2 Deparaffining of paraffin sections

In order to remove paraffin from tissue sections, paraffin sections of back skin or tumours were incubated twice in xylol for 10min and 15min. Slides were incubated in a series of ethanol solutions with 100%, 90%, 70% and 50% ethanol for 5 min. Sections were rehydrated in ddH_2O and tap water different staining methods were performed as described in the following chapter.

4.6.3 Haematoxylin-Eosin (H&E) staining

Back skin sections were incubated for 2 min in hematoxylin, followed by an incubation step of 3 min in dH_2O. Then sections were incubated for 10 sec in eosin, followed by short incubations in: 70 % ethanol, 95 % ethanol, isopropanol and xylol. Skin sections were mounted with Pertex

4.6.4 Immunofluorescence (IF)

4.6.4.1 IF staining with Paraffin embedded sections

Sections of back skin or tumours were unmasked for 40-45min in a steamer (2100-Retriver) under pressure at 121°C using the antigen retrieval solutions:

Demasking buffer

10x buffers, target retrieval solution (Dako real) for BrdU staining
10x R-buffer, (Electron Microscopy Science) for P53 staining
10x citrate buffer, target retrieval solution (Dako) for all other staining

Subsequently, the sections were washed for 5 min with 1x PBS and blocked with 10% serum derived from the species from which the secondary antibody was purified or in 0.25% FGS. The sections were incubated for 1-2h at RT in a humidified chamber. After washing the

samples with 1x PBS the slides were incubated in a humidified chamber O/N with the primary antibody (Table 10) diluted in blocking solution. After washing in PBS, the slides were incubated with the secondary antibody coupled to Alexa-488 or Alexa-594 (Table 11) diluted in blocking solutions. Nuclei were counterstained using propidium iodide (PI) or DAPI (Sigma Aldrich). After a final washing, the slides were mounted with Mowiol/DABKO and stored at 4°C in the dark.

4.6.4.2 IF staining of frozen sections

Skin or tumour was removed from the dorsal region of mice and immediately embedded in OCT mounting media and placed on dry ice for cryo-sectioning. The cryo-sections (4-7µm) were fixed with 1-4% (w/v) PFA/PBS or ice-cold acetone for 5-10 min at RT or in -20°C, respectively depending on the antibody used in the experiment. Tissue were blocked in 1xPBS containing 1-2% BSA or 0.25 fish skin gelatin (FSG) and in case for 1-2h in a humidified chamber. After washing with blocking solution the slides were incubated with the primary antibody (Table 10) diluted in blocking solution O/N at 4°C in a humidified chamber. After washing in 1x PBS the slides were incubated with the secondary antibody coupled to Alexa-488 or Alexa-594 (Table 11) for 1-2h diluted in blocking solution. Nuclei were counterstained using PI or DAPI (Sigma Aldrich). After a final washing, the slides were mounted with Mowiol/DABKO and stored at 4°C in the dark.

4.6.4.3 IF staining using anti-Lrig antibody

For immunofluorescent staining the cryo-sections (4-7µm) were fixed with 2% (w/v) PFA/PBS 15 min at RT, respectively depending on the antibody used in the experiment. Tissue were blocked in 1xPBS containing (2% BSA, 0.5%FSG, 0.1%Tx100) for 2-3h in a humidified chamber. After washing with blocking solution the slides were incubated with primary antibody (Table 10) 1:50 diluted in blocking solution (2% BSA, 0.5%FSG, 0.1%Tx100 in 1x PBS) O/N at 4°C in a humidified chamber. After washing in 1x PBS the slides were incubated with the secondary antibody coupled to Alexa-488 (Table 11) diluted 1:1000 in blocking solution for 1-2h at RT.

Nuclei were counterstained using DAPI (Sigma Aldrich). After a final washing with PBS followed with ddH_2O, the slides were mounted with Mowiol/DABKO and stored at 4°C in the dark.

4.6.4.4 IF staining using anti-Plet1 and -SCD1 antibody

For immunofluorescent staining cryo-sections (4-7µm) were immediately blocked in 0.25% FGA/PBS for 2h in a humidified chamber at RT. After washing with 1x PBS the slides were incubated with the first primary antibody anti-Scd1-S15(Table 10) diluted 1:100 in blocking solution O/N at 4°C in a humidified chamber. After washing in 1x PBS the slides were incubated with the first secondary antibody coupled to Alexa-594 (Table 11) diluted 1:500 in blocking solution for 1-2h at RT, followed by three time PBS washing and were fixed with 4% (w/v) PFA/PBS for 5min at RT. After washing with 1x PBS tissue were blocked in 1% BSA/PBS in 15min RT in a humidified chamber. After washing with PBS the slides were incubated with the second primary antibody anti-Plet1 (Table 10) 1:5 diluted in blocking solution (1% BSA/PBS) for 5h in RT. After washing in 1x PBS the slides were incubated with the second secondary antibody coupled to Alexa-488 (Table 11) diluted 1:500 in blocking solution for 1h at RT. Nuclei were counterstained using DAPI (Sigma Aldrich). After a final washing with PBS followed with ddH_2O, the slides were mounted with Mowiol/DABKO and stored at 4°C in the dark.

4.6.4.5 IF staining of paraffin sections using anti-K6a and -SCD1 antibodies

The paraffin-embedded back skin and tumour tissue (5-10µm) were dehydrated and unmasked for 40-45min in steamer (2100-Retriver) at 121°C using the antigen retrieval (Dako real). After washing with PBS slides were blocked in 0.25% FGS/PBS for 2h in a humidified chamber at RT. After washing with 1x PBS the slides were incubated with the first primary anti- SCD1-S15 antibody (Table 13) diluted 1:100 in blocking solution O/N at 4°C in a humidified chamber. The next day, after washing in PBS the slides were incubated with the a

cocktail of first secondary antibody coupled to Alexa-488 (Table 14) diluted 1:750 and second primary antibody anti-K6a (Table 13) dilute 1:400 in blocking solution O/N at 4°C. Next day after washing in PBS the slides were incubated with the second secondary antibody coupled to Alexa-594 (Table 11) for 1h diluted 1:500 in blocking solutions. Nuclei were counterstained using DAPI (Sigma Aldrich). After a final washing with PBS followed with ddH_2O, the slides were mounted with Mowiol/DABKO and stored at 4°C in the dark.

4.6.4.6 IF staining of paraffin sections using anti-BrdU and -K14 antibody

The paraffin-embedded back skin and tumour tissue (5-10µm) were dehydrated and unmasked for 40-45min in steamer (2100-Retriver) at 121°C using the antigen retrieval (Dako real). After washing with PBS slieds were blocked in 10% NGS/PBS for 2h in a humidified chamber at RT. After washing with 1x PBS the slides were incubated with the first primary anti-BrdU antibody (Table 13) diluted 1:10 in blocking solution O/N at 4°C in a humidified chamber. After washing in 1x PBS the slides were incubated with the a cocktail of first secondary antibody coupled to Alexa-488 lgG1 (Table 14) diluted 1:1000 and second primary antibody anti-K14 (Table 13) dilutet 1:2000 in blocking solution for 2h at RT, followed by three time PBS washing. After washing in 1x PBS the slides were incubated with the second secondary antibody coupled to Alexa-594 (Table 11) for 1h diluted 1:500 in blocking solution. Nuclei were counterstained using DAPI (Sigma Aldrich). After a final washing with PBS followed with ddH_2O, the slides were mounted with Mowiol/DABKO and stored at 4°C in the dark.

4.6.4.7 IF staining of paraffin sections using anti-BrdU and –K6 antibody

The paraffin-embedded back skin and tumour tissue (5-10µm) were dehydrated and unmasked for 40-45min in steamer (2100-Retriver) at 121°C using the antigen retrieval (Dako real). After washing with PBS slides were blocked in 10% NGS/PBS for 2h in a humidified chamber at RT. After washing with 1x PBS the slides were incubated with the first primary anti-BrdU antibody (Table 13) diluted 1:10 in blocking solution O/N at 4°C in a humidified

chamber. After washing in 1x PBS the slides were incubated with the a cocktail of first secondary antibody coupled to Alexa-488 lgG1 (Table 14) diluted 1:1000 and second primary antibody anti-K6a (Table 13) dilute 1:600 in blocking solution for 2h at RT, followed by three time PBS washing. After washing in 1x PBS the slides were incubated with the second secondary antibody coupled to Alexa-594 (Table 11) for 1h diluted 1:500 in blocking solution. Nuclei were counterstained using DAPI (Sigma Aldrich). After a final washing with PBS followed with ddH_2O, the slides were mounted with Mowiol/DABKO and stored at 4°C in the dark.

4.6.4.8 IF staining of Whole Mount (WM) tissue

Fixed epidermal sheets were blocked for 1h with buffer containing 0.5% milk powder, 0.25%FGS and 0.5% TritonX-100 in TBS-WM (0,9% NaCl, 20mM HEPS, PH7.2) (Braun et al., 2003). Following O/N incubation with primary antibodies at RT (gentle agitation), WMs were washed with 0.2% Tween-20/PBS for 4h. Secondary antibodies were then applied O/N at RT and washing steps were repeated for 4h. Epidermal sheets were rinsed with ddH_2O before mounting with Mowiol/DABKO and stored at 4°C in the dark.

4.6.4.9 IF staining of cells

For immunofluorescent staining cells were seeded overnight on cover slips, washed with 1x PBS and fixed with 4% PFA/PBS 5min. To remove the PFA cells were washed again in 1x PBS and treated with 0.2-0.5% Triton X-100 detergent in 1x PBS for 2-10min at RT and antibodies gain access into the cells. Afterwards, cells were blocked in with 10% serum derived from the species from which the secondary antibody was taken or in 0.25% FGS or 1% BSA for 1h at RT dependent on staining. Then were incubated with primary antibody (Table 13) diluted in blocking solution for 2h at RT or O/N at 4°C. After this first incubation, the cells were washed three times with 1x PBS and incubated again for 1h at RT with the appropriate secondary antibody (Table 14) followed by three washing steps in 1x PBS alone and one wash step in

ddH_2O. Nuclei were counterstained using PI or DAPI (Sigma Aldrich). After a final washing, the slides were mounted with Mowiol/DABKO and stored at 4°C in the dark.

4.6.4.10 IF staining of cells with anti-BrdU antibody

For immunofluorescent staining cells were seeded overnight on cover slips, washed with 1x PBS and incubate with keratinocytes medium which contain 1:100 or 1:200 BrdU (16mg/ml in H_2O) for 1h at at 37°C and 5% CO_2. Further cells were washed three time with 1x PBS and fixed with 4% PFA/PBS 10min at RT. To remove the PFA, cells were washed again three time with 1x PBS and treated with solution containing 2N HCl and 0.5% Triton X-100/PBS detergent for 10min at 37°C followed by two time 1x PBS wash step. Afterwards, cells were blocked in with blocking solution (4.1.3) for 30-60 min at RT then washed again with 1x PBS. Then cells were incubated with primary antibody (Table 13) 1:25 diluted in 1%BSA/PBS auf shaker for 45min at RT. After this first incubation, the cells were washed five times and incubated again for 30min at RT with the appropriate secondary antibody (Table 14) 1:500 dilution in blocking solution followed by five washing steps in with 0.01% Tween-20/PBS and one wash step in ddH_2O. Nuclei were counterstained using PI or DAPI (Sigma Aldrich). After a final washing, the slides were mounted with Mowiol/DABKO and stored at 4°C in the dark.

4.6.4.11 TUNEL assay

DeadEnd™ Fluorometric TUNEL System was used for TUNEL-assy. Cells were fixed in 4% formaldehyde in PBS for 25 min at 4°C. The slides were washed twice in PBS, 5 min each time and premeabilised in 0.2% Triton-X-100/PBS for 5 min. Slides were washed twice in PBS, 5 minutes each time. Further, cells were equilibrated with 100µl Equilibration Buffer at RT for 5–10 min. Cells were incubated with 50µl of TdT for 60min at 37°C in a humidified chamber. Afterward, slides were immersed in 2X SSC for 15min and washed three time with PBS, 5min each time. Nuclei were counterstained using DAPI (Sigma Aldrich). After a final washing, the slides were mounted with Mowiol/DABKO and stored at 4°C in the dark. (www.promega.com/tbs).

Table13: Primary antibodies used for IF

Antibody	Host	Dilution	Reference
K14	rabbit	1:1000 1:2000 (costaining with BrdU)	Covance
K10	rabbit	1:250	Covance
K15	mouse IgG2a	1:750	Neomarker
K81 (hHb1)	guinea pig	1:750	Progen
K6a	rabbit	1:600	Covance
Involucrin	rabbit	1:750	Covance
SCD1 (S-15)	goat	1:100	Santa Cruz
BrdU	mouse	1:10 tissue 1:25 cells	BD
Ki67	mouse	1:200	TEC-3, DAKO
Lrig1	goat	1:50	R&D System
Plet1	rat	1:5	Raymond et al., 2010
P53 (CM5)	rabitt	1:500	Novocastra Leica,Microsystems

Table 14: Secondary antibodies used for IF

Antibody	Host	Dilution	Reference
Alexa-488 mouse IgG1	goat	1:1000 tissue 1:500 cells	Invitrogen
Alexa-488 mouse IgG2a	goat	1.1000	Invitrogen
Alexa-488 rabbit IgG	donkey	1.1000	Invitrogen
Alexa-488 chicken IgG	goat	1.500	Invitrogen
Alexa-594 rabbit IgG	donkey	1:500 1:1000	Invitrogen
Alexa-488 goat IgG	donkey	1:1000	Invitrogen
Alexa-488 guinea pig	goat	1:750	Invitrogen
Alexa-488 rat IgG	donkey	1:500	Invitrogen

4.9 Statistical Methods

Statistical analysis of differences in tumor multiplicity were carried out using non-parametric methods, as tumor burden data is non-normative (Matsumoto et al., 2003, Abel et al., 2009). Data sets were analysed for statistical significance using a two-tailed unpaired Student´s *t*-test. All *P*-values below 0.05 were considered significant. All statistical analyses were done using Microsoft Exel and GraphPad Prism 5, SPSS 7.

4.10 Computer programs and data bases

Table 15: Programs and data bases

Data base/program	Internet adresse	application
Blast	http://blast.ncbi.nlm.nih.gov/Blast.cgi	primer alignment
Ensemble.org	http://www.ensembl.org/index.html	gene/exon structure primer localization
Fast PCR		primer analysis
GraphPad Prim 5	http://www.graphpad.com/prism/Prism.htm	statistical analysis
Image J	http://rsb.info.nih.gov/ij/ http://rsb.info.nih.gov/nih-image	western blot analysis
Lucia G & G/F V.4.82		Image processing
Primer 3	http://fokker.wi.mit.edu/primer3/input.htm	primer design
Step One Plus Version2		qRT-PCR quantification

5 Results

In order to address the function of Ihh signalling in skin development and tumour formation Ihh loss-of-function studies were performed. Conventional *Ihh* knockout mice, which have been generated previously, die during embryonic development at day E10.5 to E12.5 or directly after birth due to circulatory abnormalities and respiratory failure (St-Jacques et al., 1999). Consequently, *Ihh* null mice could not be used for studying the role of Ihh in postnatal skin development and tumourigenesis. Therefore we generated epidermal specific *Ihh* knockout mice (*Ihh* EKO) to study the function of Ihh during the skin morphogenesis and epidermal regeneration in normal and patho-physiological conditions.

5.1 Generation of epidermal specific *Ihh* knockout mice (*Ihh* EKO)

To generate a conditional epidermal knockout for *Ihh*, homozygous mice carrying a floxed *Ihh* gene (*Ihh* fl/fl) (Razzaque et al., 2005) were crossed with mice expressing Cre-recombinase under control of the human Keratin 14 promoter (K14Cre) (Hafner et al., 2004) (Fig. 10A). In mice epidermal Keratin 14 (K14) expression begins from embryonic stage day 9.5 (E9.5) and remains constantly active throughout life (Koster and Roop, 2004). The K14 promoter is active in the proliferating basal layer of the interfollicular epidermis (IFE), the sebaceous gland (SG) and the outer root sheat (ORS) of the hair follicle (HF) (Fig. 10B). Crossing of K14Cre mice with different reporter strains [Rosa26 (Mao et al., 1999) and $pLuh_{flox/flox}$ (Ayral et al., 1998)] it was shown that from E15 onwards the complete IFE, SG and HF contain active Cre-recombinase (Hafner et al., 2004).

In *Ihh* floxed mice the start codon and exon1 of the *Ihh* gene are flanked by loxP sites (Fig. 10C). The floxed region encodes the part of the Ihh peptide (Hh-N), which is functionally important for binding to the Patched receptor and consequently for the transduction of the Hh signal (chapter 3.2.1). The Cre enzyme is active in basal keratinocytes of the skin and therefore exon1, including the start codon are deleted and *Ihh* cannot be translated. Consequently, all descendent cells, including the differentiated keratinocytes, lack functional Ihh.

To examine the efficiency of Cre recombinase in keratinocytes, PCR analysis was performed of genomic DNA (gDNA) isolated from tail biopsies or split epidermis from the tail of mice at postnatal day 2 (P2) (Fig. 10D). Primers designed for amplifying the exon1 region of *Ihh* (Fig. 10C) can identify the *Ihh* floxed (flox 1,2kb) and *Ihh* deleted allele (Δ400bp). PCR analysis of gDNA from homozygous *Ihh* EKO (K14Cre// *Ihh* fl/ fl) tails (k1, K2, k4) shows both the *Ihh* deleted (Δ400bp) and floxed (flox 1,2kb) band. This is expected since the DNA is derived from tissues both with and without Cre expression. The DNA amplified from tails of control (CO) mice lacking Cre (*Ihh* fl/ fl) show only the non-deleted floxed band (flox 1,2kb).

In contrast, the PCR analysis of gDNA from homozygous *Ihh* EKO (K14Cre//*Ihh*fl/fl) epidermis shows a single *Ihh* deleted band (Δ400bp) resulting from effective Cre recombination in *Ihh* EKO mice (k1, k2, k4). The additional unexpected band (~750 bp) seen in the PCR analysis of tail biopsies from homozygous *Ihh* EKO mice might result from the hybridisation of floxed and deleted products. The PCR analysis was performed with several littermates and in different postnatal stages (P0-P3), always yielding the same results. Also gDNA sequencing of epidermis from CO and *Ihh* EKO mice showed the expected nucleotide deletions in the floxed region of *Ihh* EKO mice, while the CO mice contained the complete Ihh gene (data not shown).

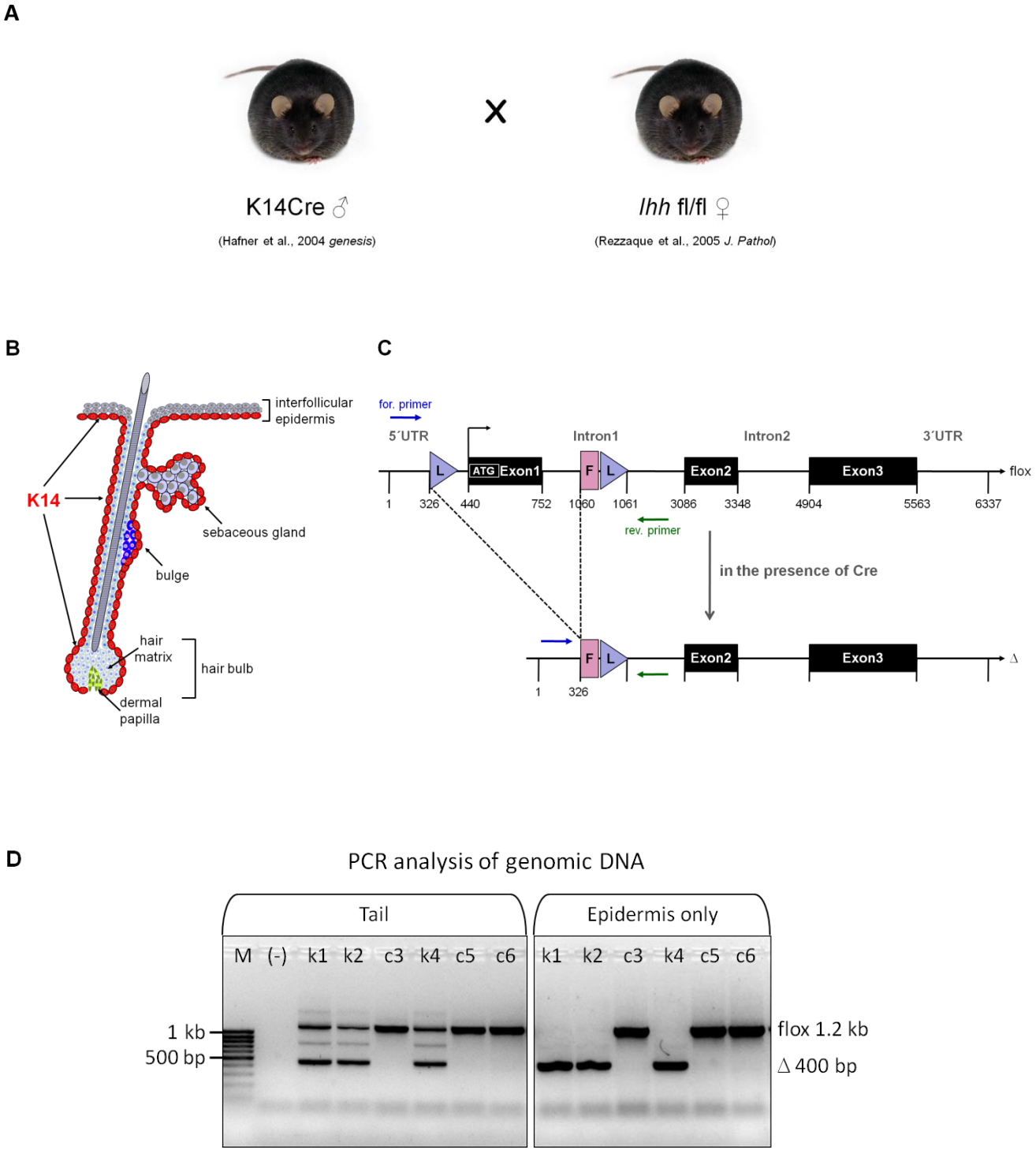

Figure 10: Generation of epidermal specific Indian hedgehog knockout mice (*Ihh* EKO).
(A) Mice expressing the Cre recombinase enzyme under the control of the Keratin 14 promoter (K14Cre) were crossed with mice homozygous for floxed Indian hedgehog allele (*Ihh* fl/fl). **(B)** The Keratin 14 (K14) promoter induces Cre expression in the basal cells of Interfollicular epidermis (IFE), Hair follicle (HF) and Sebaceous gland (SG). **(C)** Genomic map of the mouse *Ihh* locus shows loxP site flanking exon1 and start codon (ATG) and position of primers for PCR detection of *Ihh* exon1 deletion. **(D)** PCR analysis of genomic DNA isolated from tail biopsies showing both deleted and wt for *Ihh* allele from homozygous *Ihh* EKO mice (k1, k2, k4). PCR analysis of genomic DNA from split epidermis from homozygous *Ihh* EKO tail showing the high efficiency of deletion in the epidermis (k1, k2, k4) and no deletion in epidermis of CO (*Ihh* fl/fl) mice (c3, c5, c6). The size of loxP-flanked allele fragments (flox: c3, c5, c6) is 1,2kb and the size of deleted allele band (Δ: k1, k2, k4) is 400bp.

PCR analyses of primary keratinocytes isolated from *Ihh* EKO (K14Cre//Ihh fl/fl) and CO (Ihh fl/fl) littermates in postnatal day 2 (P2) confirmed the results from mouse biopsies. A single undeleted *Ihh* floxed band (flox 1,2kb) was amplified in primary keratinocytes of CO mice (c3, c5, c6) (Fig. 11). In contrast, gDNA amplification of *Ihh* EKO primary keratinocytes showed only the *Ihh* deleted allele (∆400bp) (k1, k2, k4). This means that the K14 promoter and Cre enzyme are fully active already at postnatal day 2.

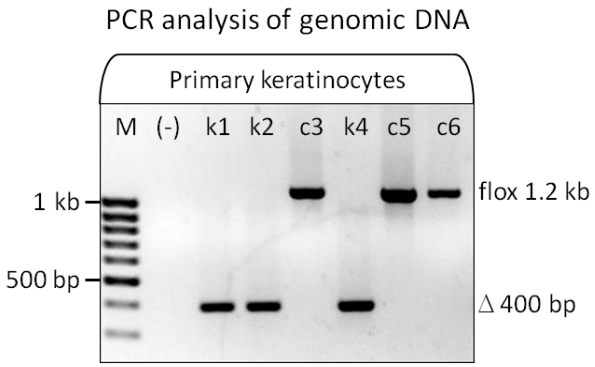

Figure 11: High efficiency of *Ihh* deletion in primary keratinocytes.
PCR analysis of genomic DNA isolated from primary keratinocytes of new born mice (P2) showing homozygous deletion of *Ihh* homozygous allele with high efficiency (k1, k2, k4). The expected size of floxed allele band (flox: c3, c5, c6) is 1,2kb and the size of deleted allele band (∆: k1, k2, k4) is 400bp.

Since *Ihh* EKO epidermis contains only the deleted *Ihh* allele and epidermis of CO mice contains only the complete *Ihh* allele, for further analysis *Ihh* fl/fl littermates are used as controls (CO) for the evaluation of *Ihh* EKO mice.

5.2 Analysis of epidermal morphology of *Ihh* EKO mice

Ihh EKO mice showed no general macroscopic abnormalities in size, weight or behaviour. Moreover, no differences in appearance of growth and density of dorsal and ventral hair and whiskers were observed. In addition in *Ihh* EKO mice, the time course of hair cycle regeneration was normal and showed no delay. To examine whether there is any microscopic morphological alteration in the skin of *Ihh* EKO mice compared to CO a histological analysis was performed.

5.2.1 Analysis skin morphology of *Ihh* EKO mice

Previous studies suggested a potential role of Ihh signalling for sebaceous gland (SG) physiology (Niemann et al., 2003; Allen et al., 2003; Takeda et al., 2006; Lo Celso et al., 2008) (chapter 3.4). Therefore, the skin of *Ihh* EKO mice was analysed focusing on SGs. Histological analysis of back and tail skin sections revealed normal development of SG, HF and IFE as analysed between postnatal day 0 to day 10 (P0-P10) (Fig. 12A). Generally, the first mature sebocytes are detectable shortly after birth as SGs develop during HF formation (Niemann, 2009). Formation of SG and HF was also investigated by epidermal whole-mount technique (Fig. 12B). No morphological alteration in size and shape of SGs and HFs were seen in absence of epidermal Ihh. Initial analysis of other skin compartments including dermis, subcutaneous fat and muscles also revealed no morphological abnormalities in P0 to P10 stages of development.

Previous studies performed in non-skin tissues suggested that Ihh regulates cell proliferation and differentiation (Vortkamp et al., 1996; St-Jacques et al., 1999; Zhang et al., 2001; van den Brink 2007; Tsiairis and McMahon, 2009; Bellon e al., 2009; Cortes et al., 2009). Therefore, we examined epidermal development in *Ihh* EKO mice in more detail using differentiation and proliferation markers.

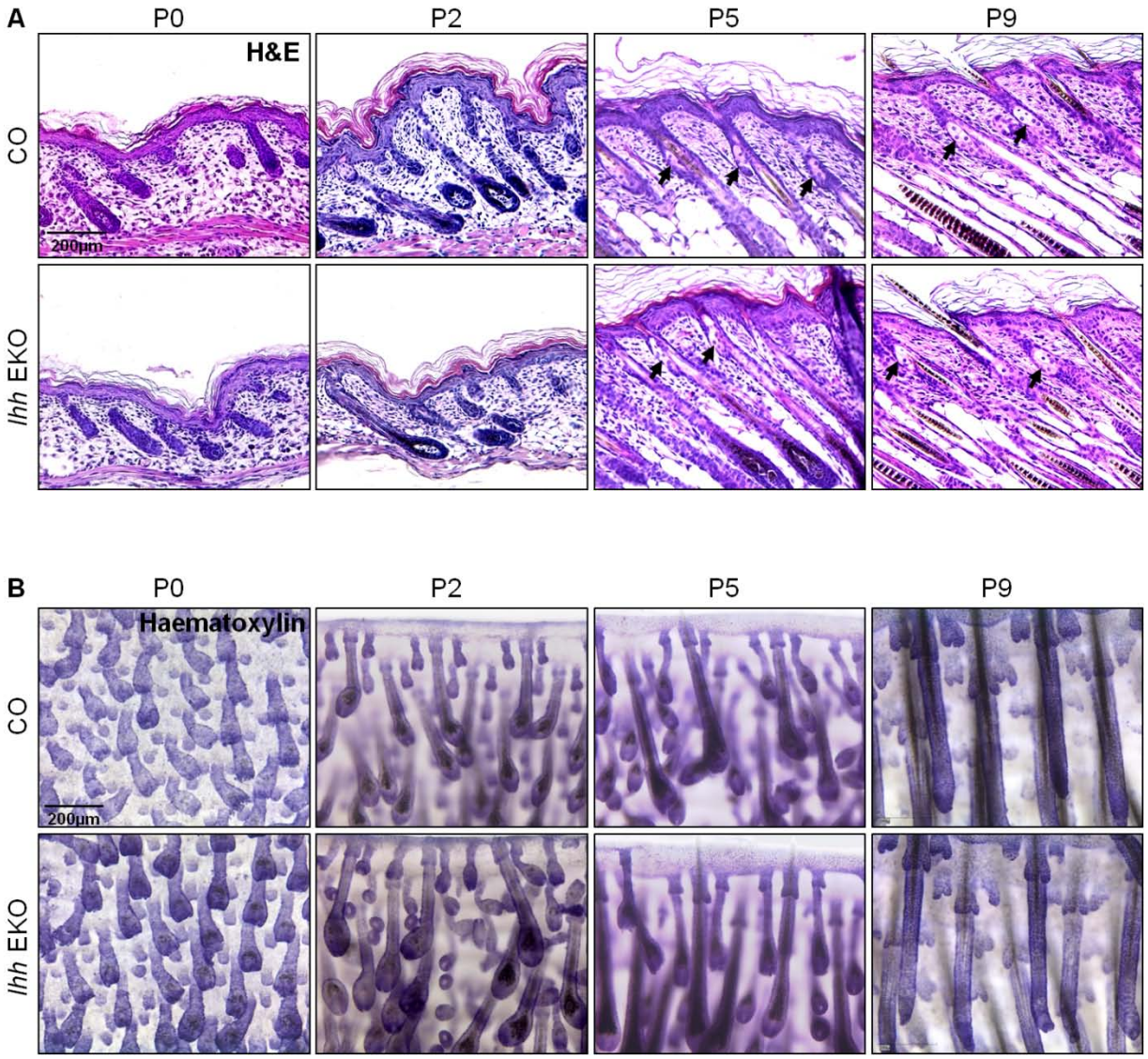

Figure 12: No morphological abnormalities in back and tail skin during postnatal development (P0-P9) of *Ihh* EKO mice.

(A) Histological analyses of back skin sections from *Ihh* EKO and control (CO) mice in early postnatal stages (P0-P9) show no morphological change in SG, HF and IFE**. (B)** Epidermal whole mounts (WM) isolated from tail skin (P0-P9) of *Ihh* EKO (lower panel) also show no morphological abnormalities in HF and SG during morphogenesis compared to CO. The analysis of all postnatal stages (P0-P9) was done with n=8-15 mice per genotype with matched littermate controls. Scale bars 200µm **(A)** and **(B).** H&E: Haematoxylin-eosin staining

5.2.2 Sebaceous gland formation is not altered in *Ihh* EKO mice

To examine whether absence of Ihh affects the differentiation of SGs, expression of stearoyl-coenzyme A desaturase 1 (SCD1) was analysed. SCD1 has been shown to be an early sebocyte differentiation marker (Zheng et al., 1999, Miyazaki et al., 2001). In this experiment, sections of back skin (Fig. 13A) and epidermal whole mounts from tails (Fig. 13B) of *Ihh* EKO and CO mice (P0-P9) were stained with antibody against SCD1 (green), K14 (red) and DAPI (blue). In all postnatal stages (P0-P9) the expression pattern of SCD1 was not altered in SGs of *Ihh* EKO mice compared to CO. In addition, K14 expression in basal cells of all epidermal compartments was not altered.

Taking together these data indicate that absence of epidermal Ihh does not affect development and differentiation of SGs. Whether the differentiation of SG, IFE or HF is altered at later stages in *Ihh* EKO remains to be analysed in more detail.

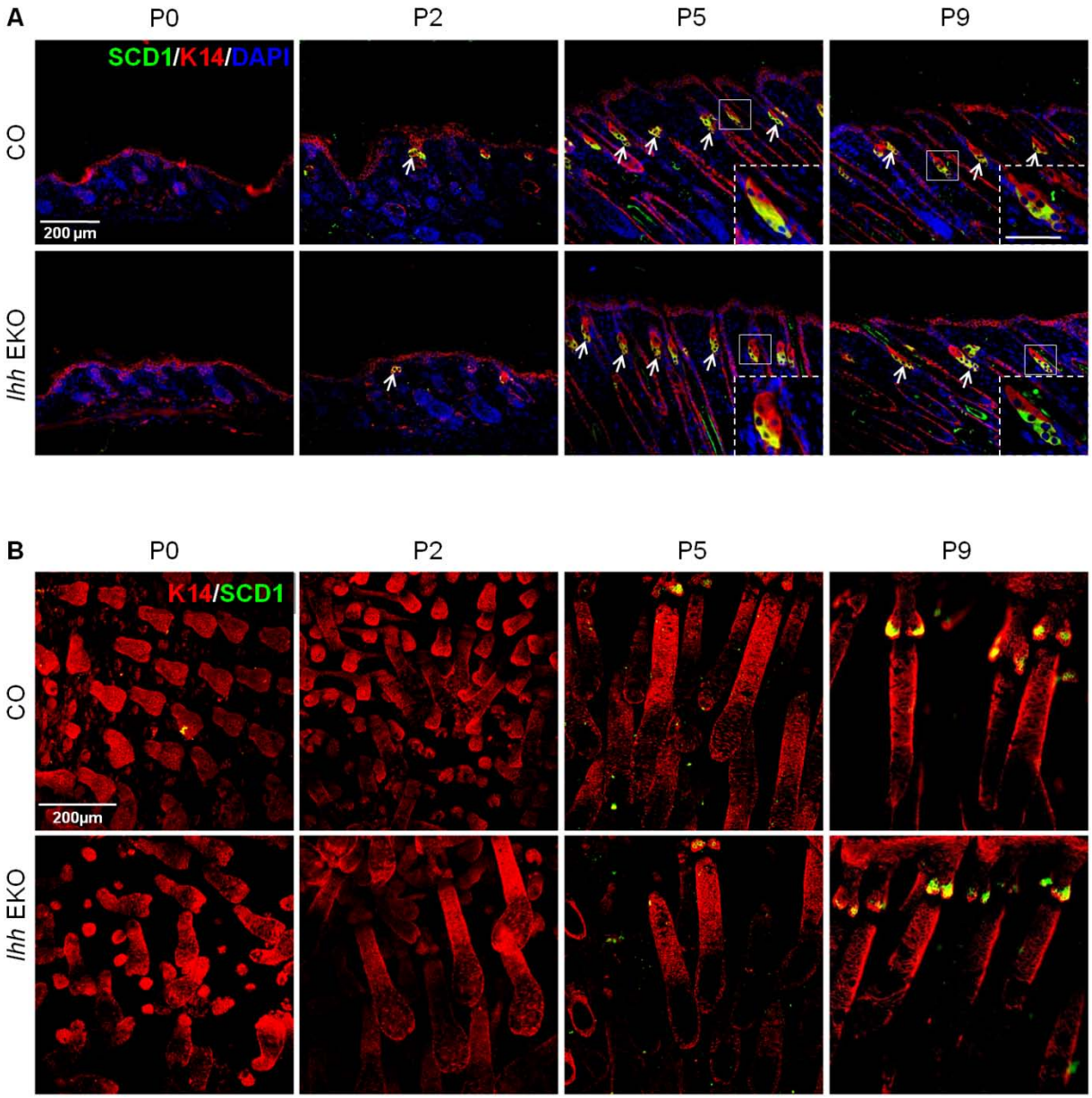

Figure 13: SG morphogenesis and differentiation is not altered in the absence of epidermal Ihh.
(A) Sebocyte differentiation marker SCD1 (green), co-stained with K14 (red) and DAPI (blue) for nuclear staining. In the back skin of *Ihh* EKO mice (lower panel) the expression pattern of SCD1 during the SG developmental stages (P0-P9) is not changed compared to control (CO) (upper panel). P5-P9 inset of higher magnification of marked region. White arrows point to sebaceous gland. **(B)** WM epidermis isolated from tail (P0-P9) show also normal SCD1 expression in *Ihh* EKO mice (lower panel) compared to CO (upper panel). The Immunofluorescents (IF) analysis of all postnatal stages (P0-P9) was done with n=3-5 mice per genotype with matched littermate controls. SCD1 (green) co-stained with K14 (red). Scale bars 200µm **(A)**, µm **(B)** and 50µm **(**Inset **A).**

5.2.3 Ihh stimulates epidermal proliferation in neonatal mice

To test if proliferation of epidermal tissue is altered in *Ihh* EKO mice different proliferation markers were used. We examined the BrdU incorporation after a 1h pulse labelling in the back skin of *Ihh* EKO mice. Skin sections of mice from P0 to P10 were stained with antibodies against BrdU (green) and K14 (red) (Fig 14). Interestingly, during the early postnatal stages (P0-P2) in *Ihh* EKO mice the number of BrdU positive cells was reduced whereas in later stages (P3-10) it was unchanged.

Analysis of Ki67 confirmed our results of reduced proliferation in *Ihh* EKO mice. In both studies the effect on proliferation seems to be most pronounced in the IFE. To examine this in more detail we quantified the BrdU incorporation in different epidermal compartments separately.

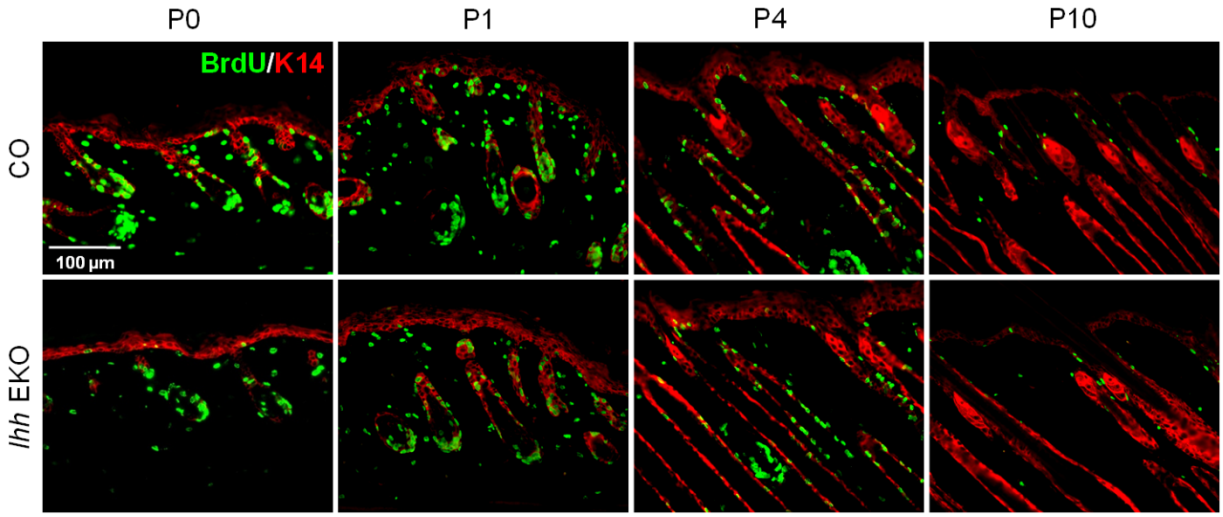

Figure 14: Reduced epidermal cell proliferation in the absence of Ihh during skin development.
Analysis of BrdU incorporation (green) of the epidermis in *Ihh* EKO mice (lower panel) compared to CO (upper panel). In the early postnatal stages (P0-P2) absence of Ihh in the epidermis significantly reduced the proliferation of IFE, but this effect is compensated in later stages (P3-P10). IF analysis with anti K14 (red) and anti BrdU (green) antibody of all postnatal stages (P0-p10) was done with n=1-7 mice per genotype with matched littermate controls. Scale bar 100µm.

BrdU positive cells within the basal layer of the IFE were counted at different developmental stages, normalised to the total number of basal cells in the IFE. In the absence of Ihh, cell proliferation within the IFE is significantly reduced at P0 (1.8 fold), P1 (1.5 fold) and P2 (1.6 fold) whereas at later stages (P3-10) no significant differences were observed (Fig 15B). Taken together, these data indicate that epidermal Ihh signalling promotes the proliferation of basal cells in the IFE during early stages of skin development. This effect might be compensated by other factors during later phases of postnatal development.

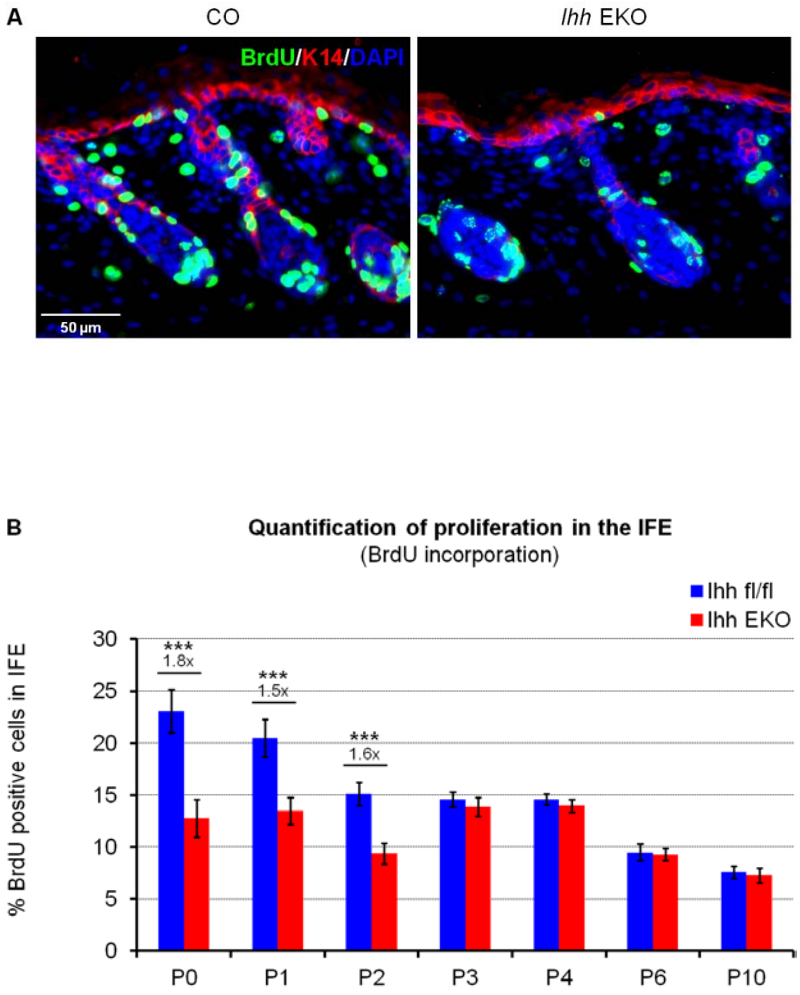

Figure 15: Reduced cellular proliferation in the IFE of neonatal *Ihh* EKO mice.
(A) Higher magnification of back skin of newborn mice (P0) stained for BrdU (green), K14 (red) and DAPI (blue). Reduction of proliferation observed in absence of Ihh within the IFE. BrdU incorporation (IP injection, 1h pulse), Scale bar 50µm **(A)**. **(B)** Quantification of BrdU positive cells within the basal layer of IFE (normalised to total number of basal cells of IFE) at different postnatal stages (P0-P10). Quantification of BrdU from each postnatal stages (P0-P10) was done with matched littermates (n=1-7 mice per genotypes) analysing 5-10 different areas per slide using ImageJ. Error bars are ± s.d., Student´s *t*-test, *** $P<5x10^{-14}$.

5.2.4 Ihh regulates epidermal proliferation by keratinocyte-intrinsic signalling

To address whether Ihh stimulates epidermal proliferation by keratinocyte-intrinsic signalling, *in vitro* studies were performed. Primary keratinocytes were isolated from newborn (P2) *Ihh* EKO and CO mice and cultured in low Ca^{2+} growth medium. In the absence of epidermal Ihh, primary keratinocytes show a significant delay until reaching confluency compared to CO. BrdU analysis revealed that in absence of Ihh the proliferation of keratinocytes is significantly reduced *in vitro* (Fig. 16A). This experiment was done in triplicate with primary keratinocytes isolated from 3 independent littermates. Quantification of BrdU positive keratinocytes indicates a 2.4 fold reduction in cell divisions in the absence of Ihh (Fig. 16C).

To test whether the reduction of cell number in absence of Ihh is due to apoptosis, TUNEL assays were performed (Fig. 16B). Only very few apoptotic cells were seen and no difference was observed between *Ihh* KO and CO cells. This experiment was also performed in triplicate with the same primary keratinocytes as for the BrdU incorporation assay.

These data demonstrate that Ihh signalling induces proliferation of keratinocytes by keratinocyte-intrinsic signalling, without affecting apoptosis. These observations raise the question of what reduced epidermal proliferation entails for skin development in *Ihh* KO mice and why Ihh regulation of cell division was only detected in neonatal stages? One possibility is that the role of Ihh in the skin during later stages becomes apparent only in stress situations or during disease processes.

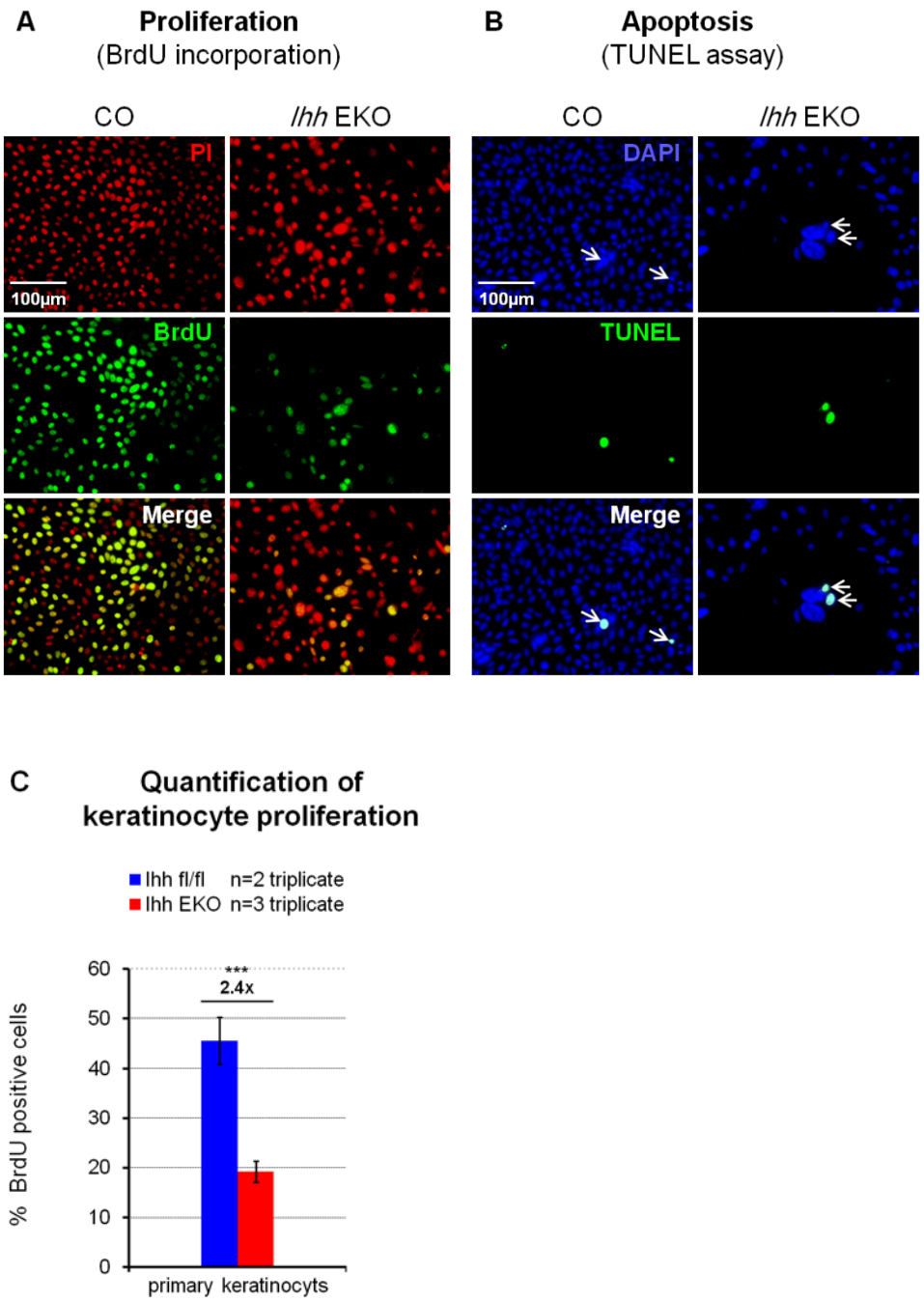

Figure 16: Ihh is required for proliferation *in vitro*.
(A) BrdU incorporation assay indicates a dramatic decrease of keratinocyte proliferation in absence of Ihh compared to CO. BrdU (green) counterstained with PI (red) for visualisation of nuclei. **(B)** TUNEL staining (green) indicates that the absence of Ihh does not affect apoptosis of primary keratinocytes compared to CO (left panel). In TUNEL assay DAPI (blue) was used for visualisation of nuclei**.** White arrows point TUNEL positive nuclei. **(C)** The quantification of BrdU positive cells indicates 2.4 fold reduction of keratinocytes proliferation in absence of Ihh (red bar; 19.2 ±2.1) compared to CO (blue bar; 45.5 ±4.7).For BrdU and TUNEL staining, including BrdU quantification analysis, primary keratinocytes were isolated from newborn littermates (P2) (n=3 *Ihh* EKO and n=2 CO mice), cultured in keratinocyte medium and stained in triplicate. 5-7 different areas from each slide were quantified using ImageJ. Scale bar 100µm **(A)** and **(B)**. Error bars are ± s.d., Student´s *t*-test, ***P<2x10^{-10}.

5.3 The function of Ihh signalling for skin tumorigenesis

To investigate the function of Ihh signalling in tumour formation, two epidermal tumour models were studied:

5.3.1 sebaceous tumours

5.3.2 squamous tumours (benign papilloma and malignant squamous cell carcinoma)

5.3.1 The function of Ihh signalling during sebaceous tumour development

To examine the role of Ihh during sebaceous tumour formation in detail, carcinogenesis experiments were performed with *Ihh* EKO (K14Cre+/-//*Ihh* fl/fl) and CO (*Ihh* fl/fl) mice, crossed to K14ΔNLef1 transgenic (tg) mice. The K14ΔNLef1 tg mouse is a sebaceous tumour model, which was previously generated and characterised by Niemann et al. (2002) (chapter 3.5.1). It has been shown that carcinogen (DMBA) treatment of K14ΔNLef1 mice is sufficient to induce sebaceous tumours at high frequency (Niemann et al. 2007) (Fig. 17). This procedure is called a one-stage carcinogenesis experiment since tumour induction does not require the additional treatment with a tumour promoter-like phorbol ester derivates. We performed one-stage carcinogenesis experiments to analyse the influence of Ihh on tumour formation in a K14ΔNLef1 background. In particular, processes of tumour formation, proliferation and differentiation of tumour cells were analysed.

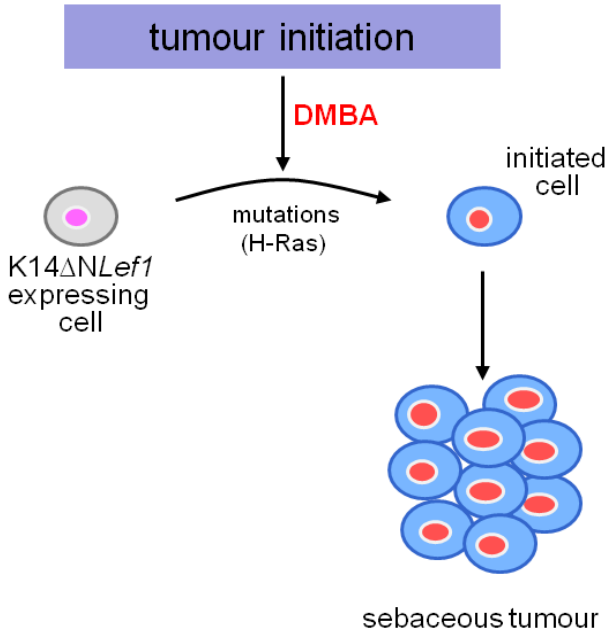

Figure 17: Scheme of tumour induction in K14ΔNLef1 mice.
In the one-stage skin carcinogenic experiments, skin of K14ΔNLef1 transgenic mice received a single sub-threshold dose of DMBA for tumour initiation resulting in sebaceous tumour development. DMBA: 7,12-dimethylbenz(*a*) anthracene.

5.3.1.1 Ihh does not affect incidence and frequency of sebaceous tumours but represses tumour growth

We generated mice with epidermal deletion of *Ihh* in a K14ΔNLef1 background (K14ΔNLef1/K14*Cre*//*Ihh* fl/fl = K14ΔNLef1/*Ihh* EKO). The animals used for the one-stage carcinogenesis experiment were 9-week-old in the second telogen. The skin of K14ΔNLef1/*Ihh* EKO (n=19) and CO (K14ΔNLef1/*Ihh* fl/fl) (n=17) littermates received a single sub-threshold dose of DMBA (100nmol/200µl) or acetone vehicle (K14ΔNLef1/*Ihh* EKO [n=5] and (K14ΔNLef1/*Ihh* fl/fl [n=4]) (Fig. 18A). Mice were monitored weekly. The first tumours developed 4 weeks after DMBA treatment while none of the mice in control groups (treated with acetone) developed tumours. Scoring of tumours was contined for up to 25 weeks after tumour initiation. In both K14ΔNLef1/*Ihh* EKO and CO mice tumour incidence was very similar (Fig. 18B).

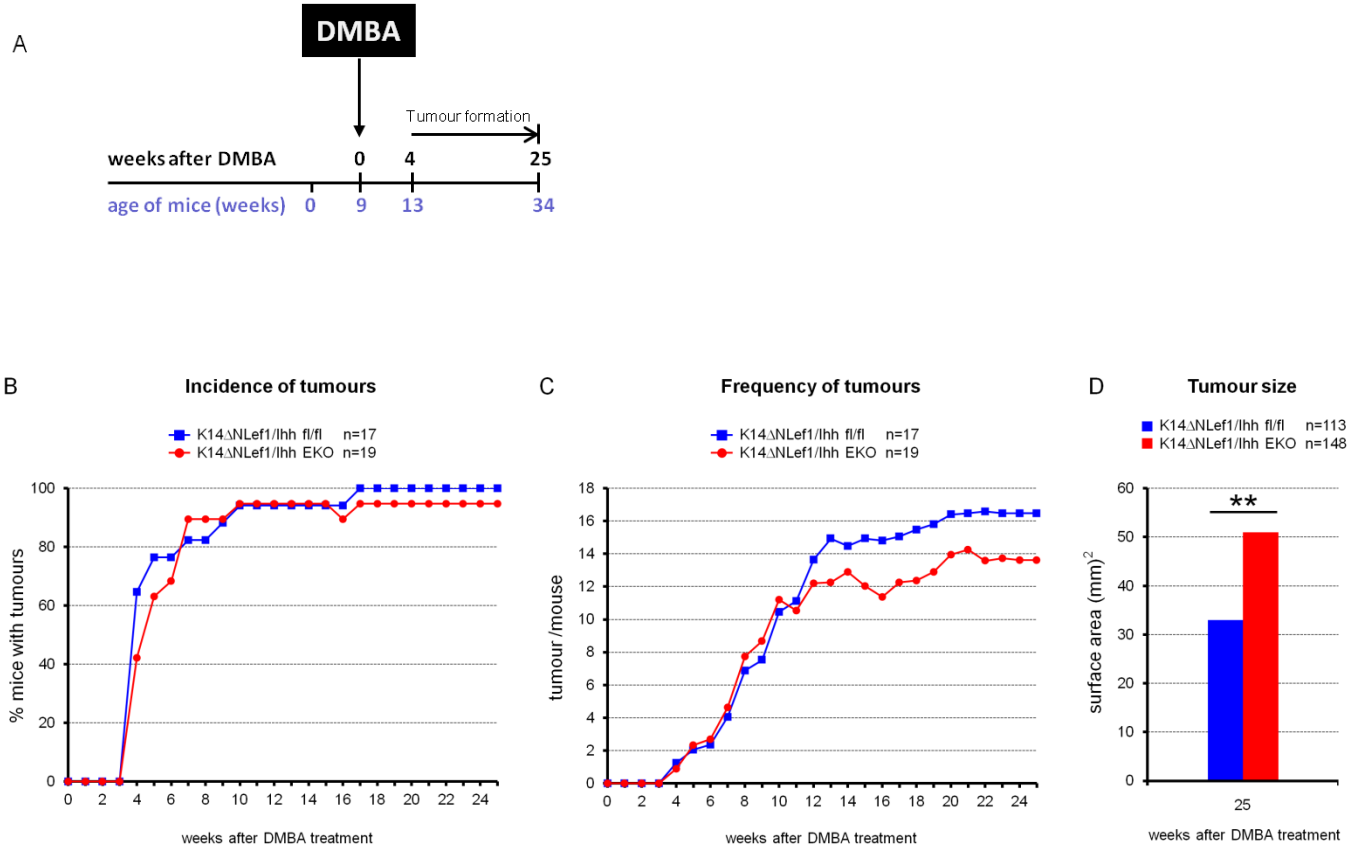

Figure 18: Repression of sebaceous tumour size in the presence of Ihh.
(A) Time line of one-stage carcinogenesis experiment. Skin of 9 week old *Ihh* EKO and CO mice, in K14ΔNLef1 background received one application of DMBA or acetone vehicle only. The first tumours were observed 4 weeks after DMBA treatment. Scoring of tumours was carried out once a week for up to 25 weeks after tumour initiation. **(B)** Incidence of tumours in K14ΔNLef1/*Ihh* EKO (red line) and K14ΔNLef1/*Ihh* fl/fl (CO) mice. **(C)** Frequency of tumours developing in K14ΔNLef1/*Ihh* EKO (red line) mice. **(D)** Measurement of tumour size at 25 weeks after DMBA treatment indicates significantly larger tumours in K14ΔNLef1/*Ihh* EKO mice (red bar) compared to K14ΔNLef1/*Ihh* fl/fl (CO) (blue bar). n=17 K14ΔNLef1/*Ihh* fl/fl (CO), n=19 K14ΔNLef1/*Ihh* EKO mice were treated with DMBA and n=4-5 mice per genotype with acetone for analysis of incidence and frequency of sebaceous tumours. n=113 tumours from n=7 K14ΔNLef1/*Ihh* fl/fl (CO) mice and n=148 tumours from n=10 K14ΔNLef1/*Ihh* EKO mice was used for the quantification of tumour size. This experiment was done in duplicate and the result was replicated. Non-parametric methods, as tumour burden data is non-normative, Student´s *t*-test, **P=0.002.

4 to 10 weeks after tumour initiation 95-100% mice in both, K14ΔNLef1/*Ihh* EKO and CO groups developed tumours after DMBA treatment. Between 1 to 12 weeks after tumour initiation the frequency of tumours was not significantly different between the two groups. While the frequency of tumours in K14ΔNLef1/*Ihh* EKO was slightly reduced from 13 to 25 weeks after tumour initiation compared to CO mice. An average number of 13.5 and 16.5 tumours were scored for K14ΔNLef1/*Ihh* EKO and CO mice at 25 weeks, respectively.

However, two-tailed unpaired student's *t*-test revealed no significance of these results (Fig. 18C). Interestingly the size of tumours developing in K14ΔNLef1/*Ihh* EKO mice (51 mm^2) was significantly larger than in CO (33 mm^2) (P=0,002) (Fig. 18D). This data indicate the incidence and frequency of tumour formation in K14ΔNLef1 mice is not affected by Ihh. On the other hand, this data suggest Ihh represses tumour size.

5.3.1.2 Ihh promotes sebocyte and sebaceous duct fate differentiation in tumours of K14ΔNLef1 mice

To further characterise the tumours developing in K14ΔNLef1/*Ihh* EKO mice the histology of the tumour tissue was investigated. In CO mice the majority of tumours are sebaceous adenoma, which arise from underneath the epidermis and upper region of HF (Niemann et al., 2002). In addition, there are some sebaceomas with sebaceous and squamouse, differentiation and very few papilloma with small areas of sebocytes. The sebaceous adenoma from CO mice are filled with a large number of well differentiated sebocytes (Fig. 19A-C). In contrast, the number of sebocytes is dramatically reduced in the sebaceous tumours of K14ΔNLef1/*Ihh* EKO mice (Fig. 19D-F). Only a few sebocytes were observed at the periphery of the tumours.

In order to further characterise the tumours and better quantify the contribution of mature sebocytes, the tumours were grouped with regard to their size: small tumours (1-4mm diameter), medium size tumours (4-8mm) and large tumours (8-16mm). Half of the tumours in both K14ΔNLef1/*Ihh* EKO and CO mice were of medium size. However, the number of large tumours was increased in K14ΔNLef1/*Ihh* EKO (34%) compared to CO mice (23%) (Fig. 19G)

The tumours which contained more than 50% sebocytes were counted and their proportion was determined relative to the total number of tumours in each group (Fig. 19H). In *Ihh* EKO mice the number of small tumours with differentiated sebocytes was higher, whereas the number of medium size and large tumours with well differentiated seboytes was significantly decreased (2.3 and 3.1 fold) compared to CO mice. These data indicate that Ihh is required for sebocyte differentiation, when tumours reach a critical size.

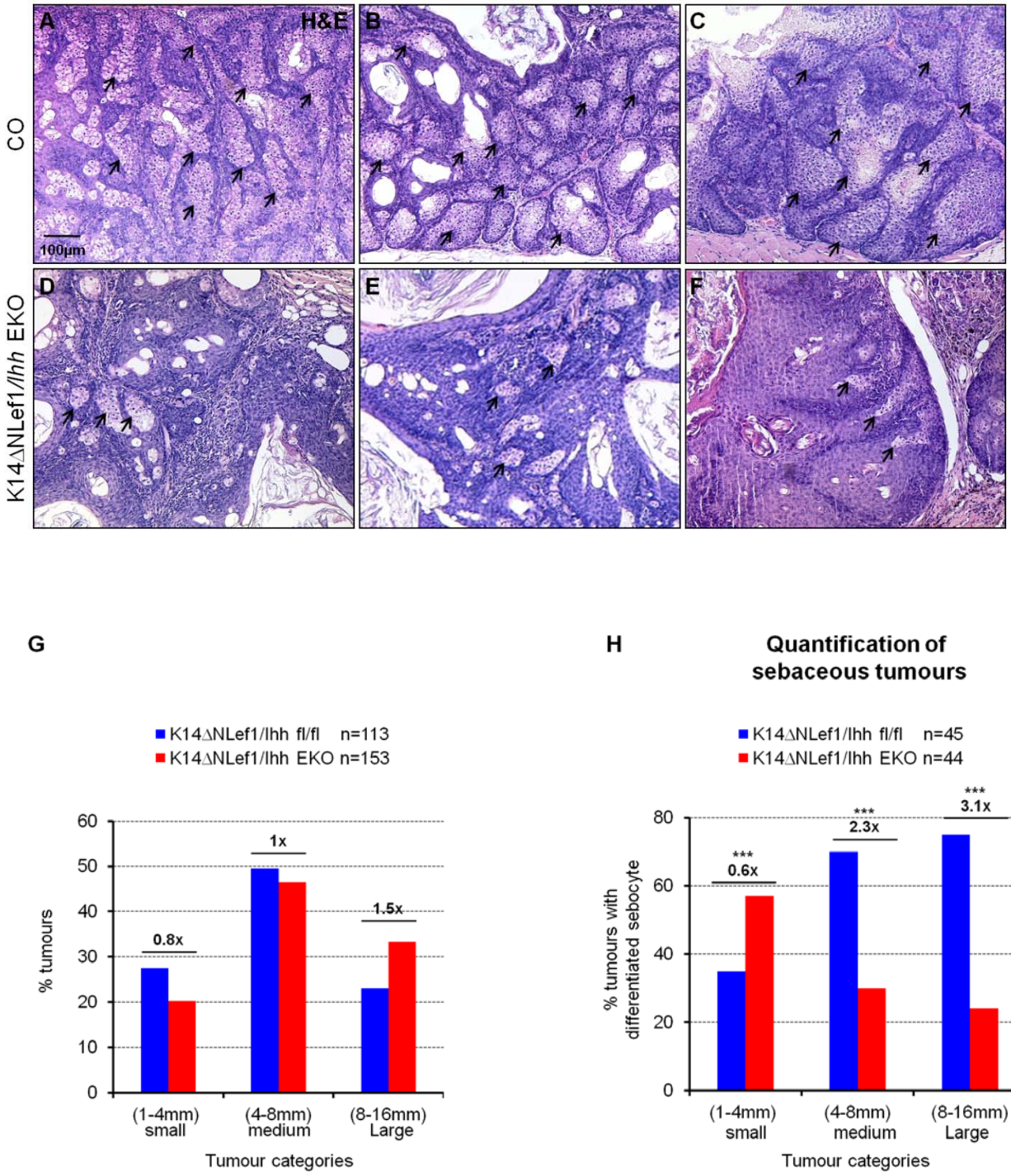

Figure 19: Reduced differentiation into sebocytes in tumours of K14ΔNLef1/*Ihh* EKO mice.
(A-F) Histological analysis of tumours from K14ΔNLef1/*Ihh* EKO mice (H&E staining) **(D-F)** indicates that number of sebocytes is decreased compared to K14ΔNLef1/*Ihh* fl/fl (CO) **(A-C).** Black arrows indicate regions of sebaceous differentiation**.** The analysis of sebaceous tumours was done with n=100-110 tumours from n=12 mice per genotype. Scale bars 100µm **(A-F)**. **(G)** For further characterisation tumours are grouped according their size (diameter), small (1-4mm), medium (4-8mm) and large (8-16mm). This graph shows the percentage of tumours relative to the total number of the tumours. **(H)** Quantification of sebaceous tumours with more than 50% sebocytes differentiation in each group. n=44-45 tumours (4-5 tumours per group) from n=4 mice per genotype, Student´s *t*-test, ***P<0.0005.

To analyse differentiation in sebaceous tumours in detail we checked for expression of the sebocyte differentiation marker SCD1 (Fig. 20). As expected in medium and large tumours of K14ΔN*Lef1*/*Ihh* EKO mice the SCD1 expression pattern is largely reduced (Fig. 20A-C) whereas the CO tumours are filled with SCD1 positive cells (Fig. 20D-F). To consider cellular heterogeneity within the tumour western blot analysis (WB) was performed to quantify SCD1 protein levels in individual sebaceous tumours (Fig. 20G-J). Lysates from large tumours of K14ΔN*Lef1*/*Ihh* EKO (k1-k9) and CO mice (c1-c9) were analysed. In *Ihh* EKO mice the majority of tumours show a significant reduction of SCD1 protein levels confirming the histological observations. Taken together, these results imply that Ihh promotes sebocyte differentiation within sebaceous tumours.

Next we wanted to know if Ihh regulates a more general program epidermal differentiation within the tumour tissue. Therefore we analysed epithelial differentiation markers characteristic for different compartments of the epidermis.

First we analysed the expression of Keratin 6a (K6a), a marker of sebaceous duct cells (Fig. 21). 2008 Gu and Coulombe reported that K6a expression by ductal cells of the SG is associated with Hh signalling. In addition, K6a marks terminally differentiated cells of the companion layer within the HF, which derive from the matrix of the hair bulb during anagen, extend to SG duct (Isthmus zone) and are located between the Outer root sheath (ORS) and Inner root sheath (IRS) (McGowan and Coulombe, 1998; Coulombe et al., 2004; Hsu et al., 2011). Tumours were stained with antibodies against K6a (red) and SCD1 (green) to examine localisation and distribution of K6a positive cells with regard to SCD1 positive seobocytes (Fig. 21). In sebaceous tumours of CO mice K6a and SCD1 both are highly expressed (Fig. 21A-D & I-K). The K6a positive cell population are mostly forms duct-like structures surrounding cysts or cavities. The layer of K6a positive cells lining the lumen of the cysts or cavities itself is surrounded by SCD1 positive sebocytes. Interestingly, in the absence of Ihh the number of K6a positive cells is dramatically reduced and this correlates with the reduction of SCD1 positive cell population (Fig. 21E-H & L-N).

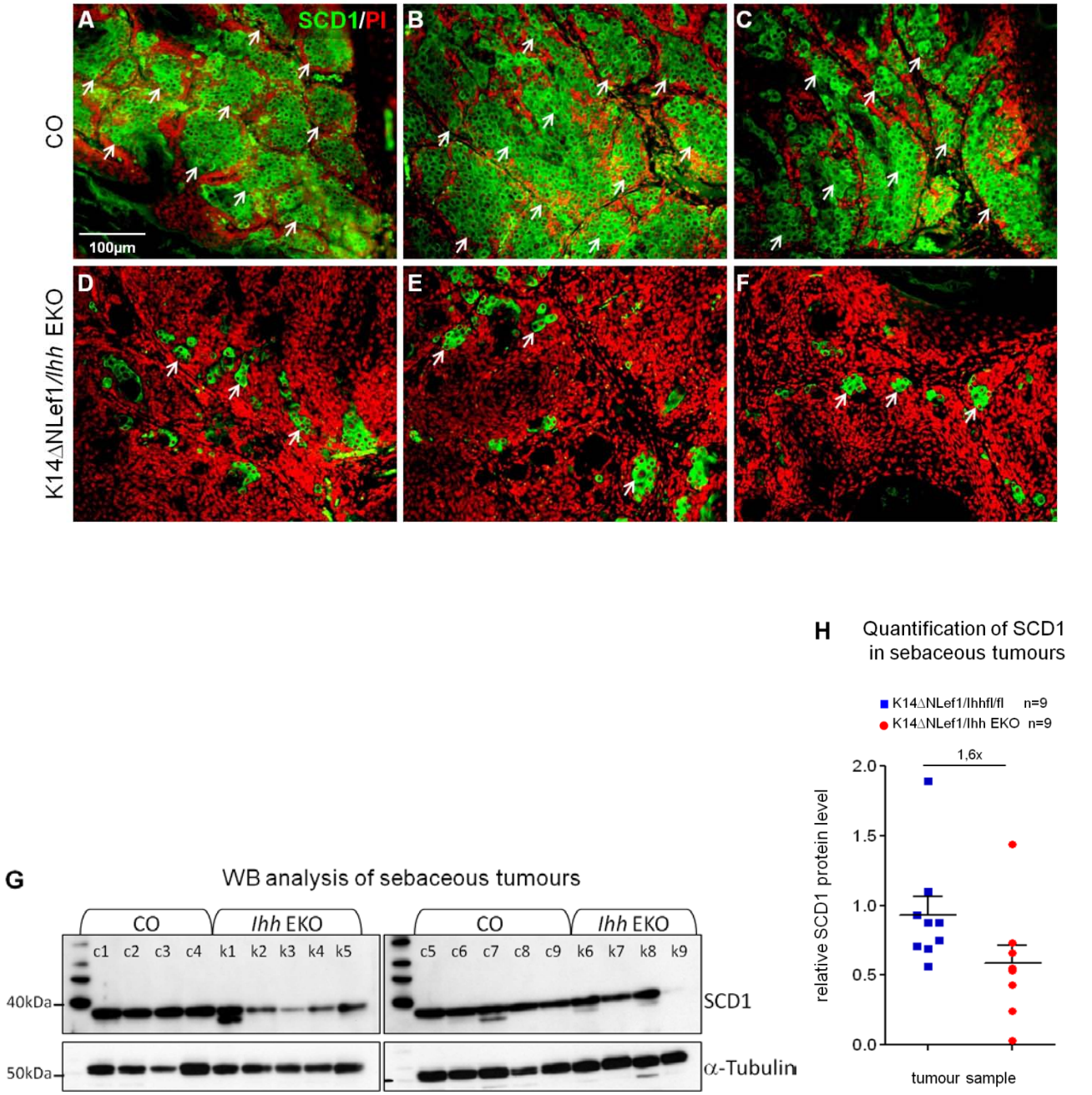

Figure 20: Decreased sebocyte differentiation in tumours of K14ΔNLef1/*Ihh* EKO mice.
(A-F) Analysis of SCD1 (green) expression in sebaceous tumours indicates dramatic reduction of differentiated sebocytes in absence of Ihh (K14ΔNLef1/*Ihh* EKO) **(D-F)** compared to K14ΔNLef1/*Ihh* fl/fl (CO) **(A-C).** White arrows point regions of sebaceous differentiation. The analysis was done with n=23-25 tumours from n=10 mice per genotype. SCD1 (green) counterstained with PI (red). Scale bars 100µm. **(G)** Western blot analysis (WB) was performed to quantify the SCD1 protein level in sebaceous tumour of K14ΔNLef1/*Ihh* EKO (k1-k9) and CO (c1-c9) mice. SCD1 =38kDa, α-Tubulin=50kDa. **(H)** Quantification of SCD1 protein level compared to α-Tubulin on WB using ImageJ program indicates a reduction of SCD1 protein in sebaceous tumours lacking Ihh (red bars) compared to CO (blue bars) by 1,6 fold higher in *Ihh* EKO tumours than CO **(D)**. Error bars are ± s.e.m.

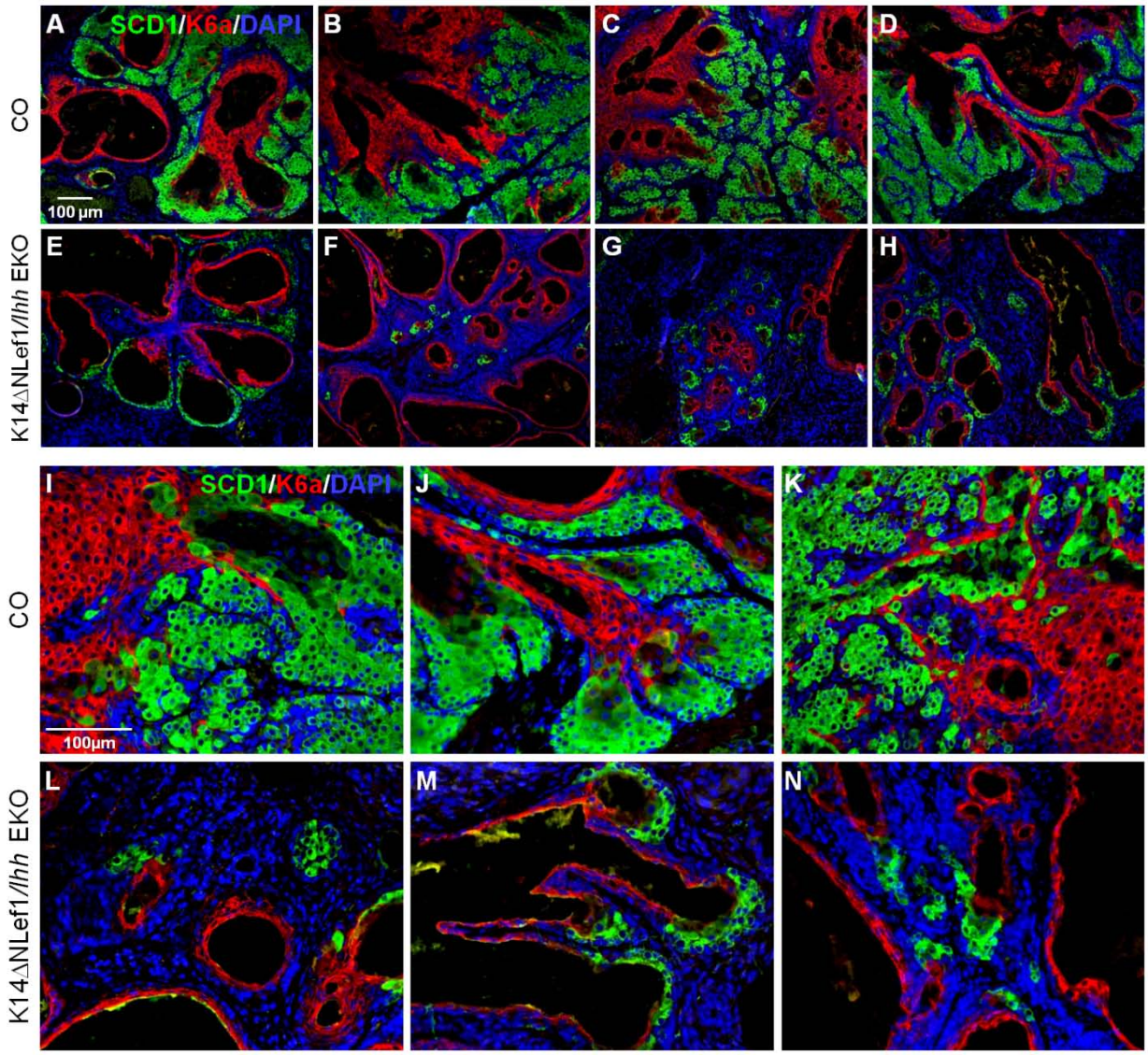

Figure 21: Ihh promotes differentiation of sebaceous duct fate in sebaceous tumours.
(A-N) Analysis of K6a (red) and SCD1 (green) in sebaceous tumours indicates dramatic reduction of K6a in the K14ΔNLef1/*Ihh* EKO **(E-H, L-N)** compared to K14ΔNLef1/*Ihh* fl/fl (CO) **(A-D, I-K).** The dramatic reduction of sebaceous duct fate correlates with reduced sebocyte differentiation in tumours. **(I-N)** Higher magnified view of tumours. The analysis was done with n=15 tumours from n=9-10 mice per genotype. Scale bars 100µm. Nuclei are counterstained with DAPI. K6a: Keratin 6a.

In wound healing experiments K6a expression is seen in proliferating cells and in epithelial tumours derived from IFE and HF K6a expression is associated with hyperproliferation (Weiss et al., 1984; Mansbridge and Knapp, 1987; Rothnagel et al., 1999; Wojcik et al, 2000). Therefore, we analysed whether in the sebaceous tumours K6a expression was associated with the proliferating cells. Dividing cells in sebaceous tumours were detected with antibodies against BrdU following a pulse of BrdU (Fig 22). Subsequent staining shows that K6a (red) positive cells did not incorporate BrdU (green), indicating that the K6a marks differentiated keratinocytes within the duct-like areas of tumours, rather than undifferentiated proliferating cells. The BrdU labelling experiment also revealed an overall reduction in proliferating cells in tumours lacking Ihh compared to tumours of control mice. The proliferation of tumour cells will be described in more detail in chapter 5.3.6.

Our data strongly indicate that Ihh promotes the differentiation of sebocytes and sebaceous duct-like cell fates in tumours of K14ΔNLef1 mice.

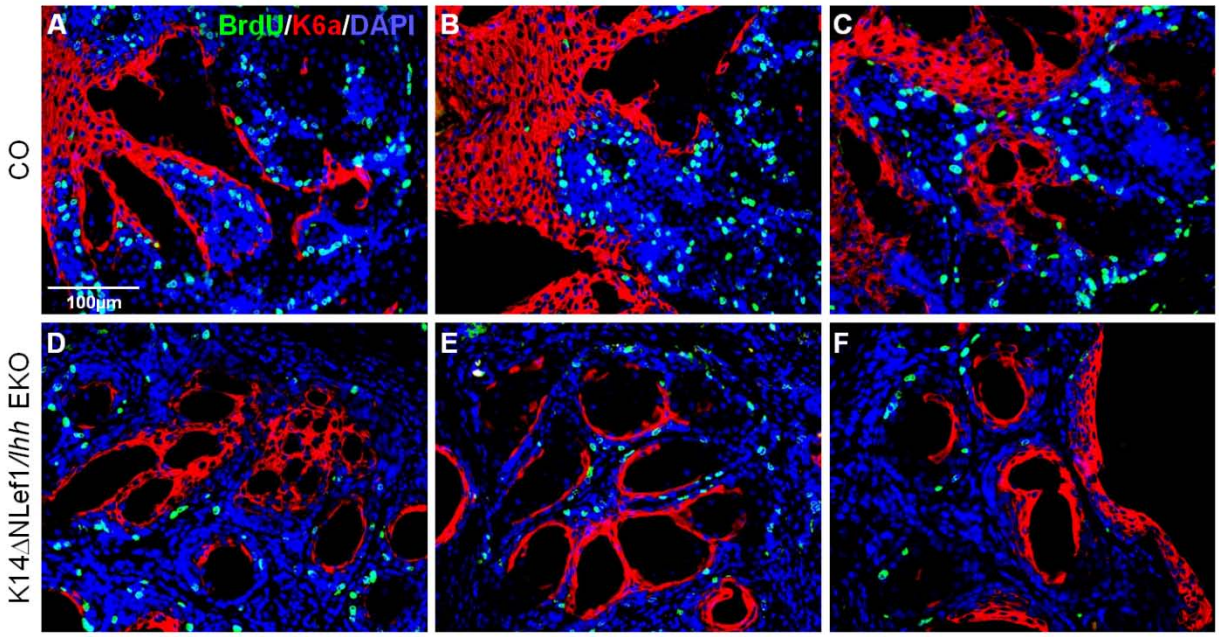

Figure 22: Analysis of proliferation in K6a positive tumour cells.
(A-F) Analysis of K6a (red) and BrdU (green) incorporation to label proliferative cells in sebaceous tumours indicates that K6a expressing cells are not proliferative. K14ΔNLef1/*Ihh* EKO mice **(D-F)** compared to K14ΔNLef1/*Ihh* fl/fl (CO) **(A-C).**The analysis was done with n=15 tumours from n=9-10 mice per genotype. Nuclei are counterstained with DAPI. Scale bar 100µm.

5.3.1.3 Altered differentiation of tumour cells upon loss of Ihh

Based on our observation that Ihh affects differentiation of sebocytes and sebaceous duct-like cell fates in tumours of K14ΔNLef1 mice we asked the question whether the differentiation of other epidermal cell lineages is also altered. For this purpose we used several epidermal differentiation markers.

Keratin 10 (K10) is expressed in keratinocytes of the spinous and granular layer of the IFE and therefore, can serve as a marker for differentiated keratinocytes of the IFE (Fuchs and Green, 1980). In sebaceous tumours of CO mice K10 was broadly expressed in cell layers surrounding the cavities (Fig. 23D). Upon loss of Ihh the number of K10 positive cells is significantly reduced and only very few cells facing the lumen of cavities express K10 (Fig. 23G). This experiment shows that Ihh influences the differentiation of K10 positive keratinocytes normally seen in tumours of K14ΔNLef1 mice. Next, we examined the terminal differentiation marker Involucrin, which is expressed in the granular layer as it differentiates into the cornified envelope and in the infudibulum. In the sebaceous tumours of CO mice Involucrin expression is strongest in regions surrounding the lumen of cavities structures (Fig. 23E). Its expression is dramatically reduced in K14ΔNLef1/*Ihh* EKO tumours: Residual expression is again found at the surface of the large cavities (Fig. 23H).

In addition to markers for the IFE we also examined markers for the HF. We tested several markers (K28, K32, K75, K82 and K81) known to be expressed in different layers within the HF. Only Keratin 81 (K81) was observed to be expressed in the sebaceous tumours. In the HF K81 is expressed in the hair cortex and hair cuticle from above the hair bulb to isthmus zone (IZ). K81 expression is also maintained in tumours derived from this region (Langbein and Schweizer, 2005). In CO sebaceous tumours K81 is expressed in several cell layers around the cavities regions (Fig. 23F); however K81 is dramatically decreased in the tumours of K14ΔNLef1/*Ihh* EKO mice (Fig. 23I).

Taken together these analyses indicate that within the sebaceous tumours Ihh affects the differentiation program of keratinocytes, which are specific for different epidermal compartments.

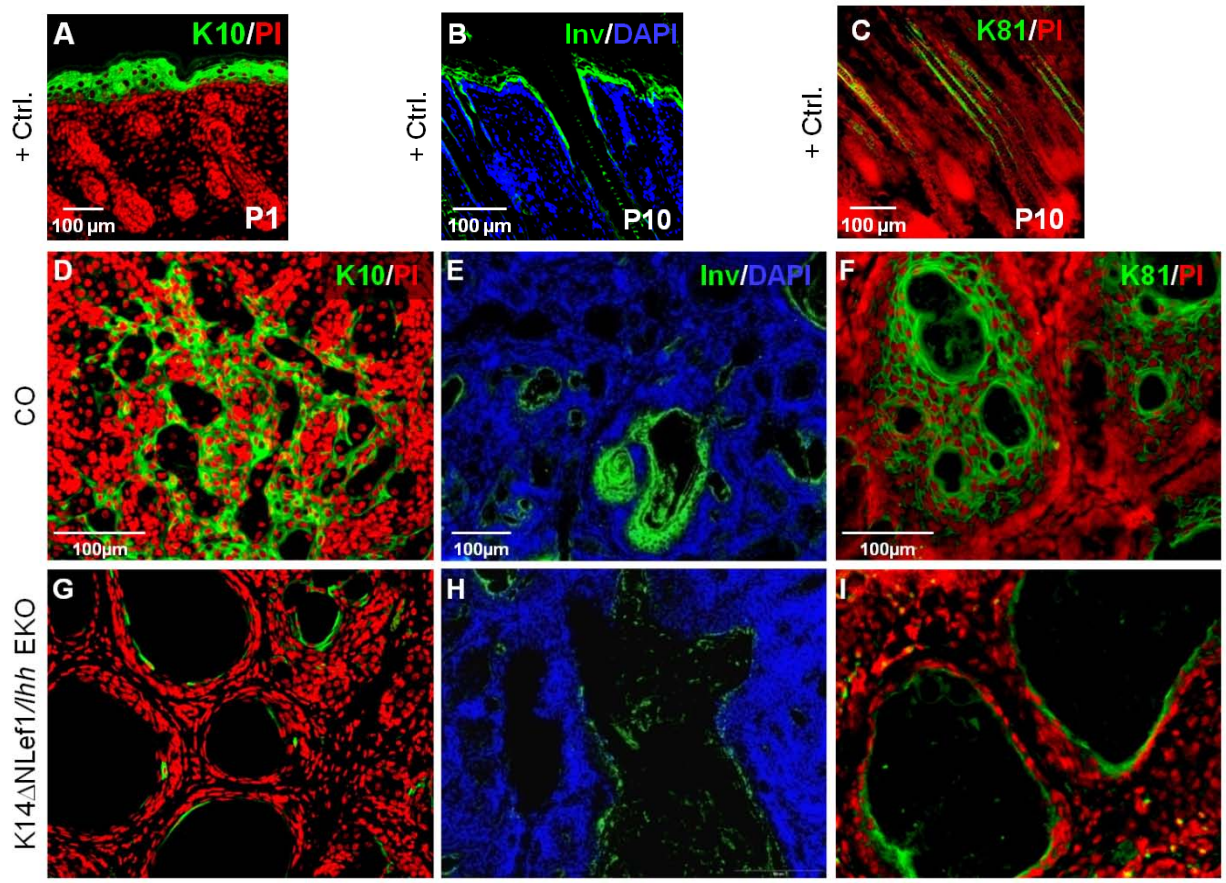

Figure 23: Altered differentiation of tumour cells in K14ΔNLef1/*Ihh* EKO mice.
(A) In normal back skin K10 (green) is expressed in the spinouse and granular layer of IFE, marking the suprabasal layer, **(B)** Involucrin (green) expressed in the spinous layer of IFE and is an early marker of the cornified envelope and **(A)** K81 (green) is expressed in the HF in the bulb to isthmus zone and marks cortex and cuticle of the HF. **(D-F)** Sebaceous tumours of K14ΔNLef1/*Ihh* fl/fl (CO) and **(G-H)** K14ΔNLef1/*Ihh* EKO mice. **(D, G)** K10 (green) co-stained with PI (red). **(E, H)** Involucrin (green) co-stained with DAPI (blue). **(F, I)** K81 (green) co-stained with PI (red). K10 analysed tumours: n=9-13 tumours from n=6-8 mice per genotype. Involucrin analysed tumours: n=3 tumours from n=3 mice per genotype. K81 analysed tumours: with n=9-13 tumours from n=6-8 mice per genotype. Scale bars 100µm, panel **(D, G, F, I)** and **(E, H)** same magnification. K10: Keratin 10; Inv: Involucrin; Keratin 81: K81.

5.3.1.4 Ihh controls the number of progenitor cells in sebaceous tumours

Given the observation that keratinocytes differentiation markers were reduced in K14ΔNLef1/*Ihh* EKO compared to CO we wondered whether this was accompanied by a change in the number of progenitor cells. We first analysed the Keratin 15 (K15) cell population. K15 is a marker for the stem cell population within the HF bulge (Liu et al., 2003; Morris et al., 2004). K15 derived progenitors contribute to HF regeneration during the hair cycle and to IFE regeneration after injury (Ito et al., 2007). In addition, recent studies done in our laboratory demonstrate that K15 derived progeny continuously reconstitutes the SG during skin homeostasis. The K15 derived cells also contribute to the development of sebaceous tumours (Petersson 2010). Therefore, we investigated if the K15 positive cell population (HFSCs) is present within sebaceous tumours and how it is affected by Ihh. Interestingly, the sebaceous tumours of both K14ΔNLef1/*Ihh* EKO and CO mice did not contain K15 positive cells (data not shown).

During normal skin homeostasis Lrig1 (Leucine-rich repeats and immunoglobulin-like domains protein 1) positive cells are localised in the junctional zone (JZ) of HF and contribute to SG and IFE renewal (Jensen et al., 2009). Plet1 (Placental expressed transcript 1) positive cells are located in the Isthmus region (IZ) which extends to the sebaceous gland. Based on their proliferative potential Plet1 positive cells have been suggested to mark a committed progenitor population of hair follicle keratinocytes (Nijhof et al., 2006).

To assess the distribution of committed progenitor cells during the sebaceous tumour development we analysed the expression of Lrig1 and Plet1 in sebaceous tumours. Lrig1 (green) labelling of CO sebaceous tumours (Fig. 24) shows an Lrig1 positive cell layer at the periphery of the sebaceous lobes within the tumours (Fig. 24A-C). In the tumours of K14ΔNLef1/*Ihh* EKO mice, Lrig1 expression appears to be reduced and its distribution is altered compared to CO tumours. Lrig1 positive cells are more concentrated in a narrow region facing the cysts in K14ΔNLef1/*Ihh* EKO tumours.

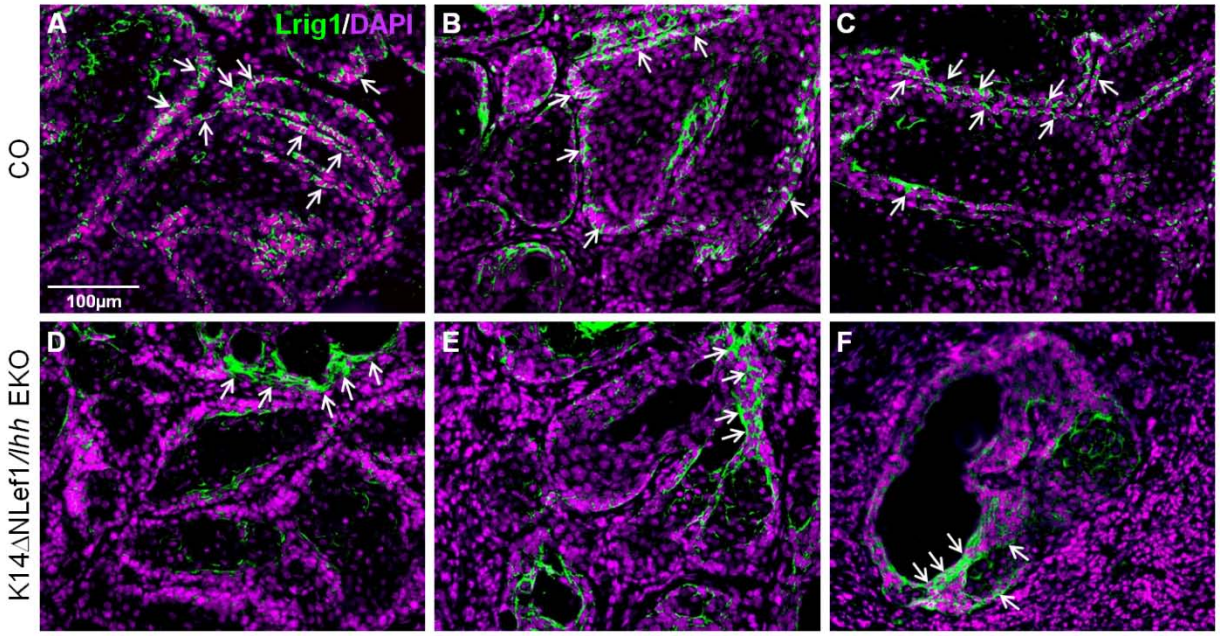

Figure 24: Expression of Lrig1 is altered in tumours of K14ΔNLef1/*Ihh* EKO.
In back skin Lrig1 (green) is expressed in the Junctional zone (JZ) of the HF and extends to the SG, contributing in to SG and IFE renewal. **(D-F)** In sebaceous tumours of K14ΔNLef1/*Ihh* EKO mice Lrig1 (green) is ectopically expressed in the duct like region and its expression is reduced compared to K14ΔNLef1/*Ihh* fl/fl (CO) mice **(A-C)**. The analysis was done with n=8-9 tumours from n=7 mice per genotype. Scale bar 100µm.

Plet1 staining using the 33A10 antibody (green) was combined with staining for the sebocyte marker SCD1 (red) (Fig. 25). In CO sebaceous tumours only a few Plet1 positive cells were observed that localised to the periphery of the cysts. The majority of the cells constituting the tumour expressed the sebocyte marker SCD1. The loss of Ihh in K14ΔNLef1/*Ihh* EKO tumours led to a dramatic change of this expression pattern. The number of Plet1 positive cells surrounding the cyst cavities strongly increased while the number of SCD1 positive cells decreased. The SCD1 positive cells were, in general, restricted to a few islands, separated from the Plet1 positive cell population. Plet1 positive cells are found predominantly, but not exclusively, around the cysts.
These data show that Ihh is involved in determining the relative number of committed progenitor cells in sebaceous tumours. One possible explanation for this result is that Ihh promotes transition from the committed progenitor fate to the terminally differentiated state in tumour cells.

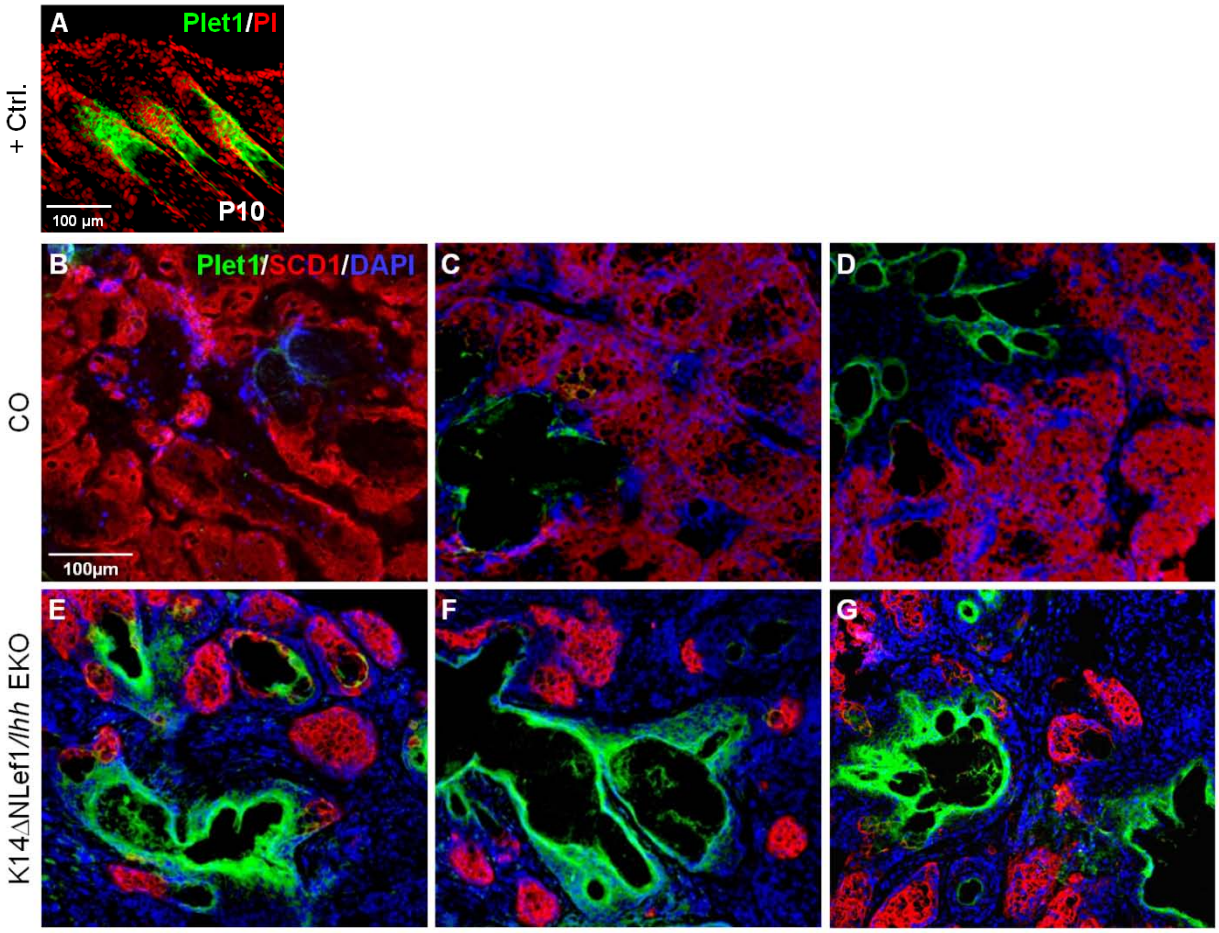

Figure 25: Increased Plet1 positive tumour cells in K14ΔNLef1/*Ihh* EKO mice.
(A) In back skin Plet1 (green) is expressed in the isthmus zone (IZ) of HF and in the sebaceous gland duct. In tumours of K14ΔNLef1/*Ihh* EKO mice Plet1 (green) expression is significantly increased **(E-G)** compared to tumours of K14ΔNLef1/*Ihh* fl/fl (CO) mice **(B-D).** Plet1 (green) counterstained with DAPI (blue). The analysis was done on n=7-9 tumours from n=6 mice per genotype. Scale bars 100µm.

5.3.1.5 Ihh induces proliferation in sebaceous tumours

So far these studies of Ihh function demonstrate that within sebaceous tumours Ihh is required for the differentiation of keratinocytes at the expense of committed progenitor cell populations. We next asked the question whether Ihh affects the proliferation of epithelial cells in sebaceous tumours. To this end we administered a pulse of Bromodeoxyuridine (BrdU) to label proliferating cells shortly before harvesting the tumour tissue. Sections of the sebaceous tumours were co-stained with BrdU (green) and K14 (red) (Fig. 26). Interestingly, after loss of Ihh the number of BrdU positive cells is dramatically reduced within sebaceous tumours (Fig. 26E-H) when compared with CO tumours (Fig. 26A-D). The majority of proliferating cells are located in the tumour lobules whereas very few cell divisions are observed within the stroma of tumours if either K14ΔNLef1/*Ihh* EKO or CO mice. In the K14ΔNLef1/*Ihh* EKO tumours the small number of BrdU positive cells was restricted to the cyst-like structures.

Quantification of BrdU positive cells (normalised to total cell number) in sebaceous tumours indicates in average a 2.2 fold reduction in absence of Ihh (11.3 ± 2) compared to CO (25.1 ± 2.9) (Fig. 26K). In addition, analysis of Ki67 immunostaining supports our observation that in sebaceous tumours of *Ihh* EKO mice keratinocyte proliferation is reduced (data not shown). This result was surprising because the determination of tumour size indicates that the tumours of K14ΔNLef1/*Ihh* EKO mice are significantly larger than tumours of CO mice (Fig. 18D). However, morphological analysis of sebaceous tumours revealed that in absence of Ihh the histology of tumours was different when compared to tumours of CO mice. The tumours lacking Ihh contain a high number of large cavities often with only thin layers of epithelial cells surrounding the lumen (e.g. compare Fig. 26C to Fig. 26G). This observation suggests that the large size of the tumours from K14ΔNLef1/*Ihh* EKO mice is caused by changes in the architecture of the tumour tissue, rather than by an increase in tumour cell number.

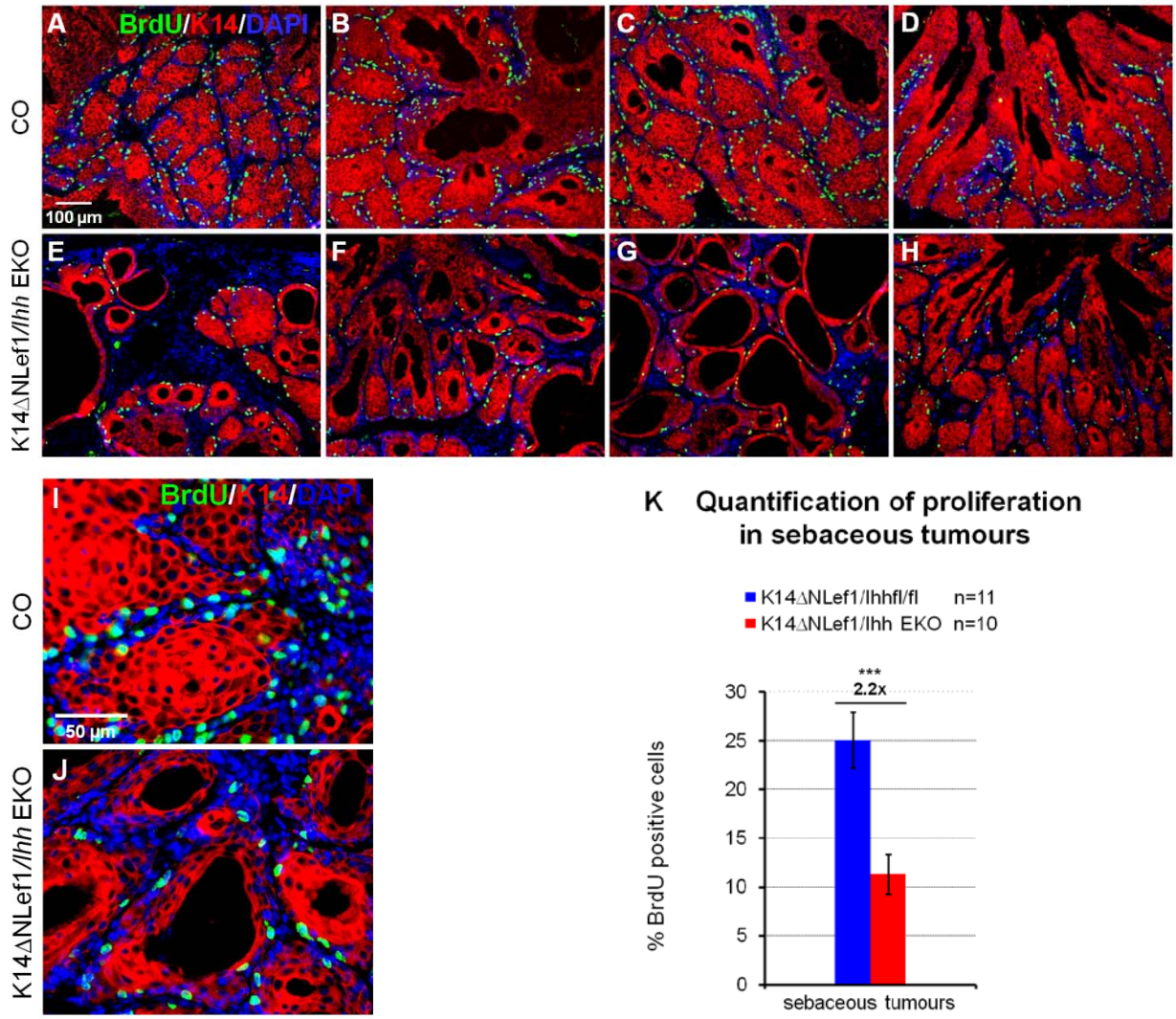

Figure 26: Reduced proliferation in sebaceous tumours of K14ΔNLef1/*Ihh* EKO mice.
(A-J) Analysis of BrdU (green) incorporation in sebaceous tumours. BrdU (green) co-stained with K14 (red) and DAPI (blue). **(E-H, J)** In sebaceous tumours of K14ΔNLef1/*Ihh* EKO mice BrdU positive cells are dramatically reduced compared to CO mice **(A-D, I). (I-J)** Higher magnification of sebaceous tumours. **(K)** Quantification of BrdU positive cells indicates a 2.2 fold reductions in sebaceous tumours lacking Ihh (red bar; 11.3 ± 2) compared to CO (blue bar; 25.1 ± 2.9). BrdU positive cells were normalised to total number of sebaceous tumour cells. The analysis was performed with n=11-20 tumours from n=7-11 mice per genotype. Scale bar 100µm **(A-H)** and 50µm **(I-J)**. Quantified 5 different areas on a single slide using ImageJ. Error bars are ± s.d., Student´s *t*-test, ***P=3x 10^{-41}.

5.3.2 The function of Ihh signaling for development of papilloma and progression into squamous cell carcinoma (SCC)

Given our observation that Ihh influences the architecture, proliferation and differentiation of sebaceous tumours we wondered whether the same applies to other types of skin tumours like papilloma and squamous cell carcinoma (SCC). To this end, we performed a two-stage carcinogenesis experiment (Fig. 27). In this experiment, a single treatment of the skin with a tumour initiator e.g. DMBA (7,12-dimethylbenz[*a*]anthracene) induces many mutations including, occasional mutations in H-Ras. Subsequently, the skin is repeatedly treated with a tumour promotion agent, the phorbol ester TPA (12-*O*-tetradecanoylphorbol-13- acetate) which stimulates proliferation, thereby expanding the cell pool containing DMBA-induced mutations. Finally, this leads to the development of benign papilloma. Eventually, a small number of papilloma will progress into malignant SCC (Fig. 27). Susceptibility to two-stage skin carcinogenesis in mice is known to be highly dependent on the genetic background of the mice (DiGiovanni, 1992). The *Ihh* EKO mice used for this study are in more tumour-resistent C57BL/6 background. Therefore, TPA was applied three times weekly with a dose of 6nmol/200µl per mouse. The application of DMBA was 100nmol/200µl per mouse (Sundberg et al., 1997; Abel et al., 2009).

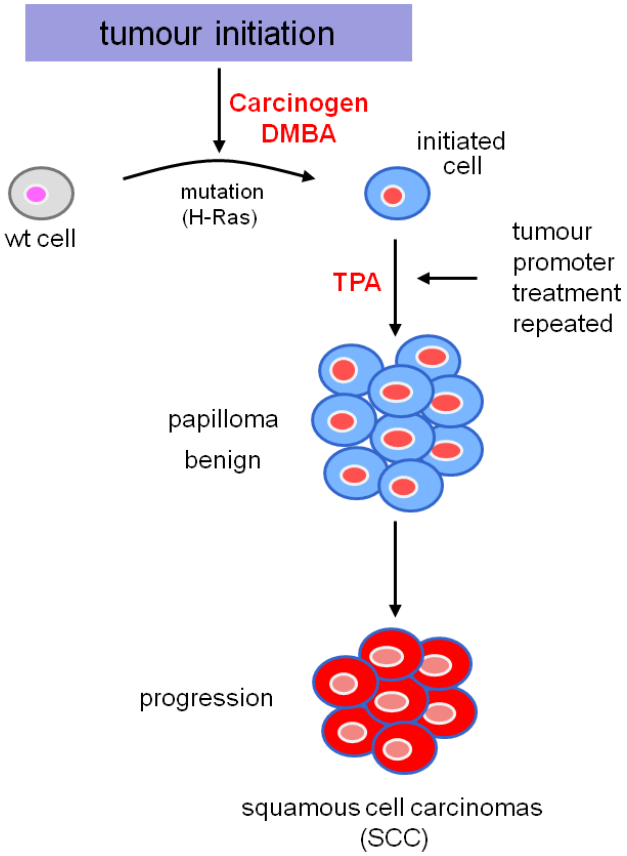

Figure 27: Scheme of a two-stage skin carcinogenesis experiment.
In the classical two-stage skin carcinogenesis experiment mice receive a single topical, sub-threshold dose of carcinogen (DMBA) for tumour initiation and repeated treatment of tumour promoter (TPA). Mice develop benign papilloma which can progress in malignant SCC. (Modified after Weinberg, 2007).

5.3.2.1 Ihh reduces the incidence and frequency of papilloma and promotes tumour growth

In order to address the function of Ihh in papilloma formation 9 weeks old mice (onset of second telogen) were used for a two-stage carcinogenesis experiment. The skin of *Ihh* EKO (n=19) and CO (*Ihh* fl/fl, n=19) littermates was treated with a single sub-threshold dose of the carcinogen DMBA to initiate mutations or with acetone vehicle (Fig. 28A). One week later mice received the tumour promoter TPA or acetone vehicle three times weekly up to 25 weeks to promote cell growth (Fig. 28A). In addition control groups, for both genotypes, Ihh EKO and CO, were treated with DMBA alone (n=5mice per genotype), TPA alone (n=5mice per genotype) and acetone alone (n=1 mouse per genotype). None of the mice in the control groups developed tumours indicating that all observed effects were due to the experimental treatment.

First tumours were observed 13 weeks after DMBA treatment for both genotypes. Scoring of tumours was carried out once a week for up to 50 weeks following DMBA treatment. Interestingly, in Ihh EKO mice both incidence (*Ihh* EKO=90% and CO=68 % mice with tumours) and tumour frequency (*Ihh* EKO=2.9 and CO=2.1 tumour/mouse) were increased then compared to CO mice. The most pronounced effect ($P<0.05$) was observed between 19 to 23 weeks after tumour initiation (Fig. 28B, C). In addition, 17-50 weeks after DMBA treatment mice lacking Ihh carried significantly smaller papilloma than CO mice (Fig. 28D) and this effect was more pronounced at later time points of the tumour experiment ($P<0.04$).

Our data indicate that Ihh suppresses the development of benign papilloma in mice, but once tumours are established Ihh promotes proliferation of tumour cells to increase size of the tumours.

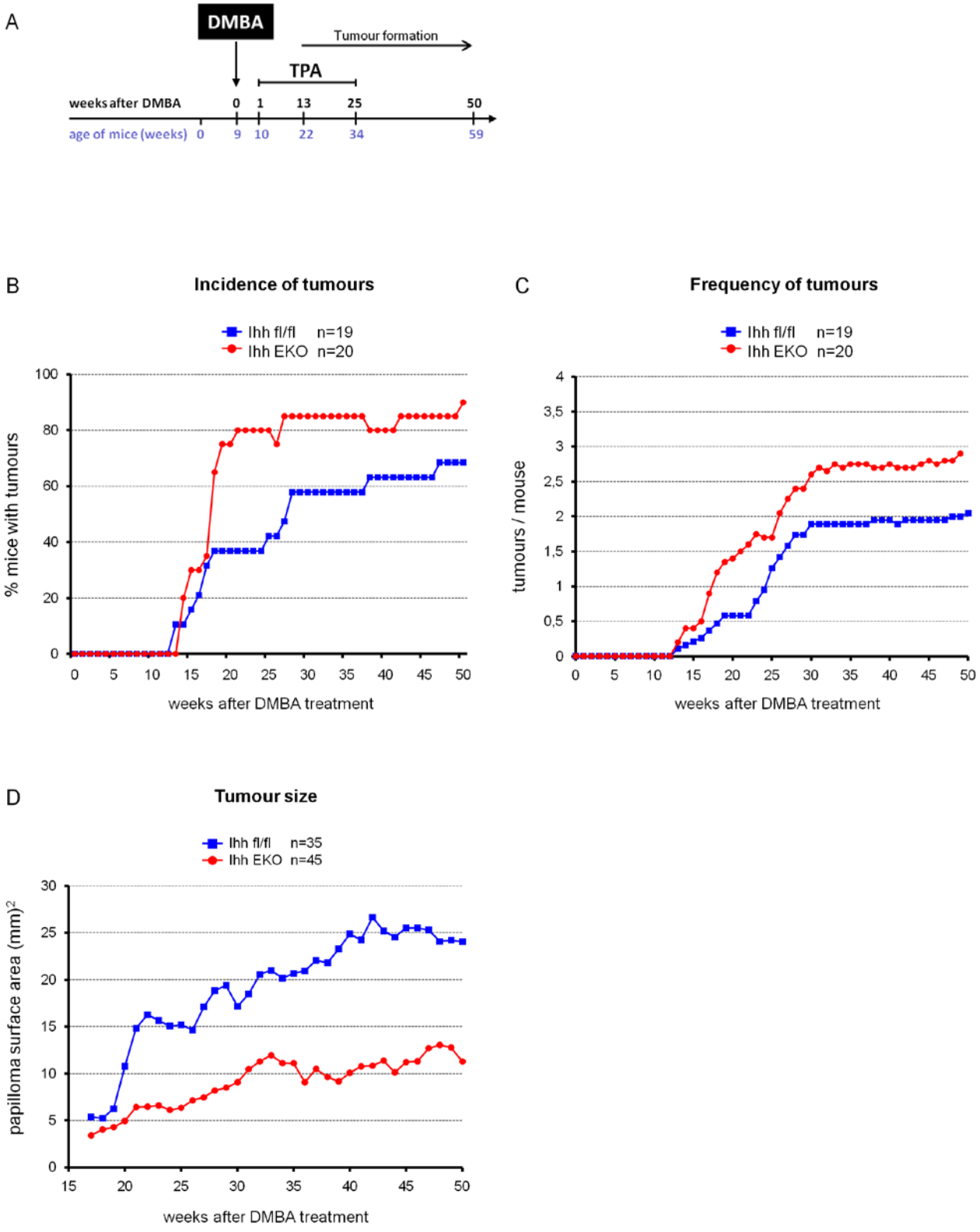

Figure 28: Ihh suppresses incidence and frequency of papilloma but increases tumour size.
(A) Time line of two-stage skin carcinogenisis experiment. **(B)** *Ihh* EKO mice (red line) showed an increased incidence of papilloma compared to CO (*Ihh* fl/fl) (blue line). **(C)** The frequency of papilloma is also higher in *Ihh* EKO (red line) mice (P<0.05 between 19-23 weeks after DMBA). **(D)** Quantification of tumour size indicates that mice lacking Ihh (red line) develop significantly larger tumours than CO mice (blue line) (P<0.05 between 34-46 weeks after DMBA). n=19 CO, n=20 *Ihh* EKO with DMBA/TPA, n=10 mice per genotype for acetone controls, Student´s *t*-test.

5.3.2.2 Increase in progression of benign papilloma into malignant carcinoma in *Ihh* EKO mice

One important observation from the two-stage carcinogenesis experiment was that a higher number of papilloma (2.5 fold) progressed to invasive SCC (19.6%) in *Ihh* EKO compared to CO mice (7.9%) (Fig. 29A). Furthermore, while conversion of papilloma into SCC was seen for the first time at 26 weeks after tumour initiation in both *Ihh* EKO and CO mice, a significantly higher number of tumours had progressed into SCC in *Ihh* EKO at the end of the experiment (55% *Ihh* EKO mice vs. 16% of CO mice) (Fig. 29B).

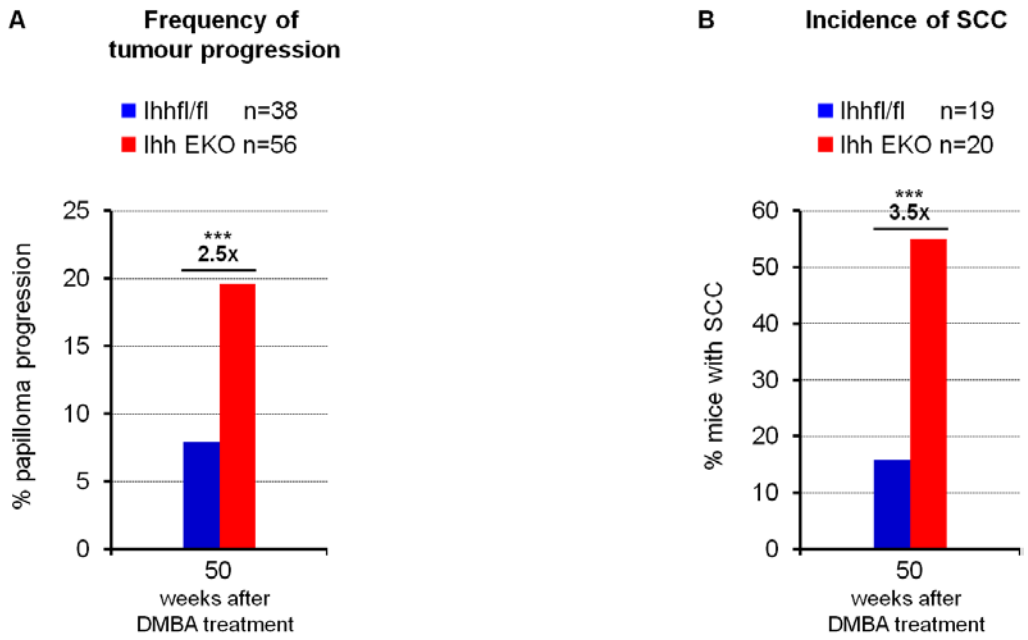

Figure 29: Increased tumour progression into SCC in *Ihh* EKO mice.
(A) Number of papilloma progressing to SCC in *Ihh* EKO mice is 2.5 fold higher than in *Ihh* fl/fl (CO) mice **(B)** incidence of formation of SCC in *Ihh* EKO (red) and CO (blue) mice. CO: n=3 SCC from n=3 mice; Ihh EKO: n=11 SCC from n=11 mice was recorded. For more detail see (Fig. 28). Student´s *t*-test, ***P<0.0005

Papilloma of CO mice show a clear layering of the thickened epidermis in which the transition to the cornified layer is always visible (Fig. 30A-C). Papilloma from Ihh EKO mice on the other hand frequently showed less differentiation of the suprabasal layers (data not shown). In particular, a

clearly discernable cornified layer was frequently lacking (Fig. 30E). This observation is corroborated by staining for K10, a marker for suprabasal keratinocytes (Fig. 30I-N). The number of K10 positive cells is strongly reduced in papilloma of *Ihh* KO mice (Fig. 30L-N) compared to papilloma of CO mice (Fig. 30I-K). Together these data suggest that Ihh influences the cellular composition of papilloma by promoting keratinocyte differentiation.

The phenotypic difference between absence and presence of Ihh is even more pronounced in the case of SCC. While SCC from CO mice show distinct epithelial lobules that allow one to distinguish stromal from epithelial areas (Fig. 30D), SCC from *Ihh* EKO mice have a more homogeneous organisation with small epithelial islands interspersed with stromal tissue (Fig. 30F). Moreover, 5 out of 11 SCC from *Ihh* EKO mice were largely composed of poorly differentiated tissue lacking separate stromal and epithelial compartments (Fig. 30G-H). In these poorly differentiated SCC high numbers of mitotic figures were observed (see insets in Fig. 30G-H). These tumours show histological similarity to spindle cell carcinoma, an aggressive, albeit relatively rarely occurring subtypes of SCC (Abel et al., 2009; Klein-Szanto, 1989).

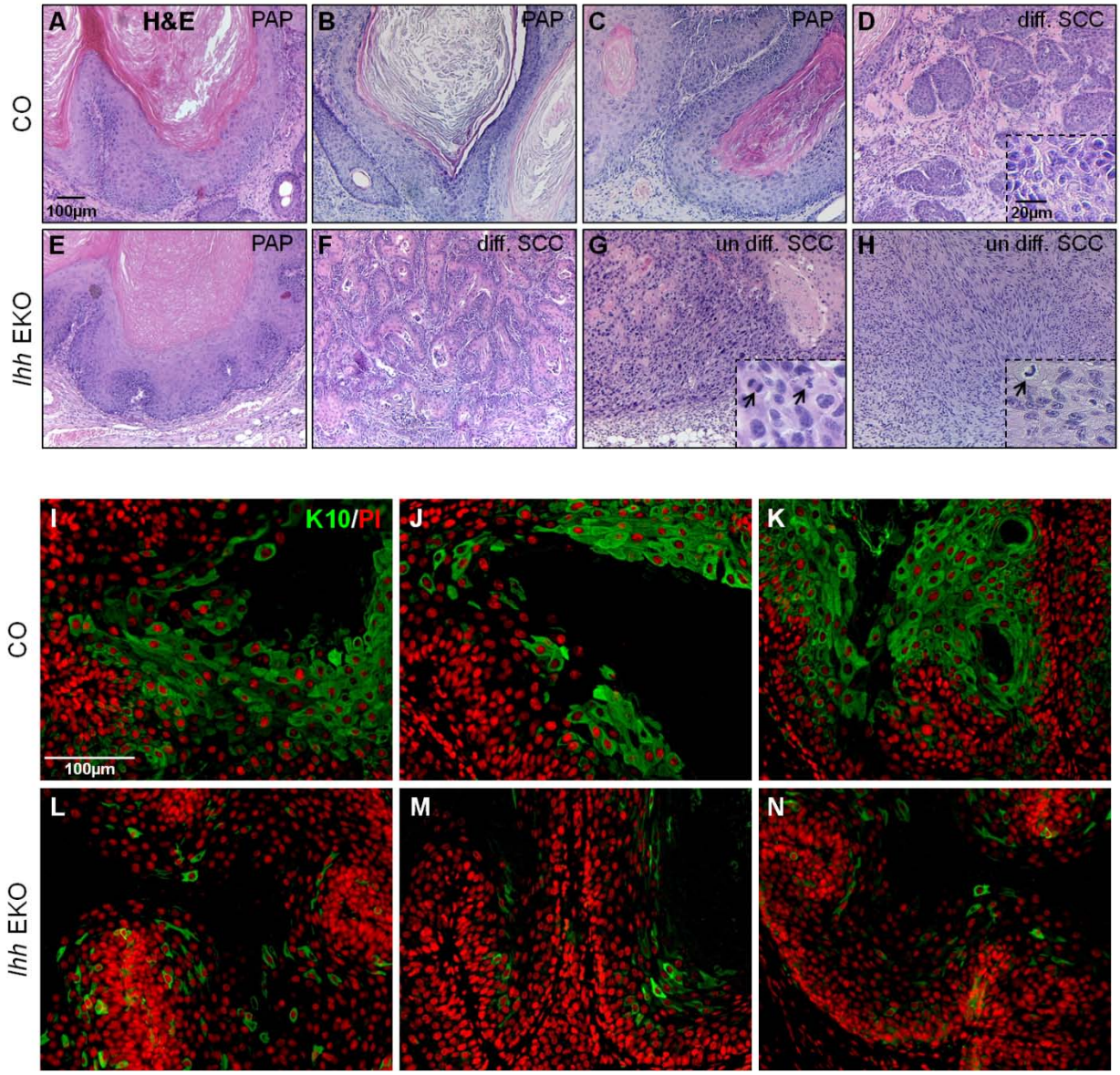

Figure 30: Reduced K10 expression in squamous tumours and increased progression into SCC in *Ihh* EKO mice. Histological analysis of papilloma (PAP) from *Ihh* EKO mice **(E)**, *Ihh* fl/fl (CO) **(A-C)** and SCC from *Ihh* EKO mice **(F-H)** compared to SCC in *Ihh* fl/fl (CO) mice **(D)**. Mitotic figures were frequently observed in poorly differentiated SCC of *Ihh* EKO mice **(G-H)** Inset of high magnified view. Black arrows point to mitotic cells**.** The analysis of tumours was done with n=38 tumours from n=19 CO mice and n=56 tumours from n=20 mice. **(I-N)** In *Ihh* EKO mice **(L-N)** the papilloma are poorly differentiated and the number of K10 (green) positive cells is reduced compared to *Ihh* fl/fl (CO) **(I-K)**. The analysis of tumours was done with n=3 tumours from n=3 mice per genotypes. Scale bar 100µm **(A-N)** and 20µm of **(**Inset **D, G, H)**

5.3.2.3 Metastasis of SCC in *Ihh* EKO mice

During the course of the tumour experiments every sacrified mouse was dissected and all organs were checked for gross-morphological abnormalities. At the end of the two-stage tumour experiment 2 out of 20 *Ihh* EKO mice (of age 60 and 68 weeks, respectively) were found to have metastases in lymph nodes (Fig 31B-C). Affected lymph nodes were found in different areas of the body. No CO mouse was observed with metastasis to any organ (Fig 31A). Histological analysis of metastases in lymph nodes (Fig 31B-C) demonstrates morphology similar to that of SCC (Fig 31A). Immunostaining for K14 (green), a marker of basal epithelial cells, shows K14 expression in the majority of keratinocytes in the SCC (Fig 31E) as well as in the cells which have invaded the lymph nodes of the two *Ihh* EKO mice (Fig 31F-G). In contrast, no K14 positive cells could be detected in lymph nodes of CO mice (Fig 31H). Although more mice need to be analysed in the future these results indicate that Ihh inhibits the occurrence of metastasis.

Taking together the two-stage carcinogenesis experiments suggests that Ihh inhibits the initiation of benign papilloma, the progression of papilloma to SCC and the acquisition of metastatic behaviour. However, the data also suggest that Ihh promotes proliferation of tumour cells.

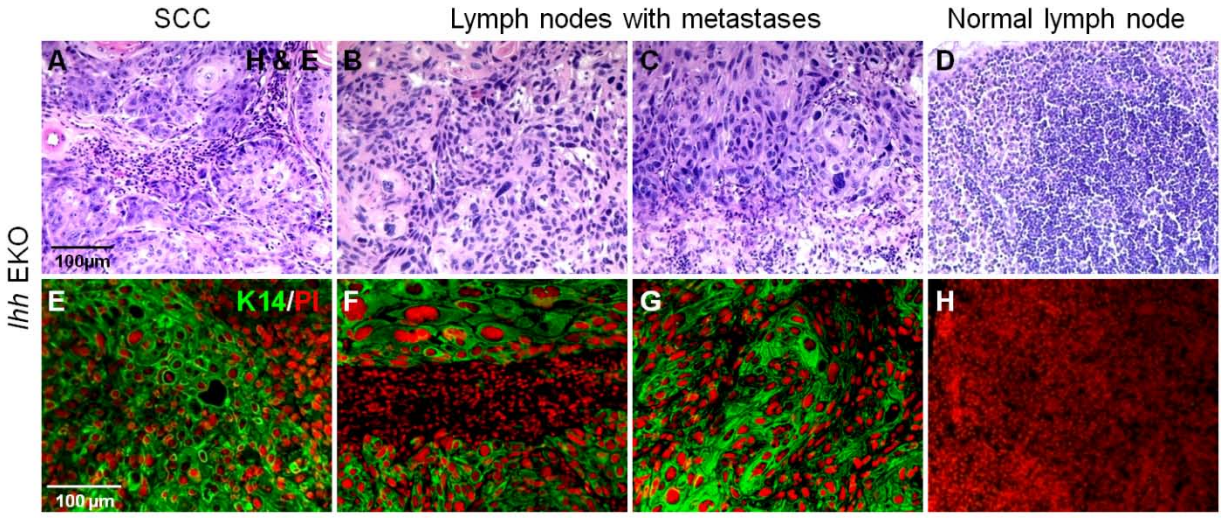

Figure 31: Ihh suppresses the metastasis of SCC.
(A) Histology of SCC, **(B-C)** lymph nodes with metastases and **(D)** lymph node with non invasive SCC in *Ihh* EKO mice. H&E: Haematoxylin-eosin staining**. (E-H)** Metastasis of lymph nodes was labelled with anti K14 (green) antibody counter stained with PI (red). Scale bars 100µm **(A-D)** and **(E-H)**.

5.3.2.4 Ihh stimulates proliferation in papilloma

Measurements of tumour size suggesed that proliferation was altered in benign papilloma of *Ihh* EKO mice. Therefore, we analysed BrdU incorporation. We restricted our analysis to papilloma of medium size (4-8mm) to avoid heterogeneity due to differences in tissue organisation. To assure that the BrdU positive nuclei were confined to epithelial cells within the heterogeneous tumour tissue, tumour sections were also immunostained with an antibody detecting K14 (Fig. 32A-J). The vast majority of keratinocytes within the papilloma are positive for K14 in both *Ihh* EKO and CO mice. In papilloma of control mice the majority of dividing cells are located at the periphery of epithelial lobes within the tumour (Fig. 32A-D, I). Only very few cells in S-phase are observed within the stroma of papilloma from both *Ihh* EKO and CO mice (data not shown). In contrast, the number of proliferating cells was dramatically reduced in absence of Ihh (Fig. 32E-H, J). The quantification of BrdU positive cells revealed a twofold reduction in mice lacking Ihh (15.8 ± 1.1) compared to CO mice (31 ± 0.9) (Fig. 32K).

These data indicate that the reduced size of papilloma measured in *Ihh* EKO mice (Fig. 27D) is a consequence of inhibited proliferation of undifferentiated tumour cells.

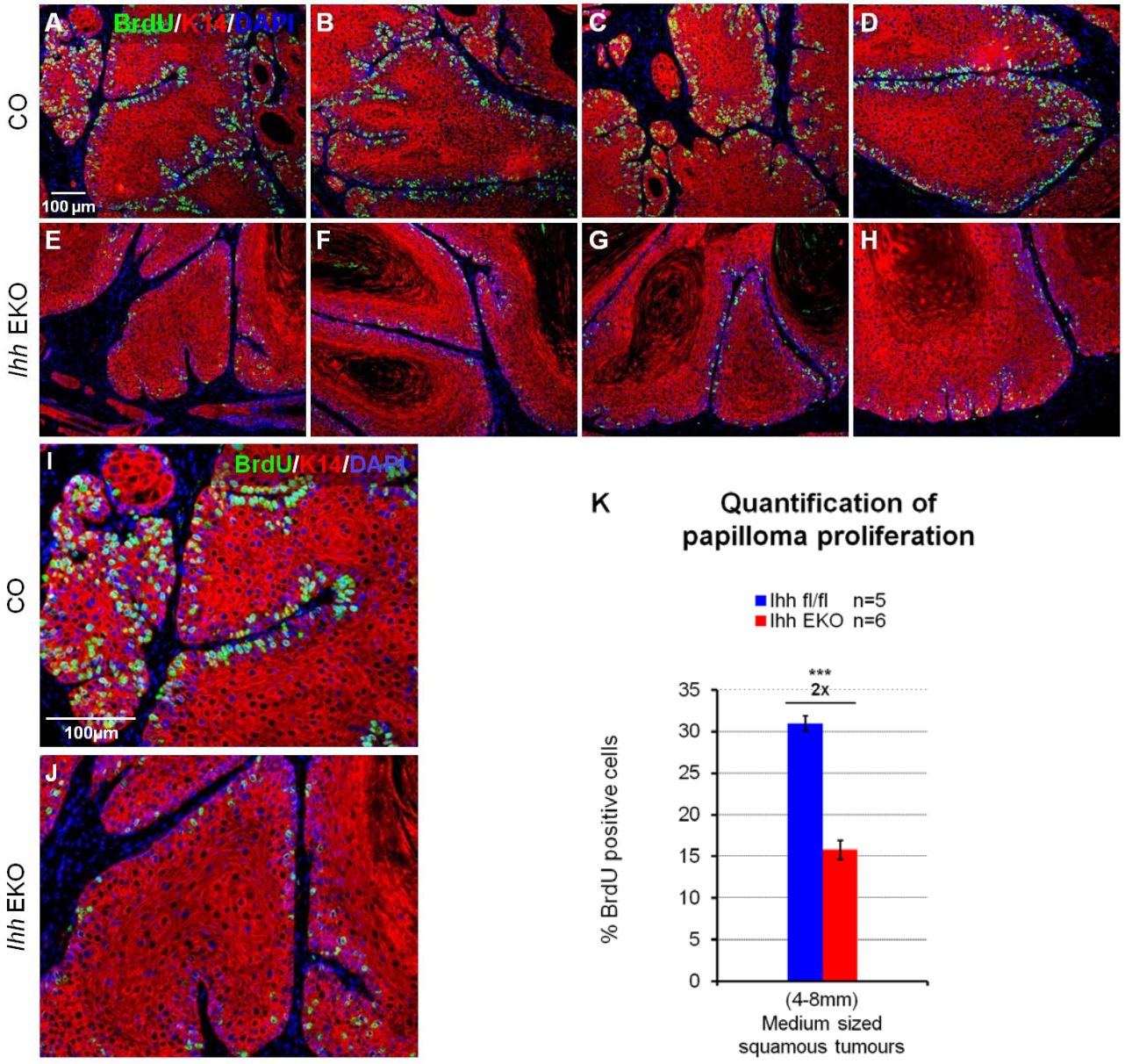

Figure 32: Reduced proliferation in squamous tumours of *Ihh* EKO mice.
(A-J) BrdU incorporation was analysed. BrdU (green) co-stained with K14 (red) and DAPI (blue). **(E-H, J)** In papilloma of *Ihh* EKO mice the BrdU positive cells are dramatically reduced compared to CO mice **(A-D, I). (I-J)** Higher magnification of papilloma co-stained with BrdU (green), K14 (red) and DAPI (blue). **(K)** Quantification of BrdU positive cells in medium size papilloma lacking Ihh (red bar; 15.8 ± 1.1) compared to CO (blue bar; 31 ± 0.9). The BrdU positive cells normalized to the total number of the DAPI positive nuclei. The analysis was done with n=5-6 tumours from n=4-5 mice per genotype. Scale bars 100µm **(A-H)** and **(I-J)**. Error bars are ± s.d., Student´s *t*-test, ***P=3x10^{-39}.

5.4 Molecular mechanisms of Ihh signalling in skin tumours and normal skin

5.4.1 Ihh regulates p53 nuclear accumulation in benign squamous papilloma

Recent studies have revealed links between the p53 tumour suppressor and Gli1 in maintaining neural stem cell number and brain tumour formation (Clement et al., 2007; Stecca and Ruiz i Altaba, 2009; Prykhozhij, 2010; Malek et al., 2011). To address the question whether Hh signalling could also play a role in regulating p53 in skin tumours, we analysed benign squamous tumours of KO and control mice for p53 expression. p53 immunfluorescence staining (green) was performed on sections of medium size papilloma (4-8mm diameter) of *Ihh* EKO and CO mice (Fig. 33A-L). Interestingly, in papilloma lacking Ihh the number of p53 positive nuclei is significantly higher than in tumours of CO mice. This observation correlates with our previous results demonstrating reduced proliferation upon loss of Ihh. Since p53 is an important mediator controlling cellular proliferation, one possible explanation for our results could be that Ihh signalling promotes proliferation by reducing p53 nuclear accumulation.

Next we investigated if regulation of p53 is also seen in other types of skin tumours lacking Ihh.

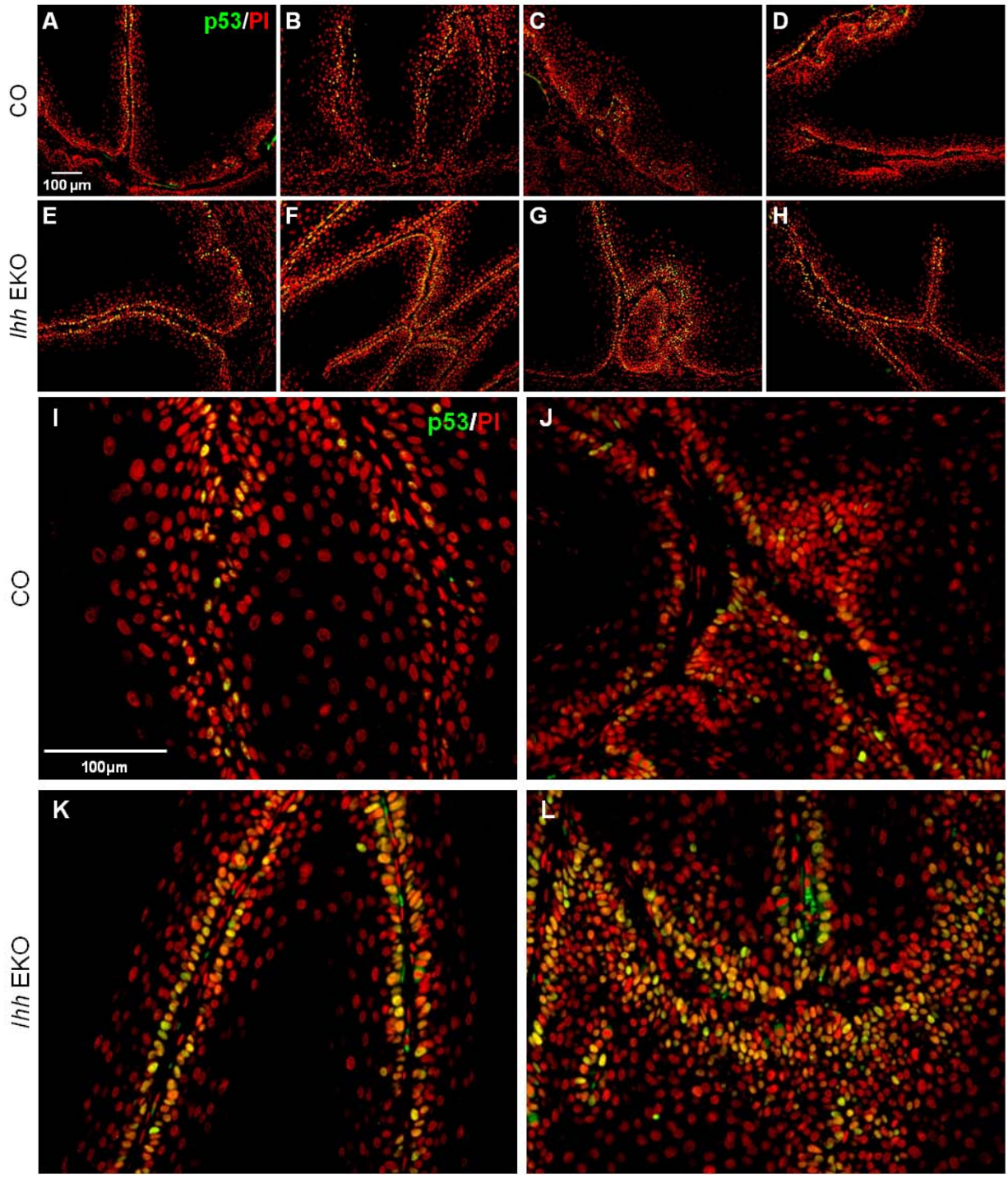

Figure 33: p53 positive cell numbers are altered in papilloma of *Ihh* EKO mice.
(A-L) Analysis of p53 (green) expression counterstained with PI (red). In papilloma of *Ihh* EKO mice **(E-H, K-L)** nuclear accumulation of p53 is dramatically increased compared to CO **(A-D, I-J). (I-L)** Higher magnified view of paillomas. n=4 tumours from n=4 CO mice and n=6 tumours from n=6 *Ihh* EKO mice were used for this analysis. Scale bars 100µm.

5.4.2 Ihh regulates p53 in sebaceouse tumours

Previously, it has been demonstrated using specific immunfluorescence staining that sebaceous tumours developing in K14 ΔNLef1 tg mice were either negative for p53 or had only a small number of p53 positive cells (Niemann et al. 2007). In addition, it was shown that Ihh expression is dramatically increased in sebaceous tumours (Niemann et al., 2003). Therefore, we inverstigated if p53 levels are changed in sebaceous tumours lacking epidermal Ihh. To this end, we performed western blots analysis to determine the p53 protein level in sebaceous tumours. Analysis of 9 tumours from n=9 K14ΔNLef1 /*Ihh* EKO (k1-k9) and n=9 CO (c1-c9) mice indicates that within the majority of sebaceous tumours lacking Ihh, p53 protein level is increased compared to tumours of CO mice (Fig. 34A). Some variation in p53 level was seen, most likely reflecting the cellular heterogeneity of tumours. On average the p53 protein level is fourfold increased in sebaceous tumours of *Ihh* EKO mice compared to CO (Fig. 34D). This data clearly indicates that in addition to squamous papilloma Ihh regulates p53 in sebaceous tumours of K14ΔN*Lef1* transgenic mice.

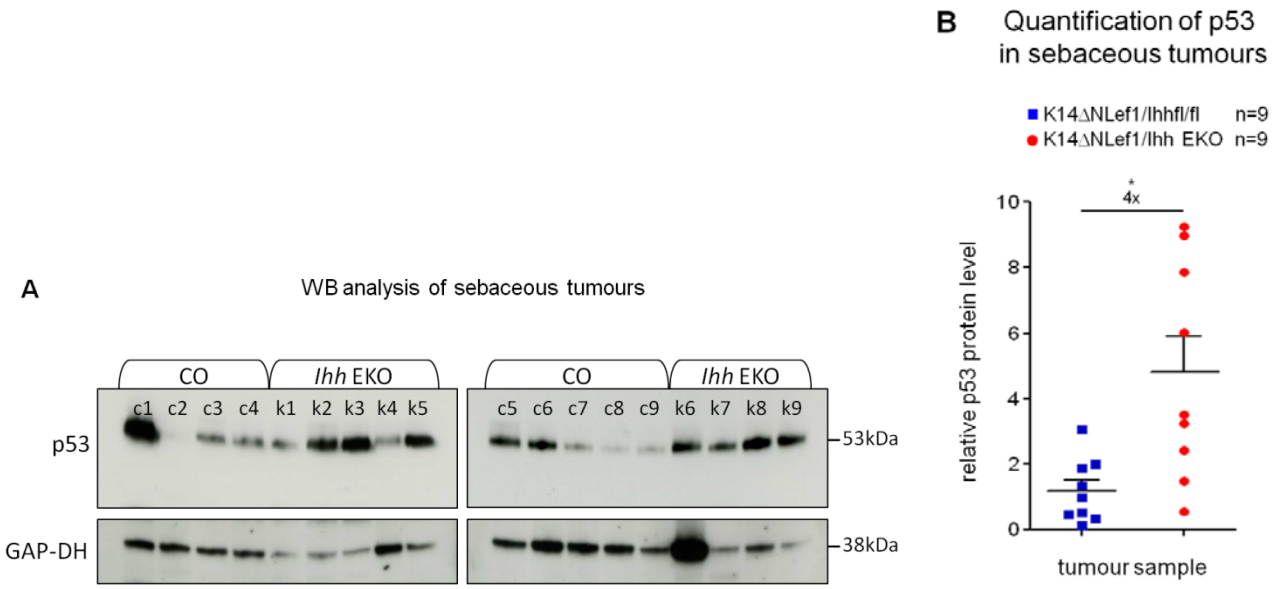

Figure 34: Ihh affects the level of p53 protein in sebaceous tumours.
(A) Western blot analysis (WB) was performed to quantify p53 protein levels in sebaceous tumours of K14ΔNLef1/*Ihh* EKO (k1-k9) and CO (c1-c9) mice. GAP-DH was used for a loading control. P53=53kDa, GAP-DAH=38kDa. **(B)** Quantification of p53 protein level using ImageJ standardised to GAP-DH. K14ΔNLef1/*Ihh* EKO (red bars) compared to K14ΔNLef1/*Ihh* fl/fl (CO) (blue bars). Error bars are ± s.e.m, Student´s *t*-test, *P<0.05.

5.4.3 Ihh regulates p53 during epidermal morphogenesis

The regulation of p53 levels seen in tumours of Ihh EKO mice raised the question whether Ihh affects p53 during normal skin development. Western blot analysis with lysates of skin samples indicates no consistent difference in total p53 protein amount during postnatal stages (P0-P10) between *Ihh* EKO and CO mice (data not shown). However, lysates were prepared from skin tissues containing dermal and epidermal cells and thus do not allow one to detect aberrant p53 levels specifically in keratinocytes. Therefore we analysed p53 expression by immunofluorescent antibody staining in the skin of neonatal mice between P0 to P10 (Fig. 35A). In skin of CO mice few p53 positive nuclei were observed. In contrast, in absence of epidermal Ihh the number of p53 positive nuclei is significantly increased until P10 during postnatal development. Quantification of these immunostainings revealed that the number of p53 positive cells was 9 to 37 fold higher in the epidermis of *Ihh* EKO mice when compared to CO littermates (Fig. 35A). Accumulation of p53 was observed in keratinocytes of the IFE, HF and SG. Interestingly, the strongest increase of the p53 signal was detected in the infundibulum of the HF. Additionally, p53 accumulation was also seen at later stages of skin development (P14) and in adult *Ihh* EKO mice (6 month and 12 month of age) (data not shown). No nuclear p53 was detected in undamaged adult skin of control mice.

Together with our analysis of skin proliferation (chapter 5.2.3) the data show a strong correlation between reduced proliferation during early postnatal stages (P0-P2) and p53 accumulation in the absence of epidermal Ihh. However, an increased number of p53 positive nuclei were also observed in the epidermis during later development and in the adult skin of *Ihh* EKO mice although no changes in epidermal proliferation was detected. In the future it will be important to understand the molecular mechanism of p53 regulation by Ihh. However, our data indicate that modulation of p53 by Ihh is not tumour specific but also occurs during normal skin homeostasis.

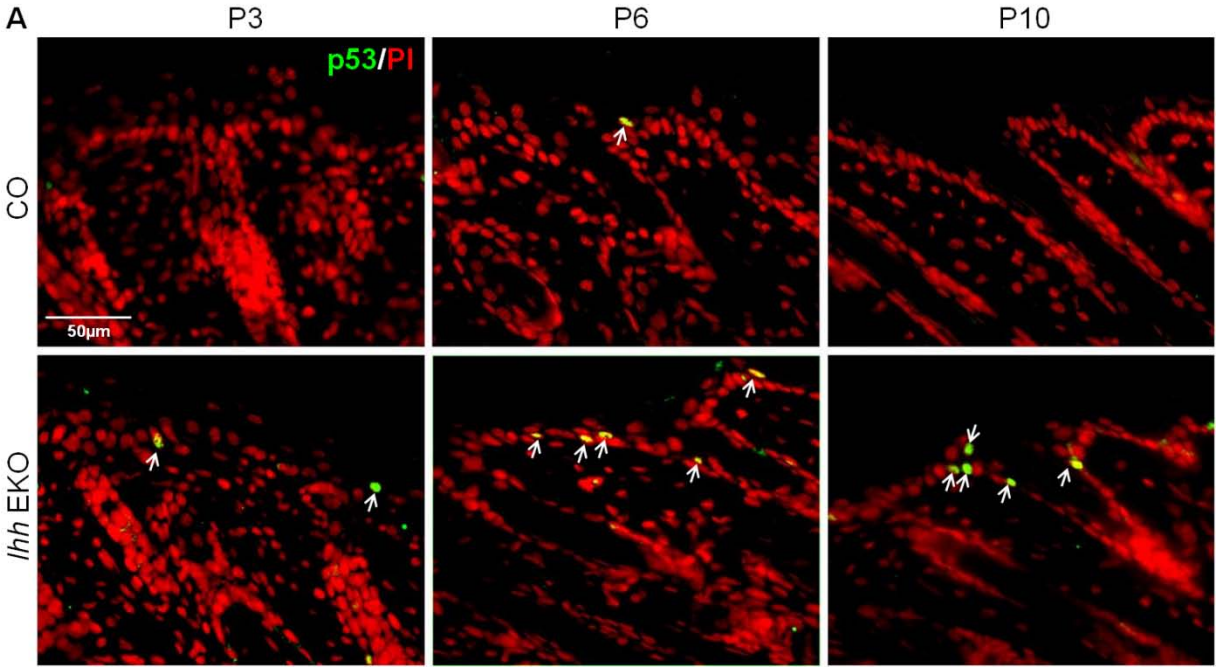

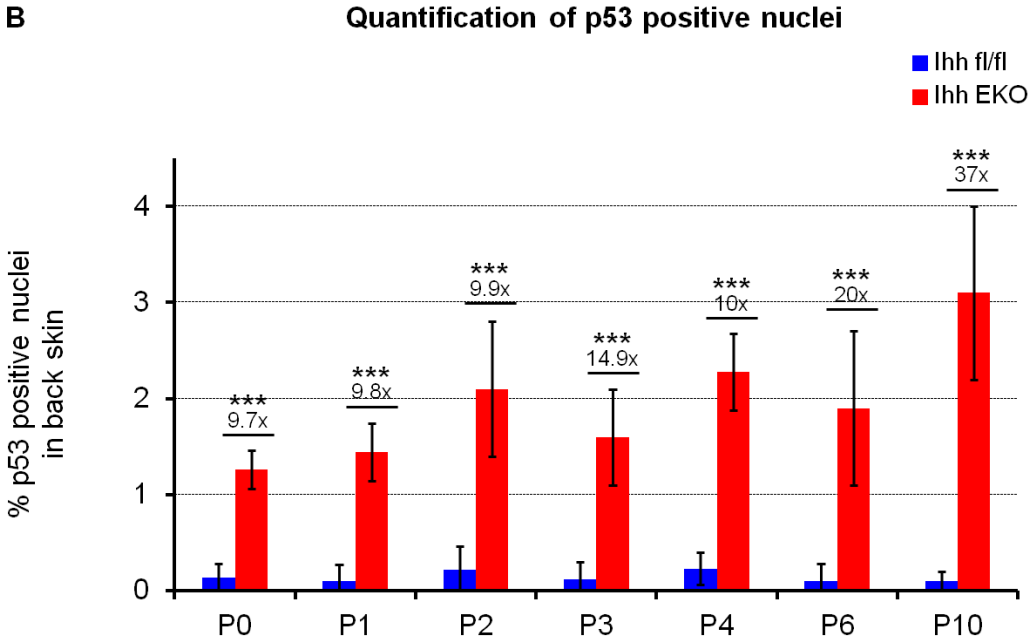

Figure 35: Stimulation of nuclear accumulation of p53 in the epidermis of *Ihh* EKO mice.
(A) Detection of p53 (green) in the skin of *Ihh* EKO (lower panel) and CO (upper panel) mice at postnatal stages (P0-P10). **(B)** Quantification of p53 positive nuclei during postnatal stages (P0-P10) in *Ihh* EKO (red bars) and CO (blue bars) mice. p53 quantification and staining of each postnatal stage (P0-P10) was done with matched littermate samples (n=2-5 mice per genotypes) in duplicate and analysing 5-10 different areas (position) per slide using ImageJ. Scale bar 50µm. Error bars are ± s.d., Student´s *t*-test, ***P<0.0005.

6 Discussion

Over the past years several groups have shown that Hh signalling plays an important role for sebaceous gland (SG) physiology both in humans and mice (Niemann et al., 2003; Allen et al., 2003, Takeda et al., 2006; Lo Celso et al., 2008; Gu and Coulombe, 2008; Bonfanti et al., 2010; Séquaris et al., unpublished data). Among the three Hh ligands only Ihh is expressed in SG during normal skin homeostasis, as well as in differentiated sebocytes of sebaceous tumours (Niemann et al., 2003; Svard et al., 2006). However the role of Ihh for skin development, and in particular for the differentiation of SG, has not been investigated by functional approaches so far. Therefore, normal skin development and skin tumour formation were investigated in mice lacking epidermal Ihh (*Ihh* EKO). This analysis has three major outcomes which will be discussed:

- Although Ihh is not essential for SG development during normal skin homeostasis, it is required for normal cell proliferation in neonatal skin.
- Ihh plays a major role in patho-physiological conditions of the skin. It affects the morphology of both sebaceous and benign squamous tumours. In particular, it plays a crucial role for the differentiation and proliferation of tumour cells.
- During normal skin homeostasis and during tumourigenesis Ihh suppresses nuclear accumulation of p53. This effect was especially striking and unexpected for normal skin development since no morphological alterations were detected during skin homeostasis

6.1 The role of Ihh during epidermal differentiation

Our analysis of epidermal differentiation of mouse skin shows that the loss of epidermal *Ihh* does not lead to gross morphological changes nor to abnormal SG differentiation. However, the sebaceous tumours of *Ihh* EKO mice demonstrate a dramatic reduction of both sebocytes and sebaceous duct fate differentiation. Based on these results and previous studies, which indicate that the Hh pathway is involved in sebocyte and sebaceous duct differentiation *in vivo* and *in vitro* (Niemann et al., 2003, Allen et al., 2003; Gu and Coulombe, 2008; Séquaris et al., unpublished data), we suggest that Ihh regulates the specification of sebocyte and sebaceous duct fate and is involved in epidermal lineage selection in tumours.

Ihh has been shown to regulate differentiation during development and homeostasis of many organs such as the lateral plate mesoderm, bone, prostate, pancreas and gut (Zhang et al., 2001; Wijgerde et al., 2002; Razzaque et al., 2005; Tsiairis and McMahon, 2009; Vortkamp et al.; 1996; St-Jacques et al., 1999; Dakubo et al., 2008; van den Brink etal., 2004; van den Brink 2007; van Dop et al., 2010). In most organs in which a role of Ihh has been described, Shh signaling also has an important function. For instance, during gut development Ihh and Shh are both expressed in the colonic crypt but in different cell populations. This is very similar to the situation in the skin where Ihh and Shh both are expressed in distinct epidermal compartments and most likely play different roles during skin development (Fig. 36). In the colon, Ihh is expressed by mature colonocytes at the luminal end of the crypt and in the junctional zone. Here, Ihh regulates colonocyte differentiation, while Shh is expressed around the precursor cells at the base of the colonic crypt to control mesenchymal patterning and to inhibit smooth muscle differentiation (Ramalho-Santos et al., 2000; Sukegawa et al., 2000; Berman et al., 2003; Mao et al., 2010; Waghray et al., 2010; Saqui-Salces and Merchant, 2010). In the skin Shh is expressed in the matrix of the hair bulb and induces proliferation of keratinocytes constituting different hair lineages (St-Jacques et al., 1998; Chiang et al., 1999; Sato et al., 1999; Wang et al., 2000; Callahan and Oro, 2001; Oro and Higgins 2003) while Ihh is expressed in differentiated sebocytes (Niemann et al., 2003). By extension from our observation that Ihh is important for sebocyte differentiation within the sebaceous tumour, we suggest that Ihh plays a similar role during normal skin homeostasis (Fig. 36).

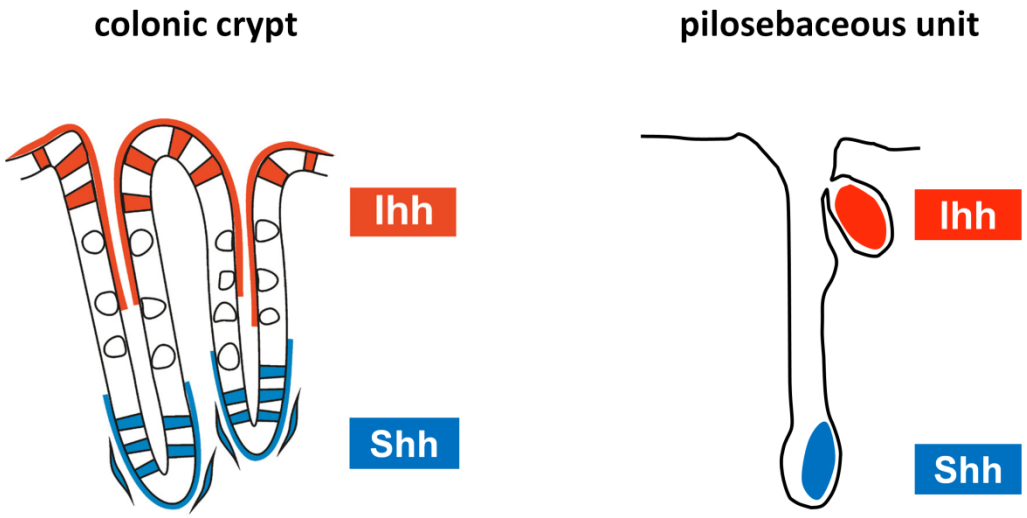

Figure 36: Hh ligand expression in the colonic crypt and the pilosebaceous unit.
Schematic view of expression pattern of ***Ihh*** **(red)** and ***Shh*** **(blue)** in the colonic crypt **(left)** (modified from van den Brink et al., 2004) and in the pilosebaceous unit **(right)**. In the colonic crypt Shh is expressed in the precursor cells at the base of the colonic crypt. Ihh is expressed by differentiated colonic enterocytes at the luminal end of the crypt and induces coloncytes differentiation. In the pilosebaceous unit, matrix cells of the hair bulb express Shh. Ihh is expressed in the mature sebocytes in SG.

During normal skin development the loss of Ihh did not lead to obvious histological abnormalities. One possible explanation for these observations is a functional compensatory mechanism by Shh. Shh and Ihh are closely related to each other and share 90% amino acid identity in the region of the signalling N-terminal peptide (Echelar et al., 1993; Ingham and McMahon, 2001). The interaction of both ligands with the same receptor, Ptch1, indicate that Shh and Ihh have a similar capacity and range of signalling during mammalian development of different organs (Ingham and McMahon, 2001; McMahon et al, 2003; Varjosalo and Taipale, 2008). Indeed, the loss-of-function analysis of Hh pathway components in organs, which express both Shh and Ihh, revealed that Shh and Ihh have partially redundant functions during tissue development and regeneration. For instance a redundant function of Shh and Ihh has been reported in muscle, pancreas, prostate and gut (Ramalho-Santos et al., 2000; Zhang et al., 2001, Aubin et al., 2002; Jason Doles, et al., 2006; Mao et al., 2010; van den Brink, 2007). In addition, Hh signals can act as a long-range signal over ~200µm (more than 100 cells) as shown in the vertebrate limb bud (Zhu and Scott, 2004; Huangfu and Anderson, 2006). During

hair morphogenesis *Shh* is up-regulated in the hair placode and later in the bulb of the HF from 14.5 day postcoital (dpc) to postnatal day 14 (P14). Therefore, potential long-range signalling of Shh and consequently a compensation of the Ihh function by Shh are possible.

Alternatively, Hh ligands may diffuse from the dermal compartment within the skin and activate the Hh pathway within the epidermal compartment. Examples for epidermal Hh ligand diffusion from other compartments have been described. For instance, a recent study shows that Shh derived from sensory nerves adjacent to the HF can induce Hh pathway activation in the stem cells of the HF bulge (Brownell et al., 2011). Signalling between epithelial and stromal compartments was also reported in tumours derived from other organs such as the pancreas (Nolan-Stevaux, 2009; Shaw and Bushman, 2007). The fact that around 50% of the small tumours (1-4mm diameter) in *Ihh* EKO mice show sebocyte differentiation, while with increased tumour size the sebocyte differentiation is dramatically reduced, might be explained by an increased distance between sebocyte precursors and the stromal compartment potentially producing Hh ligands in large tumours. In addition, the few sebocytes observed in medium (4-8mm) and large (8-16mm) tumours were mostly located at the tumour margin adjacent to stromal tissue.

Another possibility is that the Hh pathway is activated non-canonically. Indeed, it has been shown that Gli1 is regulated through a Smo-independent mechanism in neoplastic pancreatic ducts. Here, Gli transcription depends on TGF-β and K-Ras and is required independently from Shh-Ptch-Smo to maintain the transformed phenotype (Nolan-Stevaux, 2009). Such a mechanism need to be considered and might contribute to a compensation for the loss of Ihh in the skin.

To further investigate potential compensatory mechanisms, future studies should be performed in which Shh levels are monitored upon *Ihh* EKO. An accurate analysis of possible redundancy would be possible by inducing a double kockout of Shh and Ihh in the epidermis. Furthermore, the expression of all Hh ligands in the dermis should be analysed to evaluate the possibility of Hh signalling from the dermis.

6.2 A role of Ihh in controlling epidermal cell divisions

Our data reveal a general function of Ihh in regulating epidermal cell division during skin development and tumour formation. During mammalian development the Hh signalling pathway has been shown to regulate cellular proliferation in different tissues. For instance, Shh signalling has a proliferative effect in somites (Fan et al., 1995), retina (Jensen and Wallace, 1997, Wang et al., 2005), lung (Bellusci et al., 1997, Pepicelli et al., 1998), skeletal muscle (Duprez et al., 1998), granual cell precursors in the cerebellum (Wechsler-Reya and Scott, 1999; Ruiz i Altaba et al., 2002), and also the skin (Oro et al., 1997; St-Jacques et al., 1998). In neuronal cells, Hh controls proliferation through a number of different mechanisms. For instance, it can shorten the cell cycle or induce resting precursor cells to re-enter the cell cycle. Among the molecular mechanisms involved are the transcriptional up-regulation of the G1-phase cyclins D and E (Kenney and Rowitch, 2000), the direct regulation of the G2- phase cyclin B (Barnes et al., 2001), the maintenance of the phosphorylation of retinoblastoma protein (RB) (Kenney and Rowitch, 2000) and the inhibition of the cell cycle inhibitor p21 (Fan and Khavari, 1999) and p53 (Stecca and Ruiz i Altaba, 2009). Hh signalling might also be directly involved in controlling self-renewal of stem cells. In the hematopoietic system, Shh was shown to induce proliferation of early precursors by regulation of BMP signalling (Bhardwaj et al., 2001). The multiple ways by which Hh signalling can interfere with cell cycle regulation could explain why mutations in Hh pathway components have been found in many types of cancer. Since Hh exerts multiple functions in cell differentiation, abnormal Hh signalling might have different implications for each type of cancer.

Recently, a classification of tumours with aberrant Hh signalling has been proposed (Barakat et al., 2010). The tumours are grouped according to the stage when Hh becomes important for the neoplastic process. The first category comprises tumours for which tumour initiation and maintenance of tumour growth depends on mutations in Hh pathway components such as Ptch1 or Smo. Examples of this type include medulloblastoma, Rhabdomyosarcoma and BCC (Xi et al., 1997; Pazzaglia et al., 2002; Gailani et al., 1996, Hahn et al. 1996, Xi et al., 1998; Johnson et al., 1996; Dahmane et al., 1997; Goodrich et al., 1997; Oro et al., 1997; Barakat et al., 2010). The second category includes cancers in which Hh signalling does not lead to tumour initiation but is important for tumour growth and maintenance. Examples of this

category include colon and pancreas cancers (Barakat et al., 2010). There is also an unclassified group of cancers, in which the Hh pathway is implicated but its exact role is not clear yet, e.g. prostate cancer and lymphomas. It has been suggested that activation of Hh target genes in lymphomas and some other tumours might increase production of anti-apoptotic factors such as Bcl-2 and Bcl-xL (Barakat et al., 2010).

In agreement with the broadly observed function of Hh signalling in controlling proliferation, our analysis shows that lack of Ihh significantly reduces proliferation of keratinocytes during early skin development, and of primary keratinocytes in vitro without effecting apoptosis. In addition, proliferation is reduced upon loss of Ihh in papilloma and sebaceous tumours. With regard to sebaceous tumours the absence of Ihh does not change incidence and frequency of tumours. Thus, in sebaceous tumours Ihh contributes to maintenance and growth of the tumours and therefore they could be classified in the second category.

Since Ihh controls proliferation and regulates differentiation of epithelial cell lineages during sebaceous tumour formation, three possiblities are conceivable by which Ihh could contribute to tumour development:

(a) Ihh may control the transition from a multipotent SC/progenitor population to lineage specific progenitor cells. This would explain our observation that absence of Ihh not only affects sebocyte markers (SCD1, K6a positive cells), but also causes a reduction in the number of cells expressing markers for the spinous and granular cells (K10, Involucrin positive cells) as well as for cells of the HF linaege (K81 positive cells).

(b) Ihh might act on lineage-specific progenitors. The fact that Plet 1, which has been suggested to be a marker for a more committed progenitor cell fate (Nijhof et al., 2006; Raymond et al., 2010), was dramatically expanded supports this model. However, in this scenario it is more difficult to explain why loss of Ihh affects several epidermal lineages at the same time. Either Ihh is required for lineage progression of several committed progenitors or the loss of one differentiated cell type, e.g. the sebocytes leads indirectly to differentiation defects in other lineages.

(c) Ihh is not required for lineage progression but plays a role in the maintenance of the differentiated state. In this scenario sebocytes would maintain their state of differentiation

within sebaceous tumours by autocrine signalling and support the differentiation of other lineages by paracrine signalling. However, the fact that ectopic Hh signalling can induce ectopic SGs and sebaceous ducts shows that Ihh has the potential to act in an instructive way. Therefore, it is unlikely that Ihh fulfils only maintenance function in sebaceous tumours.

In combination, our data support the second model suggesting an action of Ihh on lineage-specific progenitor cells. The expression analysis of additional differentiation and progenitor markers in sebaceous tumours should make it possible to better understand how the cellular composition of these tumours changes upon loss of Ihh. This in turn will help to unravel the cellular mechanisms controlled by Ihh in tumours.

While incidence and frequency of sebaceous tumours are not altered upon loss of Ihh, papilloma lacking Ihh show increased incidence and multiplicity in spite of reduced tumour growth. The reduced tumour growth can be explained by the observation that the proliferation of keratinoyctes within these papilloma was twofold lower than in control papilloma. A preliminary marker analysis suggests that keratinocytes in papilloma lacking Ihh are less differentiated. This was also observed for sebaceous tumours. Interestingly, the reduced growth rate and the absence of differentiation in papilloma lacking Ihh is associated with a higher rate of tumour progression into SCC and metastasis. Thus, studying the role of Ihh in papilloma may provide important insights into the mechanisms underlying the transition from benign to malignant tumour growth.

6.3 Ihh controls p53 nuclear accumulation

In order to address the mechanism of Ihh signalling for epidermal cell division in the skin and in skin tumours we have analysed p53 expression. Interestingly, in the absence of Ihh there is a significant increase in nuclear accumulation of p53 in the epidermis and in papilloma. In addition, we detected increased p53 protein levels in sebaceous tumours lacking Ihh. In the skin of *Ihh* EKO mice p53 positive cells appear to be primarily localised in the basal layer of the IFE and the junctional zone. Together, these data suggest a novel function of Ihh in negatively regulating p53 during skin development and tumour formation.

In the absence of epidermal Ihh, nuclear accumulation of p53 correlates with reduced proliferation of keratinocytes in papilloma. During normal skin development epidermal loss of Ihh also causes nuclear accumulation of p53 and a reduced number of dividing keratinocytes during early stages (P0-P2). However, the change in nuclear accumulation of p53 also occurred in older Ihh EKO mice, which had normal keratinocyte proliferation. We have observed an increase in the number of p53 positive cells in up to 12 months old mice. Interestingly, these animals had normal skin morphology. Thus, the increased p53 nuclear accumulation upon loss of Ihh is a primary consequence and not always associated with reduced cell division rate or changes in tissue morphology. Therefore, our data suggest that Ihh directly regulates the p53 pathway.

The situation might be similar to that described for the relationship between Hh and p53 in neural progenitor cells where it has been shown that the number of progenitor cells is controlled by a negative feedback loop between p53 and Gli1 (Stecca and Ruiz i Altaba, 2009). p53 inhibits the activity of Gli1 by interfering with its normal nuclear localisation and by directing it to proteasomal degradation. On the other hand, in the mouse brain and several neuronal cell lines Gli1 activates Mdm2 expression, an ubiquitin ligase, which ubiquitinilates p53 resulting in its degradation (Abe et al., 2008; Stecca and Ruiz i Altaba, 2009; Prykhozhij, 2010; Malek et al., 2011).

Previously it has been shown that p53 nuclear accumulation is significantly reduced in sebaceous tumours developing in K14ΔNLef1 transgenic mice (Niemann et al., 2007).
It has been suggested that reduction of p53 accumulation is a consequence of blocking Arf in

ΔNLef1 mice. Reduced p53 levels lead to down-regulation of the cell cycle inhibitor p21 which is likely to play an important role in tumour promotion. The differentiation of sebocytes within sebaceous tumours is accompanied by increased Ihh expression. Our results show that in the absence of epidermal Ihh differentiation and proliferation of keratinocytes are reduced and p53 protein level is increased in sebaceous tumours of K14ΔNLef1 transgenic mice. This indicates that Ihh and ΔNLef1 exert the same effect on p53 protein levels in sebaceous tumours. Therefore, it is possible that the effect of ΔNLef1 on p53 is mediated by Ihh (Fig. 37a). In this case, increased levels of Ihh induced by ΔNLef1 would lead to a repression of p53. Alternatively ΔNLef1 and Ihh could act in parallel and independently negatively regulate p53 (Fig. 37b).

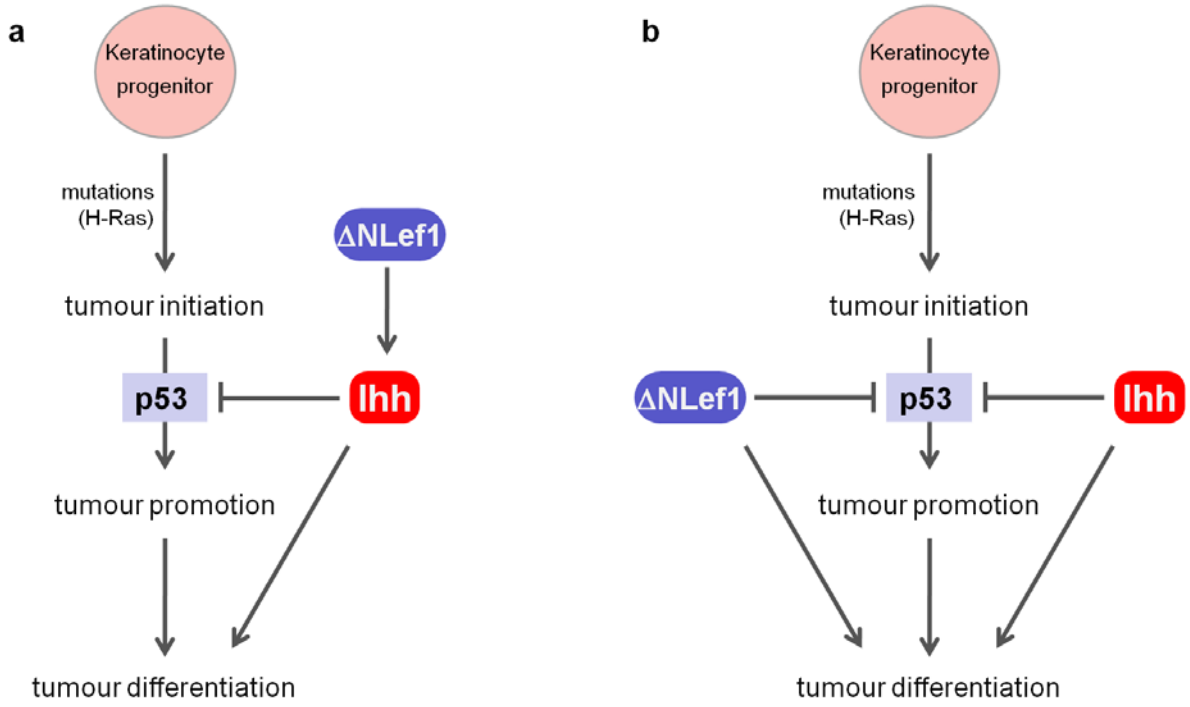

Figure 37: Regulation of p53 by Ihh signalling in sebabeous tumours.
Chemically induced H-ras mutation led to spontaneous formation of sebaceous tumours in a ΔNLef1 background. Blocking Wnt signalling by ΔNLef1 promotes tumour differentiation towards the sebocyte fate. ΔNLef1 also blocks p53 accumulation and thereby promotes tumour growth. **(a)** Ihh might act in parallel to ΔNLef1 promoting differentiation of sebocytes and blocking p53 accumulation. **(b)** The effect of ΔNLef1 may be mediated via Ihh.

6.4 Open questions and outlook

The data presented here reveal novel functions of Ihh in keratinocytes of normal skin and skin tumours, including the control of proliferation in neonatal skin, the promotion of differentiation and proliferation in skin tumours and the control of p53 protein levels both in normal skin and skin tumours. One key question resulting from our observations is why the effects of Ihh are significantly more pronounced during tumour growth than during normal skin homeostasis? In particular, how is it possible that Ihh appears to be required for keratinocyte differentiation in skin tumours considering no developmental defect was seen in normal skin lacking Ihh? Possible compensatory mechanisms the role of Shh for SG differentiation should be investigated using an inducible epidermal knockout of *Shh*. This would allow a late postnatal deletion of *Shh* minimizing general defects in hair formation. The phenotypic effects of a later loss of *Shh* should be compared to the simultaneous loss of both *Ihh* and *Shh* in the epidermis. This comparison would reveal the degree of redundancy between ligands. It would also provide hints for the existence of redundant signals from the dermis. Moreover, potential cellular abnormalities in the skin of single or double KOs could be compared to the cellular composition of skin tumours lacking Ihh. This comparison would provide insights into the cellular decision processes, which occur in presence or absence of Ihh in sebaceous tumours and papilloma. In particular, a better understanding of Ihh dependent differentiation in papilloma is required since the lack of Ihh promotes their transition to malignant SCC.

Another key question posed by this work addresses the relationship between Ihh and p53. The fact that loss of Ihh induces the nuclear accumulation of p53 even in postnatal and adult mice, which show no obvious skin abnormalities indicates that Ihh might be directly involved in the control of p53 levels. Thus, a focus of future work will be to unravel the molecular mechanism of Ihh signalling in controlling p53. The expression of several regulators of p53, for example Arf and Mdm2, should be analysed in normal skin and skin tumours in presence and absence of *Ihh*. In parallel genetic experiments would be informative. Mutant mice lacking both Ihh and p53 in the epidermis should be generated. An analysis of proliferation in the skin of these mice would reveal whether the control of cell proliferation by Ihh depends on p53.

7 Reference

Abe, Y., Oda-Sato, E., Tobiume, K., Kawauchi, K., Taya, Y., Okamoto, K., Oren, M., and Tanaka, N. (2008). Hedgehog signaling overrides p53-mediated tumor suppression by activating Mdm2. Proc Natl Acad Sci U S A 105, 4838-4843.

Abel, E. L., Angel, J. M., Kiguchi, K., and DiGiovanni, J. (2009). Multi-stage chemical carcinogenesis in mouse skin: fundamentals and applications. Nat Protoc 4, 1350-1362.

Alberts, B. (2008). Moleular Biology of the cell. 5th edn (New York, Garland Science)

Allen, M., Grachtchouk, M., Sheng, H., Grachtchouk, V., Wang, A., Wei, L., Liu, J., Ramirez, A., Metzger, D., Chambon, P., et al. (2003). Hedgehog signaling regulates sebaceous gland development. Am J Pathol 163, 2173-2178.

Andl, T., Reddy, S. T., Gaddapara, T., and Millar, S. E. (2002). WNT signals are required for the initiation of hair follicle development. Dev Cell 2, 643-653.

Apelqvist, A., Ahlgren, U., and Edlund, H. (1997). Sonic hedgehog directs specialised mesoderm differentiation in the intestine and pancreas. Curr Biol 7, 801-804.

Asplund, A., Gustafsson, A. C., Wikonkal, N. M., Sela, A., Leffell, D. J., Kidd, K., Lundeberg, J., Brash, D. E., and Ponten, F. (2005). PTCH codon 1315 polymorphism and risk for nonmelanoma skin cancer. Br J Dermatol 152, 868-873.

Asplund, A., Sivertsson, A., Backvall, H., Ahmadian, A., Lundeberg, J., and Ponten, F. (2005). Genetic mosaicism in basal cell carcinoma. Exp Dermatol 14, 593-600.

Aubin, J., Dery, U., Lemieux, M., Chailler, P., and Jeannotte, L. (2002). Stomach regional specification requires Hoxa5-driven mesenchymal-epithelial signaling. Development 129, 4075-4087.

Ayral, A-M., Kolossov, E., Serwe, M., Sablitzky, F. (1998). Reporter gege activation in transgenic mice mediated through induced Cre/loxp recombination. Transgenics 2:225-231

Aza-Blanc, P., Lin, H. Y., Ruiz i Altaba, A., and Kornberg, T. B. (2000). Expression of the vertebrate Gli proteins in Drosophila reveals a distribution of activator and repressor activities. Development 127, 4293-4301.

Bai, C. B., Stephen, D., and Joyner, A. L. (2004). All mouse ventral spinal cord patterning by hedgehog is Gli dependent and involves an activator function of Gli3. Dev Cell 6, 103-115.

Barakat, M. T., Humke, E. W., and Scott, M. P. (2010). Learning from Jekyll to control Hyde: Hedgehog signaling in development and cancer. Trends Mol Med 16, 337-348.

Barnes, E. A., Kong, M., Ollendorff, V., and Donoghue, D. J. (2001). Patched1 interacts with cyclin B1 to regulate cell cycle progression. Embo J 20, 2214-2223.

Basler, K., and Struhl, G. (1994). Compartment boundaries and the control of Drosophila limb pattern by hedgehog protein. Nature 368, 208-214.

Becker, S., Wang, Z. J., Massey, H., Arauz, A., Labosky, P., Hammerschmidt, M., St-Jacques, B., Bumcrot, D., McMahon, A., and Grabel, L. (1997). A role for Indian hedgehog in extraembryonic endoderm differentiation in F9 cells and the early mouse embryo. Dev Biol 187, 298-310.

Bellon, E., Luyten, F. P., and Tylzanowski, P. (2009). delta-EF1 is a negative regulator of Ihh in the developing growth plate. J Cell Biol 187, 685-699.

Bellusci, S., Furuta, Y., Rush, M. G., Henderson, R., Winnier, G., and Hogan, B. L. (1997). Involvement of Sonic hedgehog (Shh) in mouse embryonic lung growth and morphogenesis. Development 124, 53-63.

Berman, D. M., Karhadkar, S. S., Hallahan, A. R., Pritchard, J. I., Eberhart, C. G., Watkins, D. N., Chen, J. K., Cooper, M. K., Taipale, J., Olson, J. M., and Beachy, P. A. (2002). Medulloblastoma growth inhibition by hedgehog pathway blockade. Science 297, 1559-1561.

Berman, D. M., Karhadkar, S. S., Maitra, A., Montes De Oca, R., Gerstenblith, M. R., Briggs, K., Parker, A. R., Shimada, Y., Eshleman, J. R., Watkins, D. N., and Beachy, P. A. (2003). Widespread requirement for Hedgehog ligand stimulation in growth of digestive tract tumours. Nature 425, 846-851.

Bhardwaj, G., Murdoch, B., Wu, D., Baker, D. P., Williams, K. P., Chadwick, K., Ling, L. E., Karanu, F. N., and Bhatia, M. (2001). Sonic hedgehog induces the proliferation of primitive human hematopoietic cells via BMP regulation. Nat Immunol 2, 172-180.

Binczek, E., Jenke, B., Holz, B., Gunter, R. H., Thevis, M., and Stoffel, W. (2007). Obesity resistance of the stearoyl-CoA desaturase-deficient (scd1-/-) mouse results from disruption of the epidermal lipid barrier and adaptive thermoregulation. Biol Chem 388, 405-418.

Bitgood, M. J., Shen, L., and McMahon, A. P. (1996). Sertoli cell signaling by Desert hedgehog regulates the male germline. Curr Biol 6, 298-304.

Black, J. R., Epstein, E., Rains, W. D., Yin, Q. Z., and Casey, W. H. (2008). Magnesium-isotope fractionation during plant growth. Environ Sci Technol 42, 7831-7836.

Blanpain, C., and Fuchs, E. (2006). Epidermal stem cells of the skin. Annu Rev Cell Dev Biol 22, 339-373.

Blanpain, C., and Fuchs, E. (2009). Epidermal homeostasis: a balancing act of stem cells in the skin. Nat Rev Mol Cell Biol 10, 207-217.

Bonfanti, P., Claudinot, S., Amici, A. W., Farley, A., Blackburn, C. C., and Barrandon, Y. (2010). Microenvironmental reprogramming of thymic epithelial cells to skin multipotent stem cells. Nature 466, 978-982.

Bradfield, R. B., and Montagna, W. (1974). Letter: Scanning electron microscopy in assessment of protein-calorie malnutrition. Lancet 2, 1026.

Braun, K. M., Niemann, C., Jensen, U. B., Sundberg, J. P., Silva-Vargas, V., and Watt, F. M. (2003). Manipulation of stem cell proliferation and lineage commitment: visualisation of label-retaining cells in wholemounts of mouse epidermis. Development 130, 5241-5255.

Brewster, R., Lee, J., and Ruiz i Altaba, A. (1998). Gli/Zic factors pattern the neural plate by defining domains of cell differentiation. Nature 393, 579-583.

Brownell, I., Guevara, E., Bai, C. B., Loomis, C. A., and Joyner, A. L. (2011). Nerve-derived sonic hedgehog defines a niche for hair follicle stem cells capable of becoming epidermal stem cells. Cell Stem Cell 8, 552-565.

Brunner, M., Thurnher, D., Pammer, J., Heiduschka, G., Petzelbauer, P., Schmid, C., Schneider, S., and Erovic, B. M. (2010). Expression of hedgehog signaling molecules in Merkel cell carcinoma. Head Neck 32, 333-340.

Buglino, J. A., and Resh, M. D. (2008). Hhat is a palmitoylacyltransferase with specificity for N-palmitoylation of Sonic Hedgehog. J Biol Chem 283, 22076-22088.

Byrd, N., Becker, S., Maye, P., Narasimhaiah, R., St-Jacques, B., Zhang, X., McMahon, J., McMahon, A., and Grabel, L. (2002). Hedgehog is required for murine yolk sac angiogenesis. Development 129, 361-372.

Callahan, C. A., and Oro, A. E. (2001). Monstrous attempts at adnexogenesis: regulating hair follicle progenitors through Sonic hedgehog signaling. Curr Opin Genet Dev 11, 541-546.

Celis, J.E. (2006). Cell bology: alaboratoy handbook. Elsevier Academic, Amsterdam, NL.

Chang, D. T., Lopez, A., von Kessler, D. P., Chiang, C., Simandl, B. K., Zhao, R., Seldin, M. F., Fallon, J. F., and Beachy, P. A. (1994). Products, genetic linkage and limb patterning activity of a murine hedgehog gene. Development 120, 3339-3353.

Chen, J. K., Taipale, J., Cooper, M. K., and Beachy, P. A. (2002). Inhibition of Hedgehog signaling by direct binding of cyclopamine to Smoothened. Genes Dev 16, 2743-2748.

Chen, M. H., Li, Y. J., Kawakami, T., Xu, S. M., and Chuang, P. T. (2004). Palmitoylation is required for the production of a soluble multimeric Hedgehog protein complex and long-range signaling in vertebrates. Genes Dev 18, 641-659.

Chiang, C., Litingtung, Y., Lee, E., Young, K. E., Corden, J. L., Westphal, H., and Beachy, P. A. (1996). Cyclopia and defective axial patterning in mice lacking Sonic hedgehog gene function. Nature 383, 407-413.

Chiang, C., Swan, R. Z., Grachtchouk, M., Bolinger, M., Litingtung, Y., Robertson, E. K., Cooper, M. K., Gaffield, W., Westphal, H., Beachy, P. A., and Dlugosz, A. A. (1999). Essential role for Sonic hedgehog during hair follicle morphogenesis. Dev Biol 205, 1-9.

Chuong, C. M., Nickoloff, B. J., Elias, P. M., Goldsmith, L. A., Macher, E., Maderson, P. A., Sundberg, J. P., Tagami, H., Plonka, P. M., Thestrup-Pederson, K., et al. (2002). What is the 'true' function of skin? Exp Dermatol 11, 159-187.

Clement, V., Sanchez, P., de Tribolet, N., Radovanovic, I., and Ruiz i Altaba, A. (2007). HEDGEHOG-GLI1 signaling regulates human glioma growth, cancer stem cell self-renewal, and tumorigenicity. Curr Biol 17, 165-172.

Cortes, M., Baria, A. T., and Schwartz, N. B. (2009). Sulfation of chondroitin sulfate proteoglycans is necessary for proper Indian hedgehog signaling in the developing growth plate. Development 136, 1697-1706.

Coulombe, P. A., Tong, X., Mazzalupo, S., Wang, Z., and Wong, P. (2004). Great promises yet to be fulfilled: defining keratin intermediate filament function in vivo. Eur J Cell Biol 83, 735-746.

Dahmane, N., Lee, J., Robins, P., Heller, P., and Ruiz i Altaba, A. (1997). Activation of the transcription factor Gli1 and the Sonic hedgehog signalling pathway in skin tumours. Nature 389, 876-881.

Dai, P., Akimaru, H., Tanaka, Y., Maekawa, T., Nakafuku, M., and Ishii, S. (1999). Sonic Hedgehog-induced activation of the Gli1 promoter is mediated by GLI3. J Biol Chem 274, 8143-8152.

Dakubo, G. D., Mazerolle, C., Furimsky, M., Yu, C., St-Jacques, B., McMahon, A. P., and Wallace, V. A. (2008). Indian hedgehog signaling from endothelial cells is required for sclera and retinal pigment epithelium development in the mouse eye. Dev Biol 320, 242-255.

DiGiovanni, J. (1992). Multistage carcinogenesis in mouse skin. Pharmacol Ther 54, 63-128.

Doles, J., Cook, C., Shi, X., Valosky, J., Lipinski, R., and Bushman, W. (2006). Functional compensation in Hedgehog signaling during mouse prostate development. Dev Biol 295, 13-25.

Duprez, D., Fournier-Thibault, C., and Le Douarin, N. (1998). Sonic Hedgehog induces proliferation of committed skeletal muscle cells in the chick limb. Development 125, 495-505.

Dutton, R., Yamada, T., Turnley, A., Bartlett, P. F., and Murphy, M. (1999). Sonic hedgehog promotes neuronal differentiation of murine spinal cord precursors and collaborates with neurotrophin 3 to induce Islet-1. J Neurosci 19, 2601-2608.

Dyer, M. A., Farrington, S. M., Mohn, D., Munday, J. R., and Baron, M. H. (2001). Indian hedgehog activates hematopoiesis and vasculogenesis and can respecify prospective neurectodermal cell fate in the mouse embryo. Development 128, 1717-1730.

Echelard, Y., Epstein, D. J., St-Jacques, B., Shen, L., Mohler, J., McMahon, J. A., and McMahon, A. P. (1993). Sonic hedgehog, a member of a family of putative signaling molecules, is implicated in the regulation of CNS polarity. Cell 75, 1417-1430.

Ekker, S. C., Ungar, A. R., Greenstein, P., von Kessler, D. P., Porter, J. A., Moon, R. T., and Beachy, P. A. (1995). Patterning activities of vertebrate hedgehog proteins in the developing eye and brain. Curr Biol 5, 944-955.

Epstein, E. A., Reizian, M. A., and Chapman, M. R. (2009). Spatial clustering of the curlin secretion lipoprotein requires curli fiber assembly. J Bacteriol 191, 608-615.

Epstein, E. H. (2008). Basal cell carcinomas: attack of the hedgehog. Nat Rev Cancer 8, 743-754.

Fan, C. M., Porter, J. A., Chiang, C., Chang, D. T., Beachy, P. A., and Tessier-Lavigne, M. (1995). Long-range sclerotome induction by sonic hedgehog: direct role of the amino-terminal cleavage product and modulation by the cyclic AMP signaling pathway. Cell 81, 457-465.

Fan, C. M., and Tessier-Lavigne, M. (1994). Patterning of mammalian somites by surface ectoderm and notochord: evidence for sclerotome induction by a hedgehog homolog. Cell 79, 1175-1186.

Fan, H., and Khavari, P. A. (1999). Sonic hedgehog opposes epithelial cell cycle arrest. J Cell Biol 147, 71-76.

Fuchs, E., and Green, H. (1980). Changes in keratin gene expression during terminal differentiation of the keratinocyte. Cell 19, 1033-1042.

Fuchs, E., and Nowak, J. A. (2008). Building epithelial tissues from skin stem cells. Cold Spring Harb Symp Quant Biol 73, 333-350.

Gailani, M. R., Bale, S. J., Leffell, D. J., DiGiovanna, J. J., Peck, G. L., Poliak, S., Drum, M. A., Pastakia, B., McBride, O. W., Kase, R., and et al. (1992). Developmental defects in Gorlin syndrome related to a putative tumor suppressor gene on chromosome 9. Cell 69, 111-117.

Gailani, M. R., Leffell, D. J., Ziegler, A., Gross, E. G., Brash, D. E., and Bale, A. E. (1996). Relationship between sunlight exposure and a key genetic alteration in basal cell carcinoma. J Natl Cancer Inst 88, 349-354.

Gailani, M. R., Stahle-Backdahl, M., Leffell, D. J., Glynn, M., Zaphiropoulos, P. G., Pressman, C., Unden, A. B., Dean, M., Brash, D. E., Bale, A. E., and Toftgard, R. (1996). The role of the human homologue of Drosophila patched in sporadic basal cell carcinomas. Nat Genet 14, 78-81.

Goodrich, L. V., Milenkovic, L., Higgins, K. M., and Scott, M. P. (1997). Altered neural cell fates and medulloblastoma in mouse patched mutants. Science 277, 1109-1113.

Grachtchouk, M., Mo, R., Yu, S., Zhang, X., Sasaki, H., Hui, C. C., and Dlugosz, A. A. (2000). Basal cell carcinomas in mice overexpressing Gli2 in skin. Nat Genet 24, 216-217.

Grachtchouk, V., Grachtchouk, M., Lowe, L., Johnson, T., Wei, L., Wang, A., de Sauvage, F., and Dlugosz, A. A. (2003). The magnitude of hedgehog signaling activity defines skin tumor phenotype. Embo J 22, 2741-2751.

Gu, L. H., and Coulombe, P. A. (2008). Hedgehog signaling, keratin 6 induction, and sebaceous gland morphogenesis: implications for pachyonychia congenita and related conditions. Am J Pathol 173, 752-761.

Hafner, M., Wenk, J., Nenci, A., Pasparakis, M., Scharffetter-Kochanek, K., Smyth, N., Peters, T., Kess, D., Holtkotter, O., Shephard, P., et al. (2004). Keratin 14 Cre transgenic mice authenticate keratin 14 as an oocyte-expressed protein. Genesis 38, 176-181.

Hahn, H., Christiansen, J., Wicking, C., Zaphiropoulos, P. G., Chidambaram, A., Gerrard, B., Vorechovsky, I., Bale, A. E., Toftgard, R., Dean, M., and Wainwright, B. (1996). A mammalian patched homolog is expressed in target tissues of sonic hedgehog and maps to a region associated with developmental abnormalities. J Biol Chem 271, 12125-12128.

Hahn, H., Wicking, C., Zaphiropoulous, P. G., Gailani, M. R., Shanley, S., Chidambaram, A., Vorechovsky, I., Holmberg, E., Unden, A. B., Gillies, S., et al. (1996). Mutations of the human homolog of Drosophila patched in the nevoid basal cell carcinoma syndrome. Cell 85, 841-851.

Hahn, H., Wojnowski, L., Zimmer, A. M., Hall, J., Miller, G., and Zimmer, A. (1998). Rhabdomyosarcomas and radiation hypersensitivity in a mouse model of Gorlin syndrome. Nat Med 4, 619-622.

Heath, D. D., Iwama, G. K., and Devlin, R. H. (1994). DNA fingerprinting used to test for family effects on precocious sexual maturation in two populations of Oncorhynchus tshawytscha (Chinook salmon). Heredity 73 (Pt 6), 616-624.

Hebrok, M., Kim, S. K., St Jacques, B., McMahon, A. P., and Melton, D. A. (2000). Regulation of pancreas development by hedgehog signaling. Development 127, 4905-4913.

Hickey, G., Jacks, T., Judith, F., Taylor, J., Schoen, W. R., Krupa, D., Cunningham, P., Clark, J., and Smith, R. G. (1994). Efficacy and specificity of L-692,429, a novel nonpeptidyl growth hormone secretagogue, in beagles. Endocrinology 134, 695-701.

Hooper, J. E., and Scott, M. P. (2005). Communicating with Hedgehogs. Nat Rev Mol Cell Biol 6, 306-317.

Hsu, Y. C., Pasolli, H. A., and Fuchs, E. (2011). Dynamics between stem cells, niche, and progeny in the hair follicle. Cell 144, 92-105.

Huangfu, D., and Anderson, K. V. (2006). Signaling from Smo to Ci/Gli: conservation and divergence of Hedgehog pathways from Drosophila to vertebrates. Development 133, 3-14.

Hutchin, M. E., Kariapper, M. S., Grachtchouk, M., Wang, A., Wei, L., Cummings, D., Liu, J., Michael, L. E., Glick, A., and Dlugosz, A. A. (2005). Sustained Hedgehog signaling is required for basal cell carcinoma proliferation and survival: conditional skin tumorigenesis recapitulates the hair growth cycle. Genes Dev 19, 214-223.

Ingham, P. W., and Hidalgo, A. (1993). Regulation of wingless transcription in the Drosophila embryo. Development 117, 283-291.

Ingham, P. W., and McMahon, A. P. (2001). Hedgehog signaling in animal development: paradigms and principles. Genes Dev 15, 3059-3087.

Ito, M., Yang, Z., Andl, T., Cui, C., Kim, N., Millar, S. E., and Cotsarelis, G. (2007). Wnt-dependent de novo hair follicle regeneration in adult mouse skin after wounding. Nature 447, 316-320.

Jacks, T., Remington, L., Williams, B. O., Schmitt, E. M., Halachmi, S., Bronson, R. T., and Weinberg, R. A. (1994). Tumor spectrum analysis in p53-mutant mice. Curr Biol 4, 1-7.

Jensen, A. M., and Wallace, V. A. (1997). Expression of Sonic hedgehog and its putative role as a precursor cell mitogen in the developing mouse retina. Development 124, 363-371.

Jensen, K. B., Collins, C. A., Nascimento, E., Tan, D. W., Frye, M., Itami, S., and Watt, F. M. (2009). Lrig1 expression defines a distinct multipotent stem cell population in mammalian epidermis. Cell Stem Cell 4, 427-439.

Johnson, R. L., Rothman, A. L., Xie, J., Goodrich, L. V., Bare, J. W., Bonifas, J. M., Quinn, A. G., Myers, R. M., Cox, D. R., Epstein, E. H., Jr., and Scott, M. P. (1996). Human homolog of patched, a candidate gene for the basal cell nevus syndrome. Science 272, 1668-1671.

Karp, S. J., Schipani, E., St-Jacques, B., Hunzelman, J., Kronenberg, H., and McMahon, A. P. (2000). Indian hedgehog coordinates endochondral bone growth and morphogenesis via parathyroid hormone related-protein-dependent and -independent pathways. Development 127, 543-548.

Kastan, M. B., Zhan, Q., el-Deiry, W. S., Carrier, F., Jacks, T., Walsh, W. V., Plunkett, B. S., Vogelstein, B., and Fornace, A. J., Jr. (1992). A mammalian cell cycle checkpoint pathway utilizing p53 and GADD45 is defective in ataxia-telangiectasia. Cell 71, 587-597.

Kenney, A. M., and Rowitch, D. H. (2000). Sonic hedgehog promotes G(1) cyclin expression and sustained cell cycle progression in mammalian neuronal precursors. Mol Cell Biol 20, 9055-9067.

Klein-Szanto, A.J.P. (1989). Pathology of human and experimental skin tumors in Skin Tumors: Experimental and Clinical Aspects (eds. Conti, C.J., Slaga, T.J. & Klein-Szanto, A.J.P.) 19–53 (Raven Press, New York)

Kobayashi, T., Soegiarto, D. W., Yang, Y., Lanske, B., Schipani, E., McMahon, A. P., and Kronenberg, H. M. (2005). Indian hedgehog stimulates periarticular chondrocyte differentiation to regulate growth plate length independently of PTHrP. J Clin Invest 115, 1734-1742.

Kos, L., Chiang, C., and Mahon, K. A. (1998). Mediolateral patterning of somites: multiple axial signals, including Sonic hedgehog, regulate Nkx-3.1 expression. Mech Dev 70, 25-34.

Kosinski, C., Stange, D. E., Xu, C., Chan, A. S., Ho, C., Yuen, S. T., Mifflin, R. C., Powell, D. W., Clevers, H., Leung, S. Y., and Chen, X. (2010). Indian hedgehog regulates intestinal stem cell fate through epithelial-mesenchymal interactions during development. Gastroenterology 139, 893-903.

Krauss, S., Concordet, J. P., and Ingham, P. W. (1993). A functionally conserved homolog of the Drosophila segment polarity gene hh is expressed in tissues with polarizing activity in zebrafish embryos. Cell 75, 1431-1444.

Kumar, S., Tamura, K., and Nei, M. (1994). MEGA: Molecular Evolutionary Genetics Analysis software for microcomputers. Comput Appl Biosci 10, 189-191.

Laaff, H., Mittelviefhaus, H., Wokalek, H., and Schopf, E. (1992). [Grzybowski type eruptive keratoacanthomas and ectropion. A therapeutic problem]. Hautarzt 43, 143-147.

LeBoit, P.E. (2006). Pathology and genetics of skin tumours, volume 6. (IARC press).

Langbein, L., and Schweizer, J. (2005). Keratins of the human hair follicle. Int Rev Cytol 243, 1-78.

Lee, J. J., Ekker, S. C., von Kessler, D. P., Porter, J. A., Sun, B. I., and Beachy, P. A. (1994). Autoproteolysis in hedgehog protein biogenesis. Science 266, 1528-1537.

Lee, K., Jeong, J., Kwak, I., Yu, C. T., Lanske, B., Soegiarto, D. W., Toftgard, R., Tsai, M. J., Tsai, S., Lydon, J. P., and DeMayo, F. J. (2006). Indian hedgehog is a major mediator of progesterone signaling in the mouse uterus. Nat Genet 38, 1204-1209.

Lee, Y., Miller, H. L., Russell, H. R., Boyd, K., Curran, T., and McKinnon, P. J. (2006). Patched2 modulates tumorigenesis in patched1 heterozygous mice. Cancer Res 66, 6964-6971.

Levanat, S., Gorlin, R. J., Fallet, S., Johnson, D. R., Fantasia, J. E., and Bale, A. E. (1996). A two-hit model for developmental defects in Gorlin syndrome. Nat Genet 12, 85-87.

Levy, V., Lindon, C., Zheng, Y., Harfe, B. D., and Morgan, B. A. (2007). Epidermal stem cells arise from the hair follicle after wounding. Faseb J 21, 1358-1366.

Lewis, P. M., Dunn, M. P., McMahon, J. A., Logan, M., Martin, J. F., St-Jacques, B., and McMahon, A. P. (2001). Cholesterol modification of sonic hedgehog is required for long-range signaling activity and effective modulation of signaling by Ptc1. Cell 105, 599-612.

Li, C., Chi, S., and Xie, J. (2011). Hedgehog signaling in skin cancers. Cell Signal.

Li, E. R., Owens, D. M., Djian, P., and Watt, F. M. (2000). Expression of involucrin in normal, hyperproliferative and neoplastic mouse keratinocytes. Exp Dermatol 9, 431-438.

Li, Y., Zhang, H., Litingtung, Y., and Chiang, C. (2006). Cholesterol modification restricts the spread of Shh gradient in the limb bud. Proc Natl Acad Sci U S A 103, 6548-6553.

Lindqvist, P. G., Epstein, E., and Olsson, H. (2009). The relationship between lifestyle factors and venous thromboembolism among women: a report from the MISS study. Br J Haematol 144, 234-240.

Litingtung, Y., Dahn, R. D., Li, Y., Fallon, J. F., and Chiang, C. (2002). Shh and Gli3 are dispensable for limb skeleton formation but regulate digit number and identity. Nature 418, 979-983.

Litingtung, Y., Lei, L., Westphal, H., and Chiang, C. (1998). Sonic hedgehog is essential to foregut development. Nat Genet 20, 58-61.

Liu, A., Joyner, A. L., and Turnbull, D. H. (1998). Alteration of limb and brain patterning in early mouse embryos by ultrasound-guided injection of Shh-expressing cells. Mech Dev 75, 107-115.

Liu, F., Massague, J., and Ruiz i Altaba, A. (1998). Carboxy-terminally truncated Gli3 proteins associate with Smads. Nat Genet 20, 325-326.

Liu, Y., Lyle, S., Yang, Z., and Cotsarelis, G. (2003). Keratin 15 promoter targets putative epithelial stem cells in the hair follicle bulge. J Invest Dermatol 121, 963-968.

Lo Celso, C., Berta, M. A., Braun, K. M., Frye, M., Lyle, S., Zouboulis, C. C., and Watt, F. M. (2008). Characterization of bipotential epidermal progenitors derived from human sebaceous gland: contrasting roles of c-Myc and beta-catenin. Stem Cells 26, 1241-1252.

Ma, X., Sheng, T., Zhang, Y., Zhang, X., He, J., Huang, S., Chen, K., Sultz, J., Adegboyega, P. A., Zhang, H., and Xie, J. (2006). Hedgehog signaling is activated in subsets of esophageal cancers. Int J Cancer 118, 139-148.

Macpherson, E. E., and Montagna, W. (1974). Proceedings: The mammary glands of rhesus monkeys. J Invest Dermatol 63, 17-18.

Malek, R., Matta, J., Taylor, N., Perry, M. E., and Mendrysa, S. M. (2011). The p53 inhibitor MDM2 facilitates Sonic Hedgehog-mediated tumorigenesis and influences cerebellar foliation. PLoS One 6, e17884.

Mansbridge, J. N., and Knapp, A. M. (1987). Changes in keratinocyte maturation during wound healing. J Invest Dermatol 89, 253-263.

Mao, J., Kim, B. M., Rajurkar, M., Shivdasani, R. A., and McMahon, A. P. (2010). Hedgehog signaling controls mesenchymal growth in the developing mammalian digestive tract. Development 137, 1721-1729.

Mao, X., Fujiwara, Y., and Orkin, S. H. (1999). Improved reporter strain for monitoring Cre recombinase-mediated DNA excisions in mice. Proc Natl Acad Sci U S A 96, 5037-5042.

Masuya, H., Sagai, T., Wakana, S., Moriwaki, K., and Shiroishi, T. (1995). A duplicated zone of polarizing activity in polydactylous mouse mutants. Genes Dev 9, 1645-1653.

Matise, M. P., and Joyner, A. L. (1999). Gli genes in development and cancer. Oncogene 18, 7852-7859.

Matsumoto, T., Jiang, J., Kiguchi, K., Ruffino, L., Carbajal, S., Beltran, L., Bol, D. K., Rosenberg, M. P., and DiGiovanni, J. (2003). Targeted expression of c-Src in epidermal basal cells leads to enhanced skin tumor promotion, malignant progression, and metastasis. Cancer Res 63, 4819-4828.

Mazet, F., and Shimeld, S. M. (2002). Gene duplication and divergence in the early evolution of vertebrates. Curr Opin Genet Dev 12, 393-396.

McGowan, K., and Coulombe, P. A. (1998). The wound repair-associated keratins 6, 16, and 17. Insights into the role of intermediate filaments in specifying keratinocyte cytoarchitecture. Subcell Biochem 31, 173-204.

McMahon, A. P., Ingham, P. W., and Tabin, C. J. (2003). Developmental roles and clinical significance of hedgehog signaling. Curr Top Dev Biol 53, 1-114.

Meletis, K., Wirta, V., Hede, S. M., Nister, M., Lundeberg, J., and Frisen, J. (2006). p53 suppresses the self-renewal of adult neural stem cells. Development 133, 363-369.

Meyer, A., and Schartl, M. (1999). Gene and genome duplications in vertebrates: the one-to-four (-to-eight in fish) rule and the evolution of novel gene functions. Curr Opin Cell Biol 11, 699-704.

Mill, P., Mo, R., Fu, H., Grachtchouk, M., Kim, P. C., Dlugosz, A. A., and Hui, C. C. (2003). Sonic hedgehog-dependent activation of Gli2 is essential for embryonic hair follicle development. Genes Dev 17, 282-294.

Millar, S. E. (2002). Molecular mechanisms regulating hair follicle development. J Invest Dermatol 118, 216-225.

Miyazaki, M., Man, W. C., and Ntambi, J. M. (2001). Targeted disruption of stearoyl-CoA desaturase1 gene in mice causes atrophy of sebaceous and meibomian glands and depletion of wax esters in the eyelid. J Nutr 131, 2260-2268.

Montagna, W. (1974). An introduction to sebaceous glands. J Invest Dermatol 62, 120-123.

Montagan, W. & Parakkal, P.F. (1974). The Structure and Punction of Skin. Academic Press, New York

Morris, R. J., Liu, Y., Marles, L., Yang, Z., Trempus, C., Li, S., Lin, J. S., Sawicki, J. A., and Cotsarelis, G. (2004). Capturing and profiling adult hair follicle stem cells. Nat Biotechnol 22, 411-417.

Mullis, K.B., and Faloona, F.A. (1987). Specific synthesis of DNA in vitro via a polymerase-catalyzed chain reaction. Methods Enzymol 155:335-350.

Nelson, W. G., and Sun, T. T. (1983). The 50- and 58-kdalton keratin classes as molecular markers for stratified squamous epithelia: cell culture studies. J Cell Biol 97, 244-251.

Niemann, C. (2009). Differentiation of the sebaceous gland. Dermatoendocrinol 1, 64-67.

Niemann, C., Owens, D. M., Hulsken, J., Birchmeier, W., and Watt, F. M. (2002). Expression of DeltaNLef1 in mouse epidermis results in differentiation of hair follicles into squamous epidermal cysts and formation of skin tumours. Development 129, 95-109.

Niemann, C., Owens, D. M., Schettina, P., and Watt, F. M. (2007). Dual role of inactivating Lef1 mutations in epidermis: tumor promotion and specification of tumor type. Cancer Res 67, 2916-2921.

Niemann, C., Unden, A. B., Lyle, S., Zouboulis Ch, C., Toftgard, R., and Watt, F. M. (2003). Indian hedgehog and beta-catenin signaling: role in the sebaceous lineage of normal and neoplastic mammalian epidermis. Proc Natl Acad Sci U S A 100 Suppl 1, 11873-11880.

Niemann, C., and Watt, F. M. (2002). Designer skin: lineage commitment in postnatal epidermis. Trends Cell Biol 12, 185-192.

Nijhof, J. G., Braun, K. M., Giangreco, A., van Pelt, C., Kawamoto, H., Boyd, R. L., Willemze, R., Mullenders, L. H., Watt, F. M., de Gruijl, F. R., and van Ewijk, W. (2006). The cell-surface marker MTS24 identifies a novel population of follicular keratinocytes with characteristics of progenitor cells. Development 133, 3027-3037.

Nilsson, M., Unden, A. B., Krause, D., Malmqwist, U., Raza, K., Zaphiropoulos, P. G., and Toftgard, R. (2000). Induction of basal cell carcinomas and trichoepitheliomas in mice overexpressing GLI-1. Proc Natl Acad Sci U S A 97, 3438-3443.

Nolan-Stevaux, O., Lau, J., Truitt, M. L., Chu, G. C., Hebrok, M., Fernandez-Zapico, M. E., and Hanahan, D. (2009). GLI1 is regulated through Smoothened-independent mechanisms in neoplastic pancreatic ducts and mediates PDAC cell survival and transformation. Genes Dev 23, 24-36.

Northcott, P. A., Nakahara, Y., Wu, X., Feuk, L., Ellison, D. W., Croul, S., Mack, S., Kongkham, P. N., Peacock, J., Dubuc, A., et al. (2009). Multiple recurrent genetic events converge on control of histone lysine methylation in medulloblastoma. Nat Genet 41, 465-472.

Nothias, F., Fishell, G., and Ruiz i Altaba, A. (1998). Cooperation of intrinsic and extrinsic signals in the elaboration of regional identity in the posterior cerebral cortex. Curr Biol 8, 459-462.

Nowak, J. A., Polak, L., Pasolli, H. A., and Fuchs, E. (2008). Hair follicle stem cells are specified and function in early skin morphogenesis. Cell Stem Cell 3, 33-43.

Nusslein-Volhard, C., and Wieschaus, E. (1980). Mutations affecting segment number and polarity in Drosophila. Nature 287, 795-801.

Ochiai, T., Shibukawa, Y., Nagayama, M., Mundy, C., Yasuda, T., Okabe, T., Shimono, K., Kanyama, M., Hasegawa, H., Maeda, Y., et al. (2010). Indian hedgehog roles in post-natal TMJ development and organization. J Dent Res 89, 349-354.

Oro, A. E., and Higgins, K. (2003). Hair cycle regulation of Hedgehog signal reception. Dev Biol 255, 238-248.

Oro, A. E., Higgins, K. M., Hu, Z., Bonifas, J. M., Epstein, E. H., Jr., and Scott, M. P. (1997). Basal cell carcinomas in mice overexpressing sonic hedgehog. Science 276, 817-821.

Owens, D. M., Broad, S., Yan, X., Benitah, S. A., and Watt, F. M. (2005). Suprabasal alpha 5 beta1 integrin expression stimulates formation of epidermal squamous cell carcinomas without disrupting TGFbeta signaling or inducing spindle cell tumors. Mol Carcinog 44, 60-66.

Owens, D. M., Romero, M. R., Gardner, C., and Watt, F. M. (2003). Suprabasal alpha6beta4 integrin expression in epidermis results in enhanced tumourigenesis and disruption of TGFbeta signalling. J Cell Sci 116, 3783-3791.

Owens, D. M., and Watt, F. M. (2001). Influence of beta1 integrins on epidermal squamous cell carcinoma formation in a transgenic mouse model: alpha3beta1, but not alpha2beta1, suppresses malignant conversion. Cancer Res 61, 5248-5254.

Owens, D. M., and Watt, F. M. (2003). Contribution of stem cells and differentiated cells to epidermal tumours. Nat Rev Cancer 3, 444-451.

Pan, Y., Bai, C. B., Joyner, A. L., and Wang, B. (2006). Sonic hedgehog signaling regulates Gli2 transcriptional activity by suppressing its processing and degradation. Mol Cell Biol 26, 3365-3377.

Parmentier, L., Lakhdar, H., Blanchet-Bardon, C., Marchand, S., Dubertret, L., and Weissenbach, J. (1996). Mapping of a second locus for lamellar ichthyosis to chromosome 2q33-35. Hum Mol Genet 5, 555-559.

Parr, B. A., and McMahon, A. P. (1995). Dorsalizing signal Wnt-7a required for normal polarity of D-V and A-P axes of mouse limb. Nature 374, 350-353.

Pasca di Magliano, M., and Hebrok, M. (2003). Hedgehog signalling in cancer formation and maintenance. Nat Rev Cancer 3, 903-911.

Pazzaglia, S., Mancuso, M., Atkinson, M. J., Tanori, M., Rebessi, S., Majo, V. D., Covelli, V., Hahn, H., and Saran, A. (2002). High incidence of medulloblastoma following X-ray-irradiation of newborn Ptc1 heterozygous mice. Oncogene 21, 7580-7584.

Petersson, M. (2010). Characterisation of hair follicle stem cell function in epidermal regeneration and tumourigenesis. Dissertation. University of Cologne

Pepicelli, C. V., Lewis, P. M., and McMahon, A. P. (1998). Sonic hedgehog regulates branching morphogenesis in the mammalian lung. Curr Biol 8, 1083-1086.

Pietsch, E. C., Humbey, O., and Murphy, M. E. (2006). Polymorphisms in the p53 pathway. Oncogene 25, 1602-1611.

Polager, S., and Ginsberg, D. (2009). p53 and E2f: partners in life and death. Nat Rev Cancer 9, 738-748.

Porter, J. A., Ekker, S. C., Park, W. J., von Kessler, D. P., Young, K. E., Chen, C. H., Ma, Y., Woods, A. S., Cotter, R. J., Koonin, E. V., and Beachy, P. A. (1996). Hedgehog patterning activity: role of a lipophilic modification mediated by the carboxy-terminal autoprocessing domain. Cell 86, 21-34.

Porter, J. A., von Kessler, D. P., Ekker, S. C., Young, K. E., Lee, J. J., Moses, K., and Beachy, P. A. (1995). The product of hedgehog autoproteolytic cleavage active in local and long-range signalling. Nature 374, 363-366.

Porter, J. A., Young, K. E., and Beachy, P. A. (1996). Cholesterol modification of hedgehog signaling proteins in animal development. Science 274, 255-259.

Prykhozhij, S. V. (2010). In the absence of Sonic hedgehog, p53 induces apoptosis and inhibits retinal cell proliferation, cell-cycle exit and differentiation in zebrafish. PLoS One 5, e13549.

Puzio-Kuter, A. M., and Levine, A. J. (2009). Stem cell biology meets p53. Nat Biotechnol 27, 914-915.

Rahnama, F., Toftgard, R., and Zaphiropoulos, P. G. (2004). Distinct roles of PTCH2 splice variants in Hedgehog signalling. Biochem J 378, 325-334.

Ramalho-Santos, M., Melton, D. A., and McMahon, A. P. (2000). Hedgehog signals regulate multiple aspects of gastrointestinal development. Development 127, 2763-2772.

Raymond, K., Richter, A., Kreft, M., Frijns, E., Janssen, H., Slijper, M., Praetzel-Wunder, S., Langbein, L., and Sonnenberg, A. (2010). Expression of the orphan protein Plet-1 during trichilemmal differentiation of anagen hair follicles. J Invest Dermatol 130, 1500-1513.

Razzaque, M. S., Soegiarto, D. W., Chang, D., Long, F., and Lanske, B. (2005). Conditional deletion of Indian hedgehog from collagen type 2alpha1-expressing cells results in abnormal endochondral bone formation. J Pathol 207, 453-461.

Reifenberger, J., Wolter, M., Weber, R. G., Megahed, M., Ruzicka, T., Lichter, P., and Reifenberger, G. (1998). Missense mutations in SMOH in sporadic basal cell carcinomas of the skin and primitive neuroectodermal tumors of the central nervous system. Cancer Res 58, 1798-1803.

Riddle, R. D., Johnson, R. L., Laufer, E., and Tabin, C. (1993). Sonic hedgehog mediates the polarizing activity of the ZPA. Cell 75, 1401-1416.

Roelink, H., Augsburger, A., Heemskerk, J., Korzh, V., Norlin, S., Ruiz i Altaba, A., Tanabe, Y., Placzek, M., Edlund, T., Jessell, T. M., and et al. (1994). Floor plate and motor neuron induction by vhh-1, a vertebrate homolog of hedgehog expressed by the notochord. Cell 76, 761-775.

Rothnagel, J. A., Seki, T., Ogo, M., Longley, M. A., Wojcik, S. M., Bundman, D. S., Bickenbach, J. R., and Roop, D. R. (1999). The mouse keratin 6 isoforms are differentially expressed in the hair follicle, footpad, tongue and activated epidermis. Differentiation 65, 119-130.

Rowitch, D. H., B, S. J., Lee, S. M., Flax, J. D., Snyder, E. Y., and McMahon, A. P. (1999). Sonic hedgehog regulates proliferation and inhibits differentiation of CNS precursor cells. J Neurosci 19, 8954-8965.

Ruiz i Altaba, A. (1998). Combinatorial Gli gene function in floor plate and neuronal inductions by Sonic hedgehog. Development 125, 2203-2212.

Ruiz i Altaba, A., and Brand, A. H. (2009). Entity versus property: tracking the nature, genesis and role of stem cells in cancer. Conference on Stem cells and cancer. EMBO Rep 10, 832-836.

Ruiz i Altaba, A., Mas, C., and Stecca, B. (2007). The Gli code: an information nexus regulating cell fate, stemness and cancer. Trends Cell Biol 17, 438-447.

Ruiz i Altaba, A., Sanchez, P., and Dahmane, N. (2002). Gli and hedgehog in cancer: tumours, embryos and stem cells. Nat Rev Cancer 2, 361-372.

Sagai, T., Hosoya, M., Mizushina, Y., Tamura, M., and Shiroishi, T. (2005). Elimination of a long-range cis-regulatory module causes complete loss of limb-specific Shh expression and truncation of the mouse limb. Development 132, 797-803.

Saiki, R.K., Gelfand, D.H., Stoffel, S., Scharf, S.J., Higuchi, R., Horn, G.T., Mullis, K.B., and Erlich, H.A. (1988). Primer-directed enzymatic amplification of DNA with a thermostable DNA polymerase. Science 239:487-491.

Sambrook, J. and Russell, D.W. (2001). Molecular Cloning: A Laboratory Manual.(CSHL press, 2344 pp)

Saqui-Salces, M., and Merchant, J. L. (2010). Hedgehog signaling and gastrointestinal cancer. Biochim Biophys Acta 1803, 786-795.

Sato, N., Leopold, P. L., and Crystal, R. G. (1999). Induction of the hair growth phase in postnatal mice by localized transient expression of Sonic hedgehog. J Clin Invest 104, 855-864.

Schneider, M. R., and Paus, R. (2010). Sebocytes, multifaceted epithelial cells: lipid production and holocrine secretion. Int J Biochem Cell Biol 42, 181-185.

Segre, J. A. (2006). Epidermal barrier formation and recovery in skin disorders. J Clin Invest 116, 1150-1158.

Shaw, A., and Bushman, W. (2007). Hedgehog signaling in the prostate. J Urol 177, 832-838.

Shimomura, Y., and Christiano, A. M. (2010). Biology and genetics of hair. Annu Rev Genomics Hum Genet 11, 109-132.

Smyth, I., Narang, M. A., Evans, T., Heimann, C., Nakamura, Y., Chenevix-Trench, G., Pietsch, T., Wicking, C., and Wainwright, B. J. (1999). Isolation and characterization of human patched 2 (PTCH2), a putative tumour suppressor gene inbasal cell carcinoma and medulloblastoma on chromosome 1p32. Hum Mol Genet 8, 291-297.

Snijders, A. M., Schmidt, B. L., Fridlyand, J., Dekker, N., Pinkel, D., Jordan, R. C., and Albertson, D. G. (2005). Rare amplicons implicate frequent deregulation of cell fate specification pathways in oral squamous cell carcinoma. Oncogene 24, 4232-4242.

Stecca, B., Mas, C., Clement, V., Zbinden, M., Correa, R., Piguet, V., Beermann, F., and Ruiz, I. A. A. (2007). Melanomas require HEDGEHOG-GLI signaling regulated by interactions between GLI1 and the RAS-MEK/AKT pathways. Proc Natl Acad Sci U S A 104, 5895-5900.

Stecca, B., and Ruiz i Altaba, A. (2009). A GLI1-p53 inhibitory loop controls neural stem cell and tumour cell numbers. Embo J 28, 663-676.

St-Jacques, B., Dassule, H. R., Karavanova, I., Botchkarev, V. A., Li, J., Danielian, P. S., McMahon, J. A., Lewis, P. M., Paus, R., and McMahon, A. P. (1998). Sonic hedgehog signaling is essential for hair development. Curr Biol 8, 1058-1068.

St-Jacques, B., Hammerschmidt, M., and McMahon, A. P. (1999). Indian hedgehog signaling regulates proliferation and differentiation of chondrocytes and is essential for bone formation. Genes Dev 13, 2072-2086.

Stone, D. M., Hynes, M., Armanini, M., Swanson, T. A., Gu, Q., Johnson, R. L., Scott, M. P., Pennica, D., Goddard, A., Phillips, H., et al. (1996). The tumour-suppressor gene patched encodes a candidate receptor for Sonic hedgehog. Nature 384, 129-134.

Strigini, M., and Cohen, S. M. (1997). A Hedgehog activity gradient contributes to AP axial patterning of the Drosophila wing. Development 124, 4697-4705.

Sukegawa, A., Narita, T., Kameda, T., Saitoh, K., Nohno, T., Iba, H., Yasugi, S., and Fukuda, K. (2000). The concentric structure of the developing gut is regulated by
Sonic hedgehog derived from endodermal epithelium. Development 127, 1971-1980.

Sundberg, J. P., Sundberg, B. A., and Beamer, W. G. (1997). Comparison of chemical carcinogen skin tumor induction efficacy in inbred, mutant, and hybrid strains of mice: morphologic variations of induced tumors and absence of a papillomavirus cocarcinogen. Mol Carcinog 20, 19-32.

Svard, J., Heby-Henricson, K., Persson-Lek, M., Rozell, B., Lauth, M., Bergstrom, A., Ericson, J., Toftgard, R., and Teglund, S. (2006). Genetic elimination of Suppressor of fused reveals an essential repressor function in the mammalian Hedgehog signaling pathway. Dev Cell 10, 187-197.

Svard, J., Rozell, B., Toftgard, R., and Teglund, S. (2009). Tumor suppressor gene co-operativity in compound Patched1 and suppressor of fused heterozygous mutant mice. Mol Carcinog 48, 408-419.

Tabata, T., Eaton, S., and Kornberg, T. B. (1992). The Drosophila hedgehog gene is expressed specifically in posterior compartment cells and is a target of engrailed regulation. Genes Dev 6, 2635-2645.

Taipale, J., Cooper, M. K., Maiti, T., and Beachy, P. A. (2002). Patched acts catalytically to suppress the activity of Smoothened. Nature 418, 892-897.

Takeda, H., Lyle, S., Lazar, A. J., Zouboulis, C. C., Smyth, I., and Watt, F. M. (2006). Human sebaceous tumors harbor inactivating mutations in LEF1. Nat Med 12, 395-397.

Teglund, S., and Toftgard, R. (2010). Hedgehog beyond medulloblastoma and basal cell carcinoma. Biochim Biophys Acta 1805, 181-208.

Tsiairis, C. D., and McMahon, A. P. (2009). An Hh-dependent pathway in lateral plate mesoderm enables the generation of left/right asymmetry. Curr Biol 19, 1912-1917.

van den Brink, G. R. (2007). Hedgehog signaling in development and homeostasis of the gastrointestinal tract. Physiol Rev 87, 1343-1375.

van den Brink, G. R., Bleuming, S. A., Hardwick, J. C., Schepman, B. L., Offerhaus, G. J., Keller, J. J., Nielsen, C., Gaffield, W., van Deventer, S. J., Roberts, D. J., and Peppelenbosch, M. P. (2004). Indian Hedgehog is an antagonist of Wnt signaling in colonic epithelial cell differentiation. Nat Genet 36, 277-282.

van der Eerden, B. C., Karperien, M., Gevers, E. F., Lowik, C. W., and Wit, J. M. (2000). Expression of Indian hedgehog, parathyroid hormone-related protein, and their receptors in the postnatal growth plate of the rat: evidence for a locally acting growth restraining feedback loop after birth. J Bone Miner Res 15, 1045-1055.

van Dop, W. A., Heijmans, J., Buller, N. V., Snoek, S. A., Rosekrans, S. L., Wassenberg, E. A., van den Bergh Weerman, M. A., Lanske, B., Clarke, A. R., Winton, D. J., et al. (2010). Loss of Indian Hedgehog activates multiple aspects of a wound healing response in the mouse intestine. Gastroenterology 139, 1665-1676, 1676 e1661-1610.

van Dop, W. A., and Van Den Brink, G. R. Sonic hedgehog: a link between inflammation, gastric atrophy, and acid suppression? Gastroenterology 138, 426-429.
Varjosalo, M., and Taipale, J. (2008). Hedgehog: functions and mechanisms. Genes Dev 22, 2454-2472.

Varnat, F., Duquet, A., Malerba, M., Zbinden, M., Mas, C., Gervaz, P., and Ruiz i Altaba, A. (2009). Human colon cancer epithelial cells harbour active HEDGEHOG-GLI signalling that is essential for tumour growth, recurrence, metastasis and stem cell survival and expansion. EMBO Mol Med 1, 338-351.

Varnat, F., Zacchetti, G., and Ruiz i Altaba, A. (2010). Hedgehog pathway activity is required for the lethality and intestinal phenotypes of mice with hyperactive Wnt signaling. Mech Dev 127, 73-81.

Villani, R. M., Adolphe, C., Palmer, J., Waters, M. J., Wainwright, B. J. (2010). Patched1 inhibits epidermal progenitor cell expansion and basal cell carcinoma formation by limiting Igfbp2 activity. Cancer Prev Res 3, 1222-1234.

Vogelstein, B., Lane, D., and Levine, A. J. (2000). Surfing the p53 network. Nature 408, 307-310.

Vortkamp, A., Lee, K., Lanske, B., Segre, G. V., Kronenberg, H. M., and Tabin, C. J. (1996). Regulation of rate of cartilage differentiation by Indian hedgehog and PTH-related protein. Science 273, 613-622.

Vousden, K. H. (2002). Activation of the p53 tumor suppressor protein. Biochim Biophys Acta 1602, 47-59.

Vousden, K. H., and Lane, D. P. (2007). p53 in health and disease. Nat Rev Mol Cell Biol 8, 275-283.

Waghray, M., Zavros, Y., Saqui-Salces, M., El-Zaatari, M., Alamelumangapuram, C. B., Todisco, A., Eaton, K. A., and Merchant, J. L. (2010). Interleukin-1beta promotes gastric atrophy through suppression of Sonic Hedgehog. Gastroenterology 138, 562-572, 572 e561-562.

Wakabayashi, Y., Mao, J. H., Brown, K., Girardi, M., and Balmain, A. (2007). Promotion of Hras-induced squamous carcinomas by a polymorphic variant of the Patched gene in FVB mice. Nature 445, 761-765.

Wallace, V. A. (1999). Purkinje-cell-derived Sonic hedgehog regulates granule neuron precursor cell proliferation in the developing mouse cerebellum. Curr Biol 9, 445-448.

Wang, B., Fallon, J. F., and Beachy, P. A. (2000). Hedgehog-regulated processing of Gli3 produces an anterior/posterior repressor gradient in the developing vertebrate limb. Cell 100, 423-434.

Wang, G., Amanai, K., Wang, B., and Jiang, J. (2000). Interactions with Costal2 and suppressor of fused regulate nuclear translocation and activity of cubitus interruptus. Genes Dev 14, 2893-2905.

Wang, Y., Dakubo, G. D., Thurig, S., Mazerolle, C. J., and Wallace, V. A. (2005). Retinal ganglion cell-derived sonic hedgehog locally controls proliferation and the timing of RGC development in the embryonic mouse retina. Development 132, 5103-5113.

Watt, F. M., and Hogan, B. L. (2000). Out of Eden: stem cells and their niches. Science 287, 1427-1430.

Wechsler-Reya, R. J., and Scott, M. P. (1999). Control of neuronal precursor proliferation in the cerebellum by Sonic Hedgehog. Neuron 22, 103-114.

Weinberg, R. A. (2007). The biology of cancer. Garland Science.

Weiss, R. A., Eichner, R., and Sun, T. T. (1984). Monoclonal antibody analysis of keratin expression in epidermal diseases: a 48- and 56-kdalton keratin as molecular markers for hyperproliferative keratinocytes. J Cell Biol 98, 1397-1406.

Wijgerde, M., McMahon, J. A., Rule, M., and McMahon, A. P. (2002). A direct requirement for Hedgehog signaling for normal specification of all ventral progenitor domains in the presumptive mammalian spinal cord. Genes Dev 16, 2849-2864.

Wijgerde, M., Ooms, M., Hoogerbrugge, J. W., and Grootegoed, J. A. (2005). Hedgehog signaling in mouse ovary: Indian hedgehog and desert hedgehog from granulosa cells induce target gene expression in developing theca cells. Endocrinology 146, 3558-3566.

Wojcik, S. M., Bundman, D. S., and Roop, D. R. (2000). Delayed wound healing in keratin 6a knockout mice. Mol Cell Biol 20, 5248-5255.

Wojcik, S. M., Imakado, S., Seki, T., Longley, M. A., Petherbridge, L., Bundman, D. S., Bickenbach, J. R., Rothnagel, J. A., and Roop, D. R. (1999). Expression of MK6a dominant-negative and C-terminal mutant transgenes in mice has distinct phenotypic consequences in the epidermis and hair follicle. Differentiation 65, 97-112.

Wokalek, H., and Ruh, H. (1991). Time course of wound healing. J Biomater Appl 5, 337-362.

Xie, J., Johnson, R. L., Zhang, X., Bare, J. W., Waldman, F. M., Cogen, P. H., Menon, A. G., Warren, R. S., Chen, L. C., Scott, M. P., and Epstein, E. H., Jr. (1997). Mutations of the PATCHED gene in several types of sporadic extracutaneous tumors. Cancer Res 57, 2369-2372.

Xie, J., Murone, M., Luoh, S. M., Ryan, A., Gu, Q., Zhang, C., Bonifas, J. M., Lam, C. W., Hynes, M., Goddard, A., et al. (1998). Activating Smoothened mutations in sporadic basal-cell carcinoma. Nature 391, 90-92.

Xuan, Y. H., Jung, H. S., Choi, Y. L., Shin, Y. K., Kim, H. J., Kim, K. H., Kim, W. J., Lee, Y. J., and Kim, S. H. (2006). Enhanced expression of hedgehog signaling molecules in squamous cell carcinoma of uterine cervix and its precursor lesions. Mod Pathol 19, 1139-1147.

Yao, H. H., Whoriskey, W., and Capel, B. (2002). Desert Hedgehog/Patched 1 signaling specifies fetal Leydig cell fate in testis organogenesis. Genes Dev 16, 1433-1440.

Ye, W., Shimamura, K., Rubenstein, J. L., Hynes, M. A., and Rosenthal, A. (1998). FGF and Shh signals control dopaminergic and serotonergic cell fate in the anterior neural plate. Cell 93, 755-766.

Yonish-Rouach, E., Resnitzky, D., Lotem, J., Sachs, L., Kimchi, A., and Oren, M. (1991). Wild-type p53 induces apoptosis of myeloid leukaemic cells that is inhibited by interleukin-6. Nature 352, 345-347.

Zhang, X. M., Ramalho-Santos, M., and McMahon, A. P. (2001). Smoothened mutants reveal redundant roles for Shh and Ihh signaling including regulation of L/R symmetry by the mouse node. Cell 106, 781-792.

Zhao, C., and Malicki, J. (2007). Genetic defects of pronephric cilia in zebrafish. Mech Dev 124, 605-616.

Zhao, T., and Xu, Y. (2010). p53 and stem cells: new developments and new concerns. Trends Cell Biol 20, 170-175.

Zheng, Y., Eilertsen, K. J., Ge, L., Zhang, L., Sundberg, J. P., Prouty, S. M., Stenn, K. S., and Parimoo, S. (1999). Scd1 is expressed in sebaceous glands and is disrupted in the asebia mouse. Nat Genet 23, 268-270.

Zhu, A. J., and Scott, M. P. (2004). Incredible journey: how do developmental signals travel through tissue? Genes Dev 18, 2985-2997.

Zouboulis, C. C. (2004). Acne and sebaceous gland function. Clin Dermatol 22, 360-366.

Zuniga, A., Haramis, A. P., McMahon, A. P., and Zeller, R. (1999). Signal relay by BMP antagonism controls the SHH/FGF4 feedback loop in vertebrate limb buds. Nature 401, 598-602.

9 Erklärung

Ich versichere, dass ich die von mir vorgelegte Dissertation selbständig angefertigt, die benutzten Quellen und Hilfsmittel vollständig angegeben und die Stellen der Arbeit – einschließlich Tabellen, Karten und Abbildungen -, die anderen Werken im Wortlaut oder dass diese Dissertation noch keiner anderen Fakultät oder Universität zur Prüfung vorgelegen worden ist sowie, dass ich eine solche Veröffentlichung vor Abschluss des Promotionsverfahren nicht vornehmen werde. Die Bestimmungen dieser Promotionsordnung sind mir bekannt. Die von mir vorgelegte Dissertation ist von Prof. Dr. Jens C. Brüning betreut worden.

Köln, Mai 2011 Parisa Kakanj

Teilpublikationen: